International Journal of Genomics

Environment-Living Organism's Interactions from Physiology to Genomics

Guest Editors: Shao Hongbo, Chen Sixue, and Marian Brestic

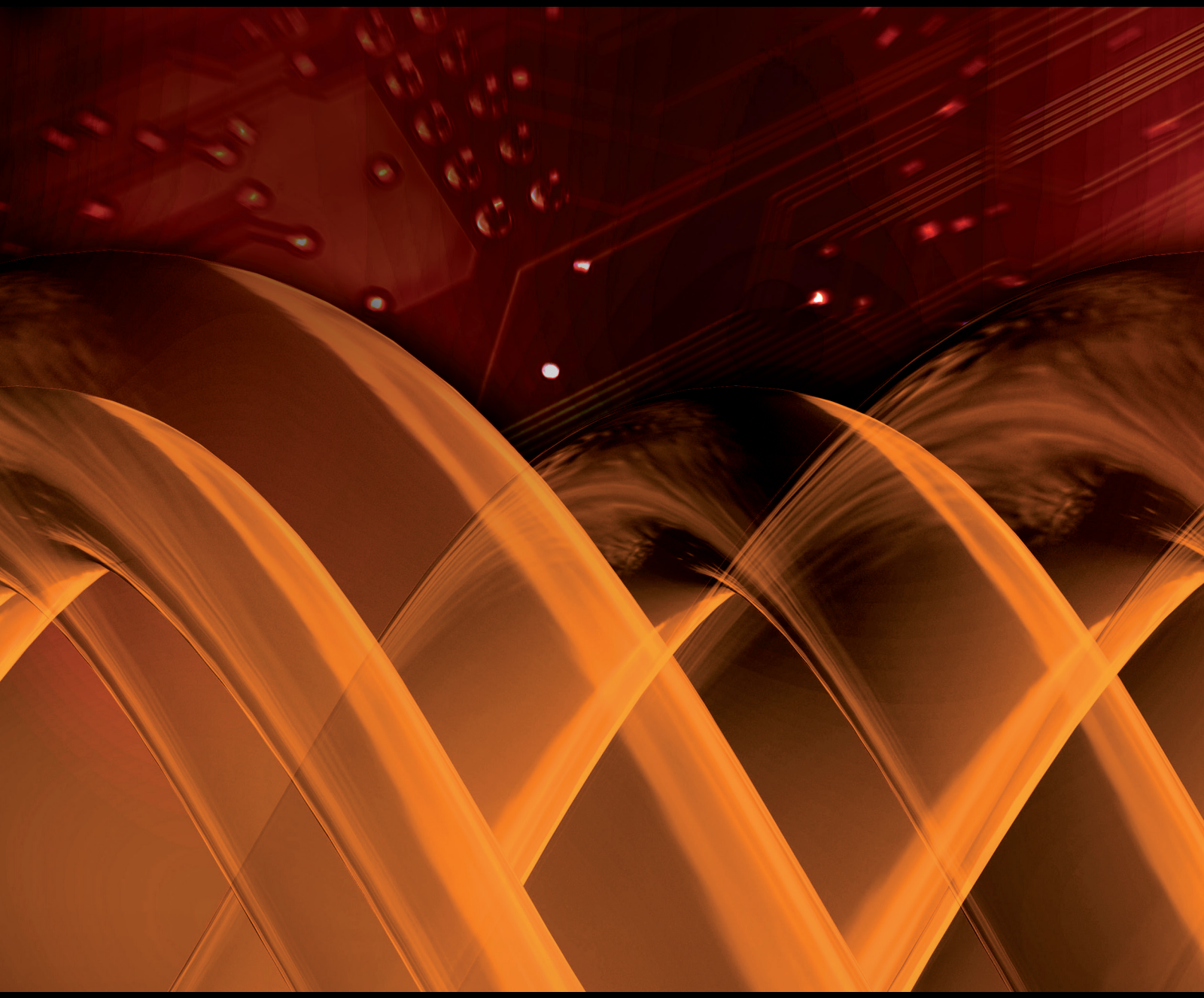

Environment-Living Organism's Interactions from Physiology to Genomics

International Journal of Genomics

Environment-Living Organism's Interactions from Physiology to Genomics

Guest Editors: Shao Hongbo, Chen Sixue, and Marian Brestic

Editorial Board

Contents

Editorial

Environment-Living Organism's Interactions from Physiology to Genomics

Shao Hongbo,[1,2] Chen Sixue,[3] and Marian Brestic[1,4]

[1] *Jiangsu Key Laboratory for Bioresources of Saline Soils, Provincial Key Laboratory of Agrobiology, Institute of Agro-Biotechnology, Jiangsu Academy of Agricultural Sciences, Nanjing 210014, China*
[2] *Key Laboratory of Coastal Biology & Bioresources Utilization, Yantai Institute of Coastal Zone Research (YIC), Chinese Academy of Sciences (CAS), Yantai 264003, China*
[3] *Cancer and Genetics Research Complex, University of Florida, 2033 Mowry Road, Gainesville, FL 32610, USA*
[4] *Department of Plant Physiology, Slovak Agricultural University, Tr. A. Hlinku 2, 949 76 Nitra, Slovakia*

Correspondence should be addressed to Shao Hongbo; shaohongbochu@126.com

Received 30 August 2015; Accepted 7 September 2015

Human beings depend on the environment for stable survival and sustainable development, so the environment and organisms should be one bi-interacting whole body. Environment-living organism's interactions in terms of physiology, molecular biology, and genomics are the essential base for establishing and crossing different disciplines where life sciences link with environmental sciences fully and they have resulted from many important subjects such as soil biology, ecophysiology, molecular ecology, and environmental genomics. These disciplines support current human beings' sustainable development by providing new ways to cope with nature.

With global economic change, large-scale urbanization, and environmental pollution, human beings face more serious challenges. To solve these problems and search for new ways we must understand environment-living organism's interacting responses by these disciplines, to which less attention has been paid for the past 20 years. In this special issue for this journal we have solicited papers from experts working with various aspects of genomic research in relation to plant biology, soil biology, agricultural sciences, aquaculture, and environmental protection. We invited researchers to present their novel results that can deeply understand environment-organisms' interactions. The special issue is dedicated to the crossing disciplines among plant biology, soil biology, microbiology, agricultural sciences, aquaculture, and ecorestoration by covering the following main aspects: (i) plants from physiology, molecular biology, and metabolisms to genomics; (ii) plant-soil interactions in terms of molecular responses; (iii) organisms-based ecorestoration; (iv) molecular microbiology related to agricultural sciences, aquaculture, and environmental protection.

In the special issue, N. Yi et al. established the linkage of water properties with the abundance and diversity of *Eichhornia crassipes* by comparative genomics and precise environmental biology methodology, providing the clear evidence for *Eichhornia crassipes* to remove nitrogen in different effluents around Dianchi Lake, China. These results can be used extensively for phytoremediation. T. Wang et al. firstly reported the results about efforts of copper nanoparticles on juvenile *Epinephelus coioides in terms of* growth parameters, digestive enzymes, body composition, and histology, providing more valuable parameters as environmental biomarkers in aquaculture and its management. G. H. Yu et al. used *SbPIP1*-transformed wheat seedlings as the materials to compare the related salt resistance. The result indicated that *SbPIP1* plays an important role in the salt stress response. Overexpression of *SbPIP1* could be used to improve the salt tolerance of important crop plants. The abiotic stresses like salinity, drought, and low and high temperature negatively affect plant growth and productivity. Dehydration-responsive element binding (DREB) transcription factor (TF) plays a key role for abiotic stress tolerance in plants. X. Zhang et al. reported the cloning and characterization of the SsDREB cDNA from *Suaeda salsa*. Its expression

pattern was investigated in response to exogenous ABA, salt, cold, and drought stress treatments. Overexpression of this cDNA in transgenic tobacco led to enhanced tolerance to salinity and dehydration stresses. These integrated data suggest that the *SsDREB* transcription factor is involved in the regulation of salt stress tolerance in tobacco by the activation of different downstream gene expression. Unlike animals, plants are not mobile organism and cannot go away from adverse environmental conditions. Owing to these reasons, they create special system to adjust themselves in external stress conditions through instant transmit signals. Due to the temporary fluctuations in cytosolic calcium concentration, plant cells receive the signals from external stimuli, so they can accept the signals using their own machineries and decode the signal to secondary messenger. Calcium is broadly well known as a ubiquitous secondary messenger because of its diverse functions in plants. Ca^{2+} is encoded in various stimuli of abiotic and biotic stresses. Abiotic stresses caused by high magnesium, high sodium, low potassium, low phosphorous, ABA, and others affect the rate of germination, photosynthesis, seedling growth, leaf expansion, total biomass accumulation, and overall growth effects of plants. In recent decades, calcineurin B-like protein- (CBL-) interacting protein kinase (CIPK) complex is widely accepted as Ca^{2+} signaling mechanism, which is involved in response to different external stresses signals (Shao et al. 2008). In adverse stresses conditions, plants evolve a stress signal that is specifying Ca^{2+} signature. The specific Ca^{2+} signatures are received by closely controlled activities of plasma membrane and other organelles channels and transporters. In addition, this signature binds to EF hands domains of the CBL proteins. Consequently, the CBL proteins bind the NAF/FISL domain of C-terminal of the CIPK thus stimulating the kinase. On the other hand, N-terminal of the CBL protein directs the CBL-CIPK system to an exact cellular target region ensuing in the stimulated CIPK phosphorylating the proper target proteins. S. M. N. Manik et al.'s review recapitulated the recent and ongoing progress of positive ions (Mg^{2+}, Na^{+}, and K^{+}), negative ions (NO_3^{-}, PO_4^{-}), and hormonal signaling, which are evolving from accumulating results of analyses of CBL and CIPK loss or gain of functions experiments in different species. Generally, this review provided further insights into the calcium sensor CBL-CIPK. Other important progresses can also be witnessed in the special issue.

All the results from the accepted papers have greatly contributed to the special issue, speeding up the extensive investigation of environment-living organism interactions. With the comprehensive application of modern methodology, more attention will be paid to this interesting and important field and it will further witness new advances.

Acknowledgments

This research was supported by Jiangsu Key Laboratory for Bioresources of Saline Soils (JKLBS2014005), One Hundred Talent Plan of Foreign Experts of Jiangsu Province (JSB2015005), the National Natural Science Foundation of China (41171216), the National Basic Research Program of China (2013CB430403), Jiangsu Autonomous Innovation of Agricultural Science & Technology [CX(15)1005], Yantai Double-Hundred Talent Plan (XY-003-02), and 135 Development Plan of YIC-CAS. More thanks also extend to all the authors and referees for their efforts in the special issue.

Shao Hongbo
Chen Sixue
Marian Brestic

Research Article

A Comparison Effect of Copper Nanoparticles versus Copper Sulphate on Juvenile *Epinephelus coioides*: Growth Parameters, Digestive Enzymes, Body Composition, and Histology as Biomarkers

Tao Wang, Xiaohua Long, Yongzhou Cheng, Zhaopu Liu, and Shaohua Yan

Jiangsu Provincial Key Laboratory of Marine Biology, College of Resources and Environmental Sciences, Nanjing Agricultural University, Nanjing 210095, China

Correspondence should be addressed to Xiaohua Long; longxiaohua2014@126.com

Received 23 December 2014; Revised 2 February 2015; Accepted 18 February 2015

Academic Editor: Marián Brestič

Copper nanoparticles (Cu-NPs) are components in numerous commercial products, but little is known about their potential hazard in the marine environments. In this study the effects of Cu-NPs and soluble Cu on juvenile *Epinephelus coioides* were investigated. The fish were exposed in triplicate to control, 20 or 100 μg Cu L^{-1} as either copper sulphate ($CuSO_4$) or Cu-NPs for 25 days. The growth performance decreased with increasing $CuSO_4$ or Cu-NPs dose, more so in the $CuSO_4$ than Cu-NPs treatment. Both forms of Cu exposure inhibited activities of digestive enzymes (protease, amylase, and lipase) found in liver, stomach, and intestine. With an increase in $CuSO_4$ and Cu-NPs dose, crude protein and crude lipid decreased, but ash and moisture increased, more so in the $CuSO_4$ than Cu-NPs treatment. The Cu-NPs treatment caused pathologies in liver and gills, and the kinds of pathologies were broadly of the same type as with $CuSO_4$. With an increase in $CuSO_4$ or Cu-NPs dose, the total polyunsaturated fatty acids decreased, but total monounsaturated fatty acids and total saturated fatty acids increased compared to control. Overall, these data showed that Cu-NPs had a similar type of toxic effects as $CuSO_4$, but soluble Cu was more toxic than Cu-NPs.

1. Introduction

The contamination of aquatic ecosystems by metals is one of the main environmental issues today [1]. In the last decade, the advance of nanotechnology fueled fast growth of the nanotoxicology research and the need for information on potential hazards of this technology in aquatic environments [1, 2].

Copper nanoparticles (Cu-NPs) are one of the most used nanomaterials due to their antibacterial and other properties [3], used for example, in textiles, food storage containers, home appliances, paints, food supplements and so on [4]. Production and use of Cu-NPs likely result in their release into aquatic environments and can lead to unexpected hazards to aquatic organisms [1, 5, 6]. In addition, Cu-NPs could be accumulated in aquatic organisms and transferred to higher trophic levels, representing a health hazard to animals and humans [5, 7].

Currently, concerns have been raised about the effects of Cu-NPs on fish [2, 3, 8] and also about the sublethal effects of NPs on different body systems of fish [8, 9]. However, the majority of the published studies focused on Cu-NPs regarding a lethal dose [8], accumulation [5, 7], stress response [3, 8], osmoregulation [6, 7], and pathology [2]. To our knowledge, the effects of nanometals on digestive enzyme activities, whole-body composition, and fatty acid composition are poorly understood. Furthermore, toxicity thresholds can be rather variable in different species [9–11], and little attention has been given so far to marine teleosts.

Epinephelus coioides (grouper), a protogynous hermaphroditic fish, is widely cultured in China and Southeast Asian countries because of its excellent seafood quality and its high market value [12]. Currently, *Epinephelus coioides* species are mainly cultured in floating net cages and earthen ponds in the natural environments that can easily be affected by

environment pollution given that discharge of Cu-NPs in the aquatic environment is inevitable [2]. However, as far as we know, there is paucity of data about toxicity of Cu-NPs on *Epinephelus coioides*.

In aquaculture production, the inappropriate management often promotes proliferation of diseases in aquatic organisms [13]. Another problem related to aquaculture is the excessive growth of phytoplankton, particularly blue-green algae [14]. Copper sulphate ($CuSO_4$) is employed to control diseases and algae in aquaculture facilities [15]. Copper is an essential micronutrient required for the various functions in biological systems, such as cell structure and enzyme activities of fish [16, 17]. However, excessive Cu in the aquatic environment can be toxic [7, 18]. It has been reported that $CuSO_4$ can induce endocrine disruption and change metabolic rates [19, 20], swimming behavior [21, 22], immunological function [2, 8], enzyme activities [8], tissue histology [2, 20], and fatty acid composition [23, 24]. Recently, we found that $CuSO_4$ exposure could significantly influence oxidative stress, Na^+/K^+-ATPase activity, and cell apoptosis in the liver of juvenile *Epinephelus coioides* [6]. Nevertheless, the physiology effects after *Epinephelus coioides* exposure to $CuSO_4$ are poorly understood.

In this study, the main goal was to evaluate the effects of Cu-NPs and $CuSO_4$ on growth parameters, activities of the digestive enzymes (protease, amylase, and lipase), whole-body composition, fatty acid composition, and histology of juvenile *Epinephelus coioides*. Results of this study provide an insight into the toxicity mechanisms of Cu-NPs compared with $CuSO_4$, aiming to propose margins for a safe use of $CuSO_4$ in fish culture.

2. Materials and Methods

2.1. Experimental Design. Juvenile *Epinephelus coioides* (n = 800) were obtained from Shenzhen Dongfang Technology Co., Ltd. China and transferred to indoor tanks for 15 days to acclimate prior to the toxicity assay. During the acclimation period, the juveniles were fed once daily (at 8 am) with commercial feed. After accumulation, selected healthy juveniles (n = 525, average weight 3.1 ± 0.2 g) were randomly divided into 15 blue plastic tanks (35 fish per tank, the density approximately 1.0 g fish L^{-1}) containing 100 L of simulated seawater. The simulated seawater was made by adding sea salt (purchased from Qingdao Universal Aquaculture Company, China) to the aerated tap water [12].

Three tanks per treatment were randomly allocated and fish were exposed in triplicate to control (no added Cu), 20 μg Cu L^{-1} or 100 μg Cu L^{-1} either as $CuSO_4{\cdot}5H_2O$ or Cu-NPs for 25 days using a semistatic exposure regime (50% water change every 12 h with redosing after each change). The low concentration of 20 μg Cu L^{-1} Cu was selected because it reflects the actual environmental concentration [7]. The high Cu concentration (100 μg Cu L^{-1}) was selected because this concentration may be found in some areas with intensive manufacturing industries, agricultural and mining activities, and municipal waste depositions [25]. Water samples were taken before and after each water change and were analyzed for pH, temperature, salinity, dissolved oxygen (tested by YSI 556MPS, USA), total ammonium (by Nessler's reagent spectrophotometry), water hardness (Ca and Mg), and Cu (trace elements were measured by an Inductively Coupled Plasma Optical Emission Spectrometer, ICP-OES, Optima 7000, PerkinElmer, USA). As there were no significant differences (ANOVA, $P \leq 0.05$) among any tanks in water quality or Cu treatment concentration, data were pooled and were pH 8.1 ± 0.1, water temperature 24 ± 0.5°C, salinity 27.5 ± 0.5 g L^{-1} (w/v), total ammonium 0.15 ± 0.05 mg L^{-1}, and total hardness (mg $CaCO_3$ L^{-1}), 405 ± 4. Continuous aeration was used to ensure dissolved oxygen above 5 mg L^{-1}. The photoperiod was 12 h light:12 h dark. The actual concentrations of Cu in the seawater were 2.3 ± 0.1, 21.9 ± 1.4, 102.5 ± 3.1, 20.3 ± 2.8, and 101.2 ± 2.1 μg L^{-1} for the control, 20 and 100 μg Cu L^{-1} as $CuSO_4$, and 20 and 100 μg Cu L^{-1} as Cu-NPs treatments, respectively. During the experimental, no fish mortality was observed.

To minimize the influence of hunger throughout the experiment (a requirement in animal husbandry) [17], fish were hand-fed commercial diet (Fish Po, imported from Japan, containing 54% w/w protein and 3.0 ± 0.12 μg Cu g^{-1}) twice daily (8 am and 4 pm) at a rate of 2–2.5% w/w fresh body mass each time [12] for 25 days. Feeding was done after each water change, but prior to Cu redosing to minimize the risk of ingestion of Cu-NPs during feeding. Food was eaten within 5 minutes, with no food wasted.

2.2. Stock Solutions and Dosing. Stock solutions of $CuSO_4$ and suspensions of Cu-NPs were prepared and characterized as described in detail in our previous report [6] using the same stocks. Briefly, powder form of Cu-NPs was purchased from Shanghai Aladdin Co., Ltd. China (manufacturer's information: particles 10–30 nm; purity 99.9%). A fresh 50-mL Cu-NPs stock solution of 1.0 g Cu L^{-1} was prepared at 8 pm daily by dispersing the nanoparticles in ultrapure water (Millipore, ion free and unbuffered), sonicated for 30 min, and stirred for 1 h at room temperature. Primary particle sizes of the Cu-NPs were measured manually from micrographs obtained using transmission electron microscopy (TEM, JEOL JEM-2100, Japan). The primary particle diameters of Cu-NPs in stock suspensions were 85±29 nm (mean ± S.E.M., n = 62 particles). According to the method of Sovová et al. [26], the particle size distributions of Cu-NPs in stock suspensions prepared as described above were measured by nanoparticle tracking analysis (NTA, NanoSight LM_{10}) in 20 mg L^{-1} dilutions to avoid saturating the instrument. Dilutions of stock suspensions to 20 mg L^{-1} gave sufficient particle tracks (>100 tracks per sample) to provide reproducible data of particle size distribution in the stock suspensions. The stock suspensions were observed to contain a normal distribution of particle sizes, ranging from individual Cu-NPs of 0 to 30 nm to larger particles, almost certainly Cu-NPs aggregates >80 nm. The mean diameter of aggregates in the suspension was 210 ± 130 nm (mean ± S.E.M., n = 3).

A stock solution containing 1 g Cu L^{-1} as $CuSO_4$ was prepared by dissolving 3.929 g $CuSO_4{\cdot}5H_2O$ in 1 L of ultrapure water (Millipore, ion free and unbuffered). The $CuSO_4$ stock solution was used to dose the tanks throughout the 25-day

exposure. Dosing of all treatments was carried out following the water change and again the following morning after a subsequent water change.

2.3. Fish Sampling. Fish from each tank were weighed at the beginning and end of experiment. Fish were not fed for 24 h before sampling [17]. Six fish were randomly taken from each tank and dissected on an ice tray. The whole liver, stomach, and intestine were removed; fat was cleaned and flushed by normal saline solution (salinity 8.6 g L^{-1}, 4°C) and placed into a centrifuge tube (tissues from three out of six fish from each tank were combined) and stored at −70°C for analyzing digestive enzyme activities; the other three fish from each replicate were used for the analysis of fatty acid composition. The remaining fish from each tank were collected for analysis of whole-body composition and for histological observation. For histological observation, the left lobe of liver and the second gill arch on the left were removed and fixed in 10% v/v buffered formal saline (100 mL 40% v/v formaldehyde, 6.5 g NaH_2PO_4 (anhydrous), 4 g $NaH_2PO_4 \cdot H_2O$, diluted to 1 L with distilled water, pH 7.2).

2.4. Digestive Enzyme Quantification. The total soluble protein content was measured in diluted homogenates by Bradford's method [27] using bovine serum albumin as a standard. Total protease activity was measured according to the method of Gui et al. [28], using casein as substrate with Folin-phenol reagent. Amylase and lipase activities were measured using kits purchased from Nanjing Jiancheng Bioengineering Research Institute of China [29]. The unit of protease activity was defined as the amount of enzyme needed to catalyze the formation of 1 μg of tyrosine per 1 min at 40°C. The unit of amylase activity was defined as 10 mg starch hydrolyzed with the substrate per mg protein in tissue during 30 min at 37°C. The unit of lipase activity was estimated as consumption of 1 μmol substrate (triglyceride) during 1 min at 37°C per g protein in tissue.

2.5. Determination of Whole-Body Composition. The fish whole-body samples were freeze-dried and homogenized prior to chemical analysis. Moisture, crude protein, crude fat, and ash contents were determined according to the standard methods [30]. Moisture content was analyzed using a Craft stove at 105°C to a constant weight. Crude protein content was determined by measuring nitrogen (N × 6.25) using the Kjeldahl method. Crude fat content was measured using a micro Soxhlet Foss Soxtec Avanti (Soxtec Avanti 2050 Auto System, Foss Tecator AB, Höganas, Sweden). Ash content was determined by heating the samples in a muffle furnace at 550°C for 12 h.

2.6. Determination of Fatty Acids Composition. The lipids from whole-body of juvenile *Epinephelus coioides* were extracted with a chloroform: methanol (2 : 1 v/v) mixture by method of Dubois et al. [31] and esterified with 14% (w/v) boron trifluoride (BF_3) in methanol according to Yoshioka et al. [32]. The samples were then analyzed using a Shimadzu GC-201 gas chromatograph (Shimadzu Co., Kyoto, Japan) in a cross-linked 5% phenylmethyl silicone gum phase column (30 m × 0.32 mm i.d. × 0.25 mm film thickness; N_2 as the carrier gas), equipped with flame ionization detection. The injector and detector temperatures were set at 250°C. The column oven temperature was kept at 100°C for 3 min, raised to 180°C at the rate of 10°C min^{-1}, and then raised to 240°C at 3°C min^{-1}. The relative quantity of each fatty acid present was determined by measuring the area under the chromatograph peak corresponding to that fatty acid.

2.7. Histology. Histological analyses followed the standard techniques [33]. Briefly, the samples were dehydrated in rising concentrations of ethanol, cleared in xylene, infiltrated with rising concentrations of liquid paraffin wax at 58°C, and later embedded in paraffin blocks. The sections were cut at 7-μm-thick with a Rotary microtome (MT-1090A, India), and stained using hematoxylin and eosin (H&E). Stained sections were observed by light microscopy (Leica DM750, Switzerland).

2.8. Calculations and Statistical Analysis. The relative weight gain rate (WG, %), specific growth rate (SGR, % d^{-1}), food conversion ratio (FCR), and protein efficiency ratio (PER) were calculated as follows [28, 34]:

$$\begin{aligned} \mathrm{WG}\,(\%) &= \frac{[(w_t - w_0) \times 100]}{w_0}, \\ \mathrm{SGR_d}\left(\%\ \mathrm{day}^{-1}\right) &= \left(\frac{(\ln(w_t) - \ln(w_0))}{t}\right) \times 100, \\ \mathrm{FCR} &= \frac{C}{(w_t - w_0)}, \\ \mathrm{PER} &= \frac{(w_t - w_0)}{(C \times \text{protein content})}, \end{aligned} \tag{1}$$

where w_t and w_0 are the final and initial wet body weight (g) of juvenile *Epinephelus coioides*, respectively, t is the duration of experiment (25 days), and C is the mean total food intake on a dry weight basis [35]. The diet contained 54% w/w protein.

Experimental data were analysed by one-way analysis of variance (ANOVA) using SPSS (18.0; SPSS Inc., Chicago, IL, USA) for Windows. Tukey's test was used to compare differences among treatments. The $P \leq 0.05$ was considered statistically significant. All data were presented as means ± S.E.M. (standard error of the mean).

3. Results

3.1. Growth Parameters. With an increase in $CuSO_4$ or Cu-NPs concentration, WG, SGR_d, and PER were decreased compared to control, more so in the $CuSO_4$ than Cu-NPs treatments. In contrast, FCR increased with increasing $CuSO_4$ or Cu-NPs dose, with the highest FCR at 100 μg Cu L^{-1} as $CuSO_4$ (Table 1).

3.2. Digestive Enzyme Activities. The activities of protease, amylase, and lipase found in liver, stomach, and intestine were

Table 1: Effect of Cu-NPs and $CuSO_4$ on weight gain rate (WG, %), specific growth rate (SGR % d^{-1}), food conversion ratio (FCR), and protein efficiency ratio (PER) of juvenile *Epinephelus coioides* after 25-day exposure.

	Control	20 μg Cu L^{-1} as $CuSO_4$	20 μg Cu L^{-1} as Cu-NPs	100 μg Cu L^{-1} as $CuSO_4$	100 μg Cu L^{-1} as Cu-NPs
WG (%)	105.34 ± 5.16^{a}	81.25 ± 5.41^{b}	92.19 ± 4.69^{b}	47.66 ± 1.97^{d}	59.38 ± 2.55^{c}
SGR % d^{-1}	2.94 ± 0.12^{a}	2.40 ± 0.17^{b}	2.71 ± 0.13^{ab}	1.60 ± 0.06^{d}	1.93 ± 0.09^{c}
FCR	37.31 ± 1.85^{d}	48.51 ± 3.25^{c}	42.48 ± 2.16^{cd}	82.37 ± 3.26^{a}	66.16 ± 2.87^{b}
PER	1.61 ± 0.08^{a}	1.24 ± 0.08^{b}	1.41 ± 0.07^{ab}	0.73 ± 0.03^{c}	0.91 ± 0.04^{c}

Data are means ± S.E.M ($n = 3$). Significant differences ($P \leq 0.05$) among treatments were indicated by different letters in each row.

Table 2: Effect of Cu-NPs and $CuSO_4$ on whole-body composition (% on wet weight basis) of juvenile *Epinephelus coioides* after 25-day exposure.

	Control	20 μg Cu L^{-1} as $CuSO_4$	20 μg Cu L^{-1} as Cu-NPs	100 μg Cu L^{-1} as $CuSO_4$	100 μg Cu L^{-1} as Cu-NPs
Crude protein (%)	16.11 ± 0.89^{a}	14.74 ± 0.28^{ab}	15.94 ± 0.40^{a}	13.53 ± 0.60^{b}	14.85 ± 0.29^{ab}
Crude lipid (%)	7.94 ± 0.46^{a}	6.87 ± 0.28^{b}	7.57 ± 0.30^{ab}	5.30 ± 0.17^{c}	5.83 ± 0.20^{c}
Ash (%)	5.03 ± 0.11^{b}	5.11 ± 0.14^{b}	5.08 ± 0.10^{b}	5.83 ± 0.14^{a}	5.73 ± 0.17^{a}
Moisture (%)	71.32 ± 0.67^{d}	73.27 ± 0.30^{bc}	72.32 ± 0.33^{cd}	75.34 ± 0.43^{a}	73.59 ± 0.47^{b}

Data are means ± S.E.M ($n = 3$). Significant differences ($P \leq 0.05$) among treatments were indicated by different letters in each row.

decreased with increasing $CuSO_4$ or Cu-NPs dose. For liver and stomach, the $CuSO_4$ treatment resulted in lower protease, amylase, and lipase activities than the Cu-NPs treatment, but opposite results were recorded for intestine (Figure 1).

3.3. Whole-Body Composition. The whole-body composition was significantly affected by the treatments (Table 2). Crude protein and crude lipid decreased with an increase in $CuSO_4$ and Cu-NPs dose, more so in the $CuSO_4$ than Cu-NPs treatment. However, ash and moisture increased with an increase in $CuSO_4$ and Cu-NPs dose, with the highest ash and moisture at 100 μg Cu L^{-1} as $CuSO_4$ (Table 2).

3.4. Whole-Body Fatty Acid Composition. As can be seen from Table 3, eicosapentaenoic acid (EPA, C20: 5), docosahexaenoic acid (DHA, C22: 6), and docosapentaenoic acid (DPA, C22: 5) were the lowest at 100 μg Cu L^{-1} as $CuSO_4$. The total polyunsaturated fatty acids ($\sum$PUFA) decreased with an increase in $CuSO_4$ and Cu-NPs dose, and the lowest $\sum$PUFA were found at 100 μg Cu L^{-1} as $CuSO_4$. However, total monounsaturated fatty acids ($\sum$MUFA) and total saturated fatty acids ($\sum$SFA) increased with an increase in $CuSO_4$ and Cu-NPs dose, with the highest $\sum$MUFA and $\sum$SFA at 100 μg Cu L^{-1} as $CuSO_4$ (Table 3).

3.5. Histological Observations. Liver from control specimens showed the normal structure of sinusoids and vascular system. However, liver from the treatment with 100 μg Cu L^{-1} as either $CuSO_4$ or Cu-NPs showed blood cell deposition in veins and dilatation of sinusoids, with the sinusoids becoming irregular in shape (Figure 2). These injuries were greater in the $CuSO_4$ than Cu-NPs treatment. No significant histological evidence of injury in liver and gills was observed in the treatment with 20 μg Cu L^{-1} as $CuSO_4$ or Cu-NPs (data not shown). In 100 μg Cu L^{-1} as $CuSO_4$ or Cu-NPs, the gills showed areas of hyperplasia at the base of the secondary lamellae, clubbed tips at the top of some secondary lamellae, and aneurism in gill filaments (Figure 2).

4. Discussion

The water quality of the aquatic environment is the main factor controlling the health of cultured as well as wild fish [36]. Pollution of the aquatic environment by metals is a serious threat to the growth and survival of aquatic organisms including fish [37, 38]. Shaw et al. [7] reported 85% mortality of rainbow trout in 100 μg Cu L^{-1} as $CuSO_4$ and 14% mortality in 100 μg Cu L^{-1} as Cu-NPs after 4 days. In our study, almost all parameters evaluated were affected by both forms of Cu exposure, but no mortality was observed after 25 days of exposure to $CuSO_4$ or Cu-NPs (up to 100 μg Cu L^{-1}). These results may indicate differential sensitivity of different species to Cu toxicity, but further work is necessary to elucidate relevant relationships.

The present study is one of the first reports detailing the effects of Cu-NPs on juvenile *Epinephelus coioides* compared to Cu added as $CuSO_4$. Either Cu-NPs or $CuSO_4$ exposure decreased WG and SGR_d compared to control. Chen et al. [17] reported that the reduction in growth performance was most likely due to two reasons: first, Cu exposure caused increased metabolic expenditure for detoxification and maintenance of homeostasis; second, higher Cu exposure reduced feed intake, which would in turn lead to reduced growth. In our study, the food was eaten within 5 min of presentation, with no waste in any of the treatments, suggesting the increased metabolic expenditure for detoxification and maintenance of homeostasis and/or decreased digestive capabilities were the main reasons for decreased growth performance of juvenile *Epinephelus coioides* rather than decreased food intake. Indeed, growth is a complex phenomenon that partly relies

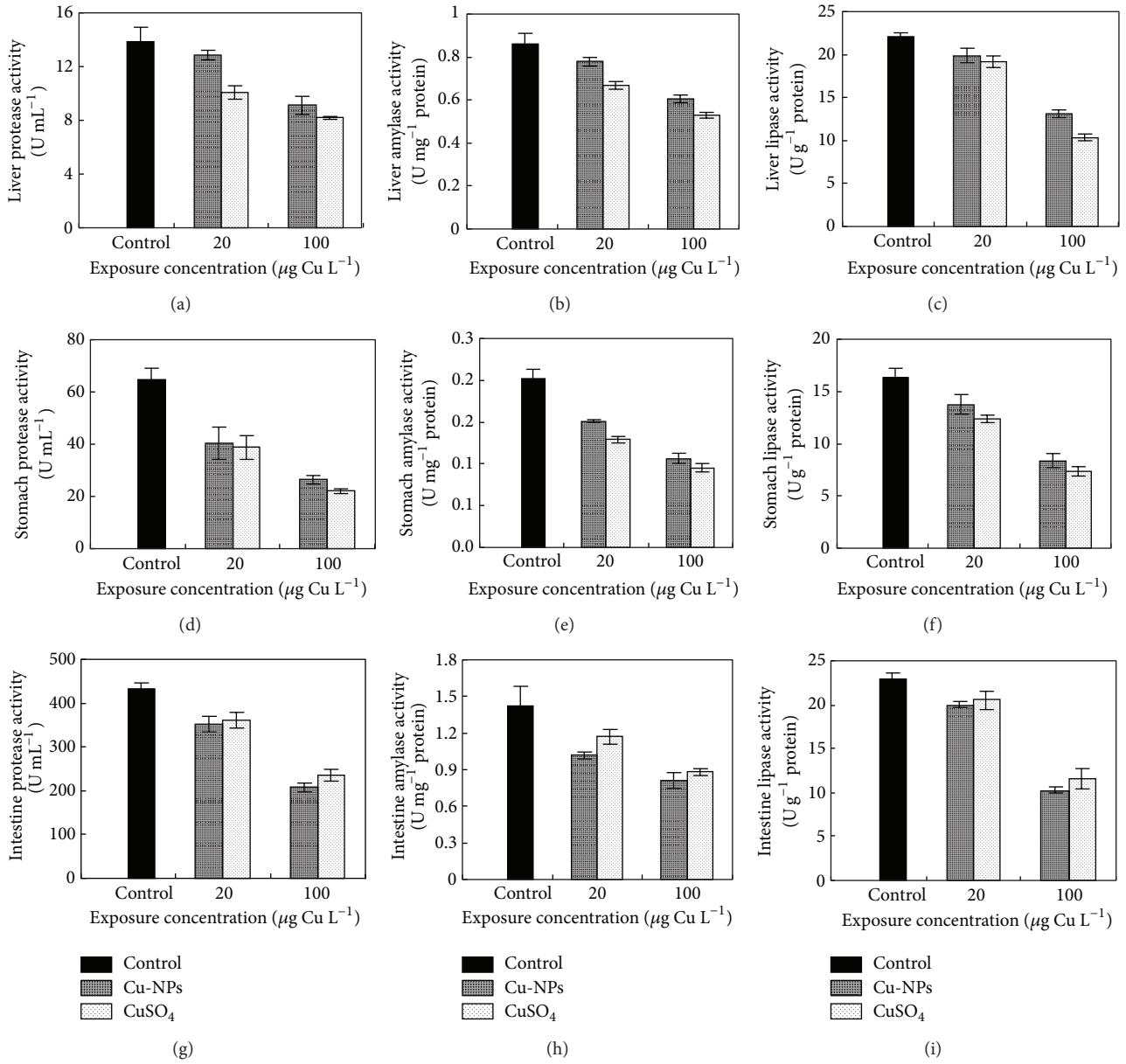

Figure 1: Effects of Cu-NPs and $CuSO_4$ on digestive enzyme activities (protease ((a), (d), (g)), amylase ((b), (e), (h)), and lipase ((c), (f), (i)) in liver ((a)–(c)), stomach ((d)–(f)), and intestines ((g)–(i)) of juvenile *Epinephelus coioides* after 25-day exposure.

on the digestive capabilities of an organism [39]. Sherwood et al. [40] reported that yellow perch living in lakes subjected to chronic exposure to metals (cadmium, copper and zinc) exhibited greater total energetic costs and lower SGR than fish in reference lakes, despite similar food consumption rates. In the study presented here, diminished growth with either form of Cu exposure was associated with increased FCR and decreased PER. Such results may be disappointing for commercial fish farming due to economic reasons because both Cu-NPs and $CuSO_4$ should be strictly monitored in the aquatic environment in actual fish production. This study also found that the $CuSO_4$ treatment resulted in a lower growth performance than the Cu-NPs treatment; in addition, the highest FCR and the lowest PER were obtained in the $CuSO_4$ treatment, indicating that soluble Cu was more harmful than Cu-NPs to fish growth and food utilization.

During ontogenetic development, marine fish undergo many changes in the structure and function of their digestive system [41, 42]. Digestive enzyme activity (e.g., protease, amylase, and lipase) can be used as an indicator of potential feed utilization and growth differences [39, 43] and to some extent may serve as an indicator of the digestive capacity in relation to the type of feed offered and the properties of aquaculture environments [42, 44]. In our study, the activities of protease, amylase, and lipase found in liver, stomach, and intestine decreased with increasing $CuSO_4$ or Cu-NPs dose, suggesting that either Cu-NPs or $CuSO_4$ exposure decreased digestive capability of juvenile *Epinephelus coioides*.

Table 3: Effects of Cu-NPs and $CuSO_4$ on whole-body fatty acid composition of juvenile *Epinephelus coioides* after 25 days exposure.

Fatty acid	Treatments				
	Control	20 μg Cu L^{-1} as $CuSO_4$	20 μg Cu L^{-1} as Cu-NPs	100 μg Cu L^{-1} as $CuSO_4$	100 μg Cu L^{-1} as Cu-NPs
	% total fatty acids				
C14:0	1.39 ± 0.06^{c}	1.41 ± 0.03^{c}	1.33 ± 0.07^{c}	2.43 ± 0.07^{a}	1.87 ± 0.10^{b}
C15:0	0.25 ± 0.03^{bc}	0.24 ± 0.02^{c}	0.36 ± 0.05^{ab}	0.39 ± 0.06^{a}	0.28 ± 0.04^{abc}
C16:0	18.13 ± 1.31^{a}	18.28 ± 1.33^{a}	17.69 ± 1.56^{a}	20.35 ± 1.44^{a}	18.26 ± 1.20^{a}
C16:1	2.51 ± 0.07^{e}	2.72 ± 0.04^{d}	2.96 ± 0.07^{c}	4.04 ± 0.09^{a}	3.42 ± 0.10^{b}
C17:0	0.36 ± 0.08^{a}	0.38 ± 0.05^{a}	0.37 ± 0.09^{a}	0.49 ± 0.11^{a}	0.36 ± 0.16^{a}
C18:0	8.22 ± 1.22^{a}	8.52 ± 1.75^{a}	8.57 ± 1.42^{a}	8.04 ± 1.11^{a}	8.34 ± 1.38^{a}
C18:1	17.16 ± 0.06^{c}	17.25 ± 0.05^{c}	17.09 ± 0.04^{c}	19.03 ± 0.07^{a}	17.79 ± 0.11^{b}
C18:2	21.77 ± 2.03^{a}	21.03 ± 2.08^{a}	20.45 ± 2.01^{a}	21.17 ± 2.33^{a}	21.99 ± 1.99^{a}
C18:3	1.72 ± 0.04^{b}	1.50 ± 0.06^{c}	1.72 ± 0.08^{b}	1.91 ± 0.09^{b}	2.13 ± 0.10^{a}
C20:0	0.30 ± 0.03^{ab}	0.37 ± 0.03^{a}	0.33 ± 0.02^{ab}	0.35 ± 0.01^{ab}	0.29 ± 0.04^{b}
C20:1	0.62 ± 0.07^{a}	0.68 ± 0.06^{a}	0.72 ± 0.08^{a}	0.73 ± 0.04^{a}	0.71 ± 0.05^{a}
C20:5 EPA	5.48 ± 0.11^{b}	5.97 ± 0.18^{a}	6.25 ± 0.14^{a}	4.00 ± 0.17^{c}	5.31 ± 0.12^{b}
C22:0	0.10 ± 0.01^{c}	0.14 ± 0.09^{c}	0.28 ± 0.02^{b}	0.47 ± 0.05^{a}	0.13 ± 0.01^{c}
C22:5DPA	1.65 ± 0.06^{ab}	1.51 ± 0.06^{b}	1.82 ± 0.09^{a}	1.20 ± 0.11^{c}	1.59 ± 0.12^{ab}
C22:6DHA	17.91 ± 1.02^{a}	17.27 ± 1.22^{ab}	17.19 ± 1.31^{ab}	12.71 ± 1.23^{c}	14.54 ± 1.11^{bc}
∑SFA	28.75 ± 0.39^{b}	29.34 ± 0.47^{b}	28.91 ± 0.46^{b}	32.53 ± 0.41^{a}	29.53 ± 0.42^{b}
∑MUFA	20.29 ± 0.07^{d}	20.65 ± 0.05^{c}	20.76 ± 0.06^{c}	23.80 ± 0.07^{a}	21.92 ± 0.09^{b}
∑PUFA	48.52 ± 0.65^{a}	47.29 ± 0.72^{ab}	47.42 ± 0.73^{ab}	41.00 ± 0.79^{c}	45.56 ± 0.69^{b}
Others	2.44 ± 0.64^{a}	2.72 ± 0.72^{a}	2.91 ± 0.72^{a}	2.67 ± 0.73^{a}	2.88 ± 0.78^{a}

Data are means ± S.E.M ($n = 3$). Significant differences ($P \leq 0.05$) among treatments were indicated by different letters in each row. EPA: eicosapentaenoic acid; DPA: dichloropropanoic acid; DHA: docosahexaenoic acid; ∑SFA: total saturated fatty acids; ∑MUFA: total monounsaturated fatty acids; ∑PUFA: total polyunsaturated fatty acids.

Several hypotheses can explain the negative effect of contaminants on digestive enzyme activities: (i) contaminants can act directly on digestive enzymes activities and/or their synthesis [16]; (ii) contaminants can act negatively on the fish behavior, for example, by decreasing the feeding activity, with indirect consequences on digestive enzymes [43, 45]; (iii) the quantity and the quality of available food may also be impacted by the pollution level, leading to a variation in the activities of digestive enzymes [42]. In this experiment, either Cu-NPs or $CuSO_4$ exposure had no appreciable effect on feeding activity (as judged from the food being eaten within 5 min of presentation regardless of the treatment). Thus, Cu exposure could act directly on digestive enzyme activities and/or synthesis, which contributed to the lower growth performance.

In liver and stomach, the $CuSO_4$ treatment resulted in lower digestive enzyme activities than the Cu-NPs treatment, but the opposite results were recorded for intestine. This result is in accordance with our previous report [6] on Cu accumulation, regarding a negative relationship between Cu accumulation (or Cu exposure concentration) and digestive enzyme activities under either form of Cu exposure. In intestine, the Cu-NPs treatment was associated with higher Cu concentration compared with the $CuSO_4$ treatment [6]; hence, digestive enzyme activities were lower in the Cu-NPs than in $CuSO_4$ treatment.

Shearer [46] reported that concentrations of crude protein and ash varied during the life cycle and were dependent on the fish size. Abdel-Tawwab et al. [47] assumed that changes in body composition such as crude protein and crude lipid contents could be linked to changes in their synthesis, deposition rate in muscle, and/or differential growth rates. Chen et al. [17] and Shearer [46] reported that deposition of lipids was influenced by several factors, but there was a general trend for percentage body lipids to decrease with decreasing fish size, and any decrease in the percentage of lipids was usually accompanied by an increase in percentage of body water. The results of the present study are in general accord with this. It is likely that the proteins and lipids in fish can be used as energy source for detoxification and the maintenance of homeostasis during metal exposure [48, 49]. In the present study, crude proteins and crude lipids decreased with an increase in $CuSO_4$ and Cu-NPs dose, more so in the $CuSO_4$ than Cu-NPs treatment, indicating that Cu ions were more harmful to energy stores (such as crude proteins and crude lipids) and weight gain of *Epinephelus coioides* than Cu-NPs. However, Chen et al. [17] found that waterborne cadmium exposure (0.49 and 0.95 mg L^{-1}) increased lipid content of yellow catfish. In conclusion, lipid metabolism under metal exposure revealed a complex regulatory mechanism and diverse biological functions of

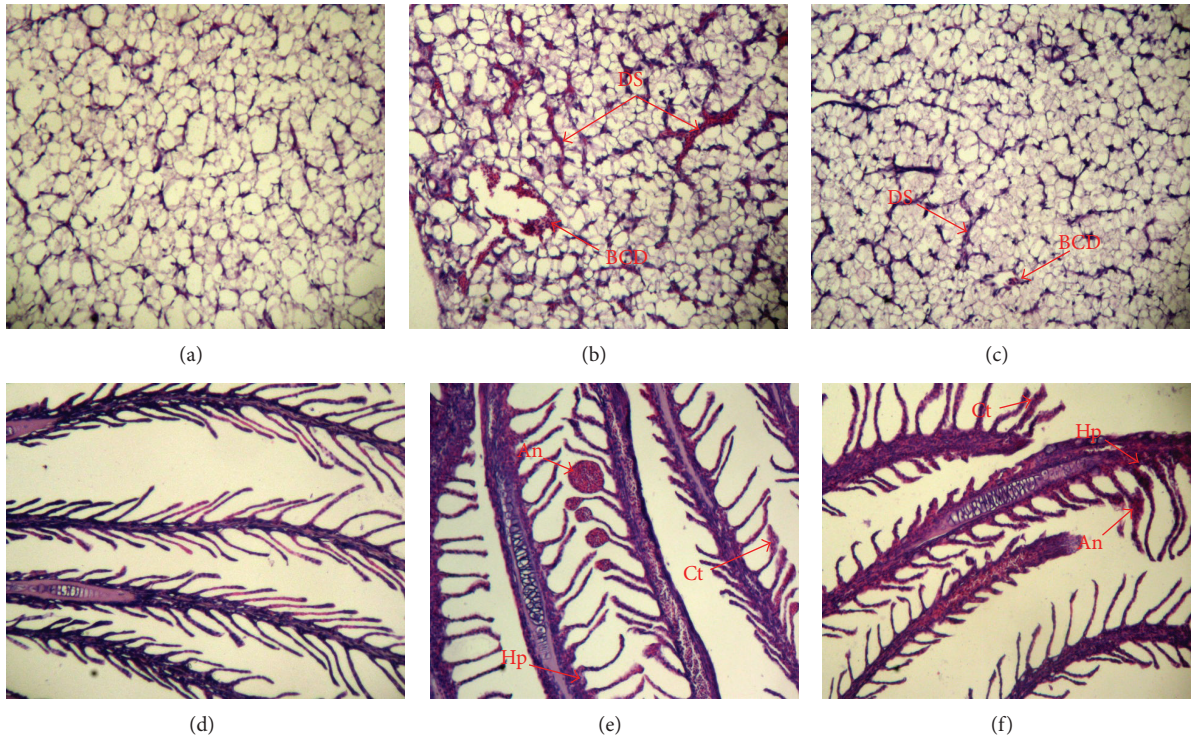

FIGURE 2: Effects of Cu-NPs and $CuSO_4$ on liver and gills morphology of juvenile *Epinephelus coioides* after 25-day exposure. (a) Liver from control, (b) liver from 100 μg Cu L^{-1} as $CuSO_4$, (c) liver from 100 μg Cu L^{-1} as Cu-NPs, (d) gills from control, (e) gills from 100 μg Cu L^{-1} as $CuSO_4$, and (f) gills from 100 μg Cu L^{-1} as Cu-NPs. In liver, all treatments showed injuries that include blood cell deposition in veins (BCD) and dilatation of sinusoids (DS). In gills, all treatments showed injuries that include hyperplasia (Hp), aneurism (An), and clubbed tips (Ct). Sections were 7-μm thick and stained with haematoxylin and eosin (H&E, ×100).

different species and organs [17, 50], so further study is needed.

Metals are highly hazardous xenobiotics. However, optimization of the lipid and fatty acid metabolism may promote the adaptation of an organism to the adverse environmental conditions (cf. Fokina et al. [24]). Sáez et al. [23] reported that the fatty acid composition in the whole body of *Gambusia holbrooki* was obviously changed after the treatment with 0.1, 0.17, or 0.25 mg Cu L^{-1} as $CuSO_4$ compared to control. Fokina et al. [24] found that saturated fatty acids (SFA) and monounsaturated fatty acids (MUFA) in gills of mussels decreased significantly after 24 h exposure to 5, 50, or 250 μg soluble Cu L^{-1}, but polyunsaturated fatty acids (PUFA) content in gills increased (primarily a rise in EPA, DHA, and AA acids). Borlongan [51] reported that EPA and DHA were the essential fatty acids for fish, but marine fish may have limited ability to synthesize them. Furthermore, DHA and EPA were closely related to the physiological functions of fish, including the antioxidant, immune, and anti-inflammatory responses, as well as protecting the retina and improving vision [12, 52]. In our study, EPA, DHA, and DPA were significantly influenced by the $CuSO_4$ or Cu-NPs treatment, with the lowest content at 100 μg Cu L^{-1} as $CuSO_4$, indicating that the physiological functions of juvenile *Epinephelus coioides* might be impaired by either form of Cu treatment, even though more so by Cu ions than Cu-NPs. With an increase in $CuSO_4$ or Cu-NPs dose, $\sum$PUFA decreased, but $\sum$MUFA and $\sum$SFA increased compared to control. These results may be related to the oxidative stress of juvenile *Epinephelus coioides* under either form of Cu exposure [6].

Metals may alter the structure of cell membranes by stimulating lipid peroxidation [53] caused by free oxygen radicals (superoxide ($O_2^{\bullet}$) transforming into higher activity oxyradicals, such as hydroxyl ($OH^{\bullet}$) and singlet oxygen ($^1O_2$)). PUFA may be attacked by these oxyradicals, which may stimulate production of lipid radicals and finally aldehydes (such as MDA), ketones, carboxylic acids, and hydrocarbons [24, 54]. In the study presented here, $\sum$PUFA content decreased and the concentration of MDA increased in juvenile *Epinephelus coioides* (also in our previous study, Wang et al. [6]) compared to control, in accordance to Fokina et al. [24] and D. E. Vance and J. E. Vance [55]. Our study also found the lowest $\sum$PUFA; in contrast, the highest $\sum$MUFA and $\sum$SFA content were found in the treatment with $CuSO_4$ (100 μg Cu L^{-1}), indicating that fatty acid composition of juvenile *Epinephelus coioides* was affected more strongly by Cu ions than Cu-NPs, and Cu ions were more harmful to the cell membranes than Cu-NPs. Therefore, the degree of Cu toxicity to cells was strongly related to the forms of Cu in the marine environment.

Histological alterations observed in liver and gills were indicative of the fish physiological status, revealing the

mechanisms of Cu exposure [56]. Liver and gills were the top two organs for Cu-NPs accumulation in juvenile *Epinephelus coioides* [6]. In the present study, no significant histological evidence of injury was observed in liver and gills in the treatment with 20 μg Cu L^{-1} as $CuSO_4$ or Cu-NPs; nevertheless, marine environments with 20 μg Cu L^{-1} pose a risk of Cu accumulation in juvenile *Epinephelus coioides* [6].

The liver is a central compartment of Cu metabolism in fish [2], and it has been used as a reference for analysis of tissue damage caused by environmental pollutants [57, 58]. In the present study, liver from fish exposed to either $CuSO_4$ or Cu-NPs (100 μg Cu L^{-1}) had blood deposition in veins and dilatation of sinusoids. In other studies, dilatation of sinusoids was one of the most evident signs of liver damage in fish exposed to Cu [8, 10]. Al-Bairuty et al. [2] found that $CuSO_4$ (100 μg Cu L^{-1}) induced some cellular necrosis and changes in the sinusoid space in liver of rainbow trout; exposure to Cu-NPs (100 μg Cu L^{-1}) produced the same type of pathology but affected a greater proportion of liver area and sinusoid space than $CuSO_4$. In contrast, in the study presented here, the dilatation of liver sinusoids was greater in the fish treated with 100 μg Cu L^{-1} as $CuSO_4$ than Cu-NPs. The difference between the two studies could be due to different fish species and different duration of exposure; it should also be kept in mind that differential susceptibility to Cu could exist between freshwater and seawater fish.

Gills are an important organ for both osmoregulation and respiratory gas exchange, and they were the primary target for toxicity of Cu-NPs [59]. In the present study, gills had areas of hyperplasia at the base of the secondary lamellae, clubbed tips at the top of some secondary lamellae, and aneurism in gill filaments at 100 μg Cu L^{-1} as $CuSO_4$ or Cu-NPs. These results were similar with the data recorded by Al-Bairuty et al. [2] and Griffitt et al. [59]. Gomes et al. [3] and Griffitt et al. [59] reported that hyperplasia at the base of the secondary lamellae would increase the diffusion distance for gas exchange, with even a small increase having profound effects on the efficiency of oxygen transfer across gills. Gill injuries from metal exposure were associated with a decrease in arterial oxygen tension, which might be recoverable depending on the extent of the injury (e.g., Zn, Lappivaara et al., [60]). Decreases in arterial oxygen tension in fish exposed to NPs have also been reported [61]. It, therefore, seems probable that the gill injury reported here would cause some hypoxia. Further research on the exercise performance and swimming behaviour of fish exposed to Cu-NPs is required to determine the functional significance of observed gill pathology.

5. Conclusions

The present study confirmed that either Cu-NPs or $CuSO_4$ exposure had obvious toxicity to juvenile *Epinephelus coioides*. Either form of Cu exposure inhibited digestive enzyme activities, which contributed to the diminished growth performance. The crude proteins and crude lipids in fish might be used as energy source for detoxification and the maintenance of homeostasis during Cu-NPs or $CuSO_4$ exposure; thus fish qualities (whole-body composition and fatty acid composition) were obviously affected after either form of Cu exposure. A similar type of pathology was caused by Cu-NPs or Cu metal salts, but greater injuries were found in liver of fish exposed to $CuSO_4$ than Cu-NPs. The studied parameters in fish treated by metals could be used as biomarkers, reflecting the adverse effects of marine environment on fish. Finally, considering the importance of this species for fish culture, a further exploration from genomic, transcriptomic, proteomic, and metabolomics should be provided to elaborate for the diminished growth performance after Cu exposure.

Conflict of Interests

The authors declare that there is no conflict of interests regarding the publication of this paper.

Acknowledgments

The authors are grateful for the financial support of the National Key Projects of Scientific and Technical Support Programs funded by the Ministry of Science and Technology of China (nos. 2011BAD13B09).

References

[1] F. Li, Z. Liang, X. Zheng, W. Zhao, M. Wu, and Z. Wang, "Toxicity of nano-TiO_2 on algae and the site of reactive oxygen species production," *Aquatic Toxicology*, vol. 158, pp. 1–13, 2015.

[2] G. A. Al-Bairuty, B. J. Shaw, R. D. Handy, and T. B. Henry, "Histopathological effects of waterborne copper nanoparticles and copper sulphate on the organs of rainbow trout (*Oncorhynchus mykiss*)," *Aquatic Toxicology*, vol. 126, pp. 104–115, 2013.

[3] T. Gomes, J. P. Pinheiro, I. Cancio, C. G. Pereira, C. Cardoso, and M. J. Bebianno, "Effects of copper nanoparticles exposure in the mussel *Mytilus galloprovincialis*," *Environmental Science & Technology*, vol. 45, no. 21, pp. 9356–9362, 2011.

[4] A. D. Maynard, R. J. Aitken, T. Butz et al., "Safe handling of nanotechnology," *Nature*, vol. 444, no. 7117, pp. 267–269, 2006.

[5] J. Zhao, Z. Wang, X. Liu, X. Xie, K. Zhang, and B. Xing, "Distribution of CuO nanoparticles in juvenile carp (*Cyprinus carpio*) and their potential toxicity," *Journal of Hazardous Materials*, vol. 197, pp. 304–310, 2011.

[6] T. Wang, X. Long, Y. Cheng, Z. Liu, and S. Yan, "The potential toxicity of copper nanoparticles and copper sulphate on juvenile *Epinephelus coioides*," *Aquatic Toxicology*, vol. 152, pp. 96–104, 2014.

[7] B. J. Shaw, G. Al-Bairuty, and R. D. Handy, "Effects of waterborne copper nanoparticles and copper sulphate on rainbow trout, (*Oncorhynchus mykiss*): physiology and accumulation," *Aquatic Toxicology*, vol. 116-117, pp. 90–101, 2012.

[8] B. J. Shaw and R. D. Handy, "Physiological effects of nanoparticles on fish: a comparison of nanometals versus metal ions," *Environment International*, vol. 37, no. 6, pp. 1083–1097, 2011.

[9] Y. Cong, G. T. Banta, H. Selck, D. Berhanu, E. Valsami-Jones, and V. E. Forbes, "Toxicity and bioaccumulation of sediment-associated silver nanoparticles in the estuarine polychaete,

Nereis (Hediste) diversicolor," *Aquatic Toxicology*, vol. 156, pp. 106–115, 2014.

[10] J. M. Arellano, V. Storch, and C. Sarasquete, "Histological changes and copper accumulation in liver and gills of the senegales sole, *Solea senegalensis*," *Ecotoxicology and Environmental Safety*, vol. 44, no. 1, pp. 62–72, 1999.

[11] M. W. Beaumont, E. W. Taylor, and P. J. Butler, "The resting membrane potential of white muscle from brown trout (*Salmo trutta*) exposed to copper in soft, acidic water," *The Journal of Experimental Biology*, vol. 203, no. 14, pp. 2229–2236, 2000.

[12] T. Wang, Y. Cheng, Z. Liu, S. Yan, and X. Long, "Effects of light intensity on growth, immune response, plasma cortisol and fatty acid composition of juvenile *Epinephelus coioides* reared in artificial seawater," *Aquaculture*, vol. 414-415, pp. 135–139, 2013.

[13] L. Burridge, J. S. Weis, F. Cabello, J. Pizarro, and K. Bostick, "Chemical use in salmon aquaculture: a review of current practices and possible environmental effects," *Aquaculture*, vol. 306, no. 1–4, pp. 7–23, 2010.

[14] W. Wang, K. Mai, W. Zhang et al., "Effects of dietary copper on survival, growth and immune response of juvenile abalone, *Haliotis discus hannai* Ino," *Aquaculture*, vol. 297, no. 1–4, pp. 122–127, 2009.

[15] Y. H. Lin, Y. Y. Shie, and S. Y. Shiau, "Dietary copper requirements of juvenile grouper, *Epinephelus malabaricus*," *Aquaculture*, vol. 274, no. 1, pp. 161–165, 2008.

[16] O. Dedourge-Geffard, F. Palais, S. Biagianti-Risbourg, and A. Geffard, "Effects of metals on feeding rate and digestive enzymes in *Gammarus fossarum*: an *in situ* experiment," *Chemosphere*, vol. 77, no. 11, pp. 1569–1576, 2009.

[17] Q.-L. Chen, Z. Luo, Y.-X. Pan et al., "Differential induction of enzymes and genes involved in lipid metabolism in liver and visceral adipose tissue of juvenile yellow catfish *Pelteobagrus fulvidraco* exposed to copper," *Aquatic Toxicology*, vol. 136-137, pp. 72–78, 2013.

[18] D. Lapointe, F. Pierron, and P. Couture, "Individual and combined effects of heat stress and aqueous or dietary copper exposure in fathead minnows (*Pimephales promelas*)," *Aquatic Toxicology*, vol. 104, no. 1-2, pp. 80–85, 2011.

[19] R. D. Handy, "Chronic effects of copper exposure versus endocrine toxicity: two sides of the same toxicological process?" *Comparative Biochemistry and Physiology Part A: Molecular and Integrative Physiology*, vol. 135, no. 1, pp. 25–38, 2003.

[20] M. Mela, I. C. Guiloski, H. B. Doria et al., "Risks of waterborne copper exposure to a cultivated freshwater Neotropical catfish (*Rhamdia quelen*)," *Ecotoxicology and Environmental Safety*, vol. 88, pp. 108–116, 2013.

[21] D. J. H. Phillips, *Quantitative Aquatic Biological Indicators*, Applied Science Publishers, London, UK, 1980.

[22] G. R. Scott and K. A. Sloman, "The effects of environmental pollutants on complex fish behaviour: integrating behavioural and physiological indicators of toxicity," *Aquatic Toxicology*, vol. 68, no. 4, pp. 369–392, 2004.

[23] M. I. Sáez, S. García-Mesa, J. J. Casas et al., "Effect of sublethal concentrations of waterborne copper on lipid peroxidation and enzymatic antioxidant response in *Gambusia holbrooki*," *Environmental Toxicology and Pharmacology*, vol. 36, no. 1, pp. 125–134, 2013.

[24] N. N. Fokina, T. R. Ruokolainen, N. N. Nemova, and I. N. Bakhmet, "Changes of blue mussels *Mytilus edulis* L. lipid composition under cadmium and copper toxic effect," *Biological Trace Element Research*, vol. 154, no. 2, pp. 217–225, 2013.

[25] US-EPA, "Aquatic life ambient freshwater quality criteria-copper (CAS Registry Number 7440-50-8)," U.S. Environmental Protection Agency Office of Water, Office of Science and Technology, Washington, DC, USA, 2007.

[26] T. Sovová, D. Boyle, K. A. Sloman, C. V. Pérez, and R. D. Handy, "Impaired behavioural response to alarm substance in rainbow trout exposed to copper nanoparticles," *Aquatic Toxicology*, vol. 152, pp. 195–204, 2014.

[27] M. M. Bradford, "A rapid and sensitive method for the quantitation of microgram quantities of protein utilizing the principle of protein dye binding," *Analytical Biochemistry*, vol. 72, no. 1-2, pp. 248–254, 1976.

[28] D. Gui, W. Liu, X. Shao, and W. Xu, "Effects of different dietary levels of cottonseed meal protein hydrolysate on growth, digestibility, body composition and serum biochemical indices in crucian carp (*Carassius auratus gibelio*)," *Animal Feed Science and Technology*, vol. 156, no. 3-4, pp. 112–120, 2010.

[29] L. Rongzhu, W. Suhua, X. Guangwei et al., "Effects of acrylonitrile on antioxidant status of different brain regions in rats," *Neurochemistry International*, vol. 55, no. 7, pp. 552–557, 2009.

[30] AOAC, *Official Methods of Analysis of Official Analytical Chemists International*, Association of Official Analytical Chemists, Arlington, Va, USA, 16th edition, 1995.

[31] M. Dubois, K. A. Gilles, J. K. Hamilton, P. A. Rebers, and F. Smith, "Colorimetric method for determination of sugars and related substances," *Analytical Chemistry*, vol. 28, no. 3, pp. 350–356, 1956.

[32] M. Yoshioka, T. Yago, Y. Yoshie-Stark, H. Arakawa, and T. Morinaga, "Effect of high frequency of intermittent light on the growth and fatty acid profile of *Isochrysis galbana*," *Aquaculture*, vol. 338–341, pp. 111–117, 2012.

[33] G. L. Humason, *Animal Tissue Techniques*, W.H. Freeman, New York, NY, USA, 1979.

[34] A. K. Biswas, M. Seoka, Y. Inoue, K. Takii, and H. Kumai, "Photoperiod influences the growth, food intake, feed efficiency and digestibility of red sea bream (*Pagrus major*)," *Aquaculture*, vol. 250, no. 3-4, pp. 666–673, 2005.

[35] S. O. Handeland, A. K. Imsland, and S. O. Stefansson, "The effect of temperature and fish size on growth, feed intake, food conversion efficiency and stomach evacuation rate of Atlantic salmon post-smolts," *Aquaculture*, vol. 283, no. 1–4, pp. 36–42, 2008.

[36] T. T. N. Yen Nhi, N. A. S. Mohd Shazili, and F. Shaharom-Harrison, "Use of cestodes as indicator of heavy-metal pollution," *Experimental Parasitology*, vol. 133, no. 1, pp. 75–79, 2013.

[37] M. Samir and M. Ibrahim, "Assessment of heavy metals pollution in water and sediments and their effect on *Oreochromis niloticus* in the northern Delta Lakes, Egypt," in *Proceedings of the 8th International Symposium on Tilapia in Aquaculture*, pp. 475–490, 2008.

[38] E. A. Shubina, M. A. Nikitin, E. V. Ponomareva, D. V. Goryunov, and O. F. Gritsenko, "Comparative study of genome divergence in salmonids with various rates of genetic isolation," *International Journal of Genomics*, vol. 2013, Article ID 629543, 16 pages, 2013.

[39] P. Gómez-Requeni, F. Bedolla-Cázares, C. Montecchia et al., "Effects of increasing the dietary lipid levels on the growth performance, body composition and digestive enzyme activities of the teleost pejerrey (*Odontesthes bonariensis*)," *Aquaculture*, vol. 416-417, pp. 15–22, 2013.

[40] G. D. Sherwood, J. B. Rasmussen, D. J. Rowan, J. Brodeur, and A. Hontela, "Bioenergetic costs of heavy metal exposure in yellow

perch (*Perca flavescens*): in situ estimates with a radiotracer (^{137}Cs) technique," *Canadian Journal of Fisheries and Aquatic Sciences*, vol. 57, no. 2, pp. 441–450, 2000.

[41] C. L. Cahu and J. L. Z. Infante, "Maturation of the pancreatic and intestinal digestive functions in sea bass (*Dicentrarchus labrax*): effect of weaning with different protein sources," *Fish Physiology and Biochemistry*, vol. 14, no. 6, pp. 431–437, 1995.

[42] C. Suzer, Ş. Saka, and K. Fırat, "Effects of illumination on early life development and digestive enzyme activities in common pandora *Pagellus erythrinus* L. larvae," *Aquaculture*, vol. 260, no. 1–4, pp. 86–93, 2006.

[43] K. Rungruangsak-Torrissen, "Important parameters for growth study," in *Proceedings of the 2nd International Symposium on Cultivation of Salmon II*, p. 14, Bergen, Norway, May 2001.

[44] O. Dedourge-Geffard, L. Charron, C. Hofbauer et al., "Temporal patterns of digestive enzyme activities and feeding rate in gammarids (*Gammarus fossarum*) exposed to inland polluted waters," *Ecotoxicology and Environmental Safety*, vol. 97, pp. 139–146, 2013.

[45] L. Maltby and M. Crane, "Responses of *Gammarus pulex* (Amphipoda, Crustacea) to metalliferous effluents: identification of toxic components and the importance of interpopulation variation," *Environmental Pollution*, vol. 84, no. 1, pp. 45–52, 1994.

[46] K. D. Shearer, "Factors affecting the proximate composition of cultured fishes with emphasis on salmonids," *Aquaculture*, vol. 119, no. 1, pp. 63–88, 1994.

[47] M. Abdel-Tawwab, A. M. Abdel-Rahman, and N. E. M. Ismael, "Evaluation of commercial live bakers' yeast, *Saccharomyces cerevisiae* as a growth and immunity promoter for Fry Nile tilapia, *Oreochromis niloticus* (L.) challenged *in situ* with *Aeromonas hydrophila*," *Aquaculture*, vol. 280, no. 1–4, pp. 185–189, 2008.

[48] S. Stefanni, R. Bettencourt, M. Pinheiro, G. de Moro, L. Bongiorni, and A. Pallavicini, "Transcriptome of the deep-sea black scabbardfish, *Aphanopus carbo* (Perciformes: Trichiuridae): tissue-specific expression patterns and candidate genes associated to depth adaptation," *International Journal of Genomics*, vol. 2014, Article ID 267482, 21 pages, 2014.

[49] J.-L. Zheng, Z. Luo, C.-X. Liu et al., "Differential effects of acute and chronic zinc (Zn) exposure on hepatic lipid deposition and metabolism in yellow catfish *Pelteobagrus fulvidraco*," *Aquatic Toxicology*, vol. 132-133, pp. 173–181, 2013.

[50] F. Pierron, M. Baudrimont, A. Bossy et al., "Impairment of lipid storage by cadmium in the European eel (*Anguilla anguilla*)," *Aquatic Toxicology*, vol. 81, no. 3, pp. 304–311, 2007.

[51] I. G. Borlongan, "The essential fatty acid requirement of milkfish (*Chanos chanos* Forsskal)," *Fish Physiology and Biochemistry*, vol. 9, no. 5-6, pp. 401–407, 1992.

[52] P. Hung, S. Kaku, S.-I. Yunoki et al., "Dietary effect of EPA-rich and DHA-rich fish oils on the immune function of Sprague-Dawley rats," *Bioscience, Biotechnology and Biochemistry*, vol. 63, no. 1, pp. 135–140, 1999.

[53] R. F. Fornazier, R. R. Ferreira, A. P. Vitória, S. M. G. Molina, P. J. Lea, and R. A. Azevedo, "Effects of cadmium on antioxidant enzyme activities in sugar cane," *Biologia Plantarum*, vol. 45, no. 1, pp. 91–97, 2002.

[54] A. Liavonchanka and I. Feussner, "Lipoxygenases: occurrence, functions and catalysis," *Journal of Plant Physiology*, vol. 163, no. 3, pp. 348–357, 2006.

[55] D. E. Vance and J. E. Vance, *Biochemistry of Lipids, Lipoproteins and Membranes*, Elsevier, 4th edition, 2002.

[56] C. Gravato, M. Teles, M. Oliveira, and M. A. Santos, "Oxidative stress, liver biotransformation and genotoxic effects induced by copper in *Anguilla anguilla* L.—the influence of pre-exposure to β-naphthoflavone," *Chemosphere*, vol. 65, no. 10, pp. 1821–1830, 2006.

[57] A. F. Amaral, N. Alvarado, I. Marigomez, R. Cunha, K. Hylland, and M. Soto, "Autometallography and metallothionein immunohistochemistry in hepatocytes of turbot (*Scophthalmus maximus* L.) after exposure to cadmium and depuration treatment," *Biomarkers*, vol. 7, no. 6, pp. 491–500, 2002.

[58] R. Cortés, M. Teles, R. Trídico, L. Acerete, and L. Tort, "Effects of cortisol administered through slow-release implants on innate immune responses in rainbow trout (*Oncorhynchus mykiss*)," *International Journal of Genomics*, vol. 2013, Article ID 619714, 7 pages, 2013.

[59] R. J. Griffitt, R. Weil, K. A. Hyndman et al., "Exposure to copper nanoparticles causes gill injury and acute lethality in zebrafish (*Danio rerio*)," *Environmental Science and Technology*, vol. 41, no. 23, pp. 8178–8186, 2007.

[60] J. Lappivaara, M. Nikinmaa, and H. Tuurala, "Arterial oxygen tension and the structure of the secondary lamellae of the gills in rainbow trout (*Oncorhynchus mykiss*) after acute exposure to zinc and during recovery," *Aquatic Toxicology*, vol. 32, no. 4, pp. 321–331, 1995.

[61] D. Boyle, G. A. Al-Bairuty, C. S. Ramsden, K. A. Sloman, T. B. Henry, and R. D. Handy, "Subtle alterations in swimming speed distributions of rainbow trout exposed to titanium dioxide nanoparticles are associated with gill rather than brain injury," *Aquatic Toxicology*, vol. 126, pp. 116–127, 2013.

Research Article

Response of Spatial Patterns of Denitrifying Bacteria Communities to Water Properties in the Stream Inlets at Dianchi Lake, China

Neng Yi,[1,2] Yan Gao,[1,2] Zhenhua Zhang,[1,2] Yan Wang,[1,2] Xinhong Liu,[1,2] Li Zhang,[1,2] and Shaohua Yan[1,2]

[1] *Institute of Agricultural Resources and Environment, Jiangsu Academy of Agricultural Sciences, 50 Zhongling Street, Nanjing 210014, China*
[2] *Key Lab of Food Quality and Safety of Jiangsu Province, State Key Laboratory Breeding Base, 50 Zhongling Street, Nanjing 210014, China*

Correspondence should be addressed to Shaohua Yan; shyan@jaas.ac.cn

Received 3 July 2015; Accepted 16 August 2015

Academic Editor: Marián Brestič

Streams are an important sink for anthropogenic N owing to their hydrological connections with terrestrial systems, but main factors influencing the community structure and abundance of denitrifiers in stream water remain unclear. To elucidate the potential impact of varying water properties of different streams on denitrifiers, the abundance and community of three denitrifying genes coding for nitrite (*nirK, nirS*) and nitrous oxide (*nosZ*) reductase were investigated in 11 streams inlets at the north part of Dianchi Lake. The DGGE results showed the significant pairwise differences in community structure of *nirK, nirS*, and *nosZ* genes among different streams. The results of redundancy analysis (RDA) confirmed that nitrogen and phosphorus concentrations, pH, and temperature in waters were the main environmental factors leading to a significant alteration in the community structure of denitrifiers among different streams. The denitrifying community size was assessed by quantitative PCR (*q*PCR) of the *nirS, nirK*, and *nosZ* genes. The abundance of *nirK, nirS*, and *nosZ* was positively associated with concentrations of total N (TN) and PO_4^{3-} ($p < 0.001$). The difference in spatial patterns between *nirK* and *nirS* community diversity, in combination with the spatial distribution of the *nirS/nirK* ratio, indicated the occurrence of habitat selection for these two types of denitrifiers in the different streams. The results indicated that the varying of N species and PO_4^{3-} together with pH and temperature would be the main factors shaping the community structure of denitrifiers. Meanwhile, the levels of N in water, together with PO_4^{3-}, tend to affect the abundance of denitrifiers.

1. Introduction

It has been commonly observed that a large but variable proportion of aquatic N removal occurred in freshwater ecosystems, including groundwater, streams, lakes, and wetlands [1, 2]. The variation in microbial abundance and community structure among different aquatic ecosystems has been recognized as one of the most important factors which contributed to the changing of N biogeochemical cycling process in different aquatic ecosystems [3, 4]. Therefore, studying the spatial patterns of functional microbial guilds can help us to understand the relationships between microbial community ecology and the related ecosystem functions. Canonical denitrification has been generally considered as the main mechanism for permanent removal of N from aquatic ecosystem through returning of N in water to the atmosphere in the form of N_2O and N_2, although some alternative pathway, such as anaerobic ammonium oxidation (Anammox), has been discovered [5]. Denitrification in aquatic ecosystems has been widely found removing large proportion of the total N inputs to watersheds and thus providing a valuable ecosystem service by alleviating the impact of increased human N inputs [1]. Several studies have reported that the function of denitrifying bacteria communities was correlated with their abundance and community structure [6–8]. Hence, studying the variation in

Table 1: Water properties of the streams at Dianchi Lake (mean ± SD).

Streams	NO_3^- (mg L^{-1})	TN (mg L^{-1})	PO_4^{3-} (mg L^{-1})	TP (mg L^{-1})	ORP (mg L^{-1})	DO (mg L^{-1})	pH	T (°C)
XBX	4.79 ± 0.39	7.44 ± 0.19	0.33 ± 0.01	0.39 ± 0.01	18.45 ± 1.63	2.15 ± 0.15	7.83 ± 0.06	19.60 ± 0.00
H	0.16 ± 0.02	23.69 ± 0.79	2.07 ± 0.07	2.10 ± 0.07	−156.80 ± 29.56	0.20 ± 0.10	7.90 ± 0.01	18.80 ± 0.00
XB	0.56 ± 0.14	6.35 ± 1.21	0.39 ± 0.01	0.45 ± 0.03	−46.55 ± 9.83	0.55 ± 0.25	7.78 ± 0.06	17.95 ± 0.05
YA	8.99 ± 0.00	15.08 ± 0.50	0.22 ± 0.01	0.28 ± 0.01	−15.95 ± 4.03	1.05 ± 0.35	7.85 ± 0.07	17.60 ± 0.10
JJ	0.43 ± 0.02	8.14 ± 0.54	0.36 ± 0.01	0.41 ± 0.01	59.55 ± 2.19	1.30 ± 0.10	7.90 ± 0.01	19.50 ± 0.00
GPG	0.08 ± 0.02	23.66 ± 0.16	1.78 ± 0.11	1.86 ± 0.04	−225.75 ± 12.80	0.20 ± 0.10	7.83 ± 0.00	17.90 ± 0.00
PLJ	5.86 ± 0.01	8.08 ± 0.19	0.16 ± 0.01	0.28 ± 0.00	48.05 ± 0.78	2.80 ± 0.00	8.03 ± 0.00	19.70 ± 0.00
XBH	5.92 ± 0.25	8.60 ± 0.19	0.13 ± 0.01	0.19 ± 0.01	37.53 ± 1.34	0.60 ± 0.00	7.77 ± 0.00	21.60 ± 0.00
CF	5.09 ± 0.03	8.63 ± 0.10	0.10 ± 0.01	0.13 ± 0.01	49.50 ± 3.25	3.80 ± 0.10	7.90 ± 0.06	21.75 ± 0.05
DG	12.00 ± 0.67	12.91 ± 0.62	0.06 ± 0.00	0.12 ± 0.02	43.90 ± 0.28	2.70 ± 0.13	7.56 ± 0.04	22.15 ± 0.05
XYL	0.08 ± 0.02	21.40 ± 2.78	0.98 ± 0.09	2.52 ± 0.16	−246.75 ± 17.18	0.45 ± 0.05	7.78 ± 0.02	21.55 ± 0.05

Stream names: XBX = Xinbaoxiang, H = Haihe, XB = Xiaba, YA = Yaoan, JJ = Jinjia, GPG = Guangpugou, PLJ = Panlongjiang, XBH = Xibahe, CF = Chuangfang, DG = Daguang, and XYL = Xinyunliang.
(1) TSN = total soluble nitrogen.

abundance and structure of denitrifying community will help to understand the variable denitrification potential as well as variable proportion of aquatic N removal that occurred among different aquatic ecosystems.

Streams are an important sink for anthropogenic N owing to their hydrological connections with terrestrial systems. The microbial communities in streams adapted to changes in the concentration and makeup of organic matter [9] and nutrients [10, 11]. Some recent studies have been concentrated on the link between the freshwater bacterioplankton dynamics and the environmental changes [12]. Numerous studies have reported that denitrifying bacteria can be affected by physical and chemical parameters such as pH, temperature (T), dissolved oxygen (DO), and N forms [12, 13] in series of laboratory incubation experiments. However, it is hard to identify the factors driving the variation in abundance and community structure of denitrifying bacteria in complicated aquatic ecosystems. Nowadays, functional markers include nitrite reductase (*nirK* and *nirS*) and nitrous oxide reductase (*nosZ*) genes have been frequently used to analyze the diversity and abundance of denitrifying bacteria community in the processes of denitrification and their response to the changing of environmental factors [8, 14–18]. Based on the analysis of these functional markers, recent research has demonstrated that the variation in the assemblage of *nirS*, *nirK*, and *nosZ* populations in soil was closely related to temperature, pH, and DO [19–21]. Furthermore, the abundance of these denitrifies varied in response to different nitrogen concentrations in soil, and a differential response of denitrifies communities structure to environmental gradients has also been reported [22]. These mean that functional genes of *nirS*, *nirK*, and *nosZ* could be sensitive indicators when studying the response of denitrifier community to variation of environmental gradients in complicated ecosystems. So far, limited studies incorporated the phosphorus concentration into the analysis of environmental gradient resulting in denitrifies community change in freshwater ecosystems [17], despite phosphorus being a vital element influencing microbial spatial patterns [23]. Therefore, in this study, we will focus on the environmental factors that have been reported to be closely related with denitrification and the variation of denitrifier community (e.g., nitrogen forms, nitrogen concentration, pH, water temperature, and DO) and the less addressed factor such as phosphorus concentration.

Dianchi Lake is the sixth largest freshwater lake in China. There are 35 streams radially flowing into the Dianchi Lake, which is a shallow plateau freshwater lake in the south-west of Kunming city, Yunnan province of China. Streams around the lake serve as ecohydrological channels that impose anthropogenic stress on the lake ecosystem and eventually cause water quality deterioration [24]. Due to the sedimentation, land reclamation, and excessive pollution, the water quality of 35 streams continued degrading from the level of drinking water quality in 1975 to the level of landscape-use only water in 2009 [24, 25]. The water quality in the north part of Dianchi Lake is the worst grade of national water quality standard. There were relatively higher NH_4^+ and NO_3^- concentration even up to 12–20 mg/L in some rivers. The pH values of all sites were alkalescent [24, 26]. More than 6 sewage treatment plants (STPs) had been in operation near 11 streams in the north lake side in recent years. The effluents from the STPs are a major cause of degraded water quality in the down streams within the basin. Generally, effluents are characterized by high concentrations of nitrogen and organic matter [27]. Along with high concentration of nitrogen, many microorganisms especially denitrifying bacterial community entrained in effluents were domesticated [28].

In the present study, in order to address the response of spatial patterns of denitrifying communities to variation in environmental factors among different streams, we investigated the water properties and the abundance and diversity of denitrifying bacterial community in 11 stream inlets with different pollution sources, some of which were receiving effluents from different sewage treatment plants in the north part of Dianchi Lake, an eutrophic lake located in Southwest China (Table 1). We hypothesized that the variation in pollution sources and effluents types, such as the main eutrophication elements of N and P, may modulate

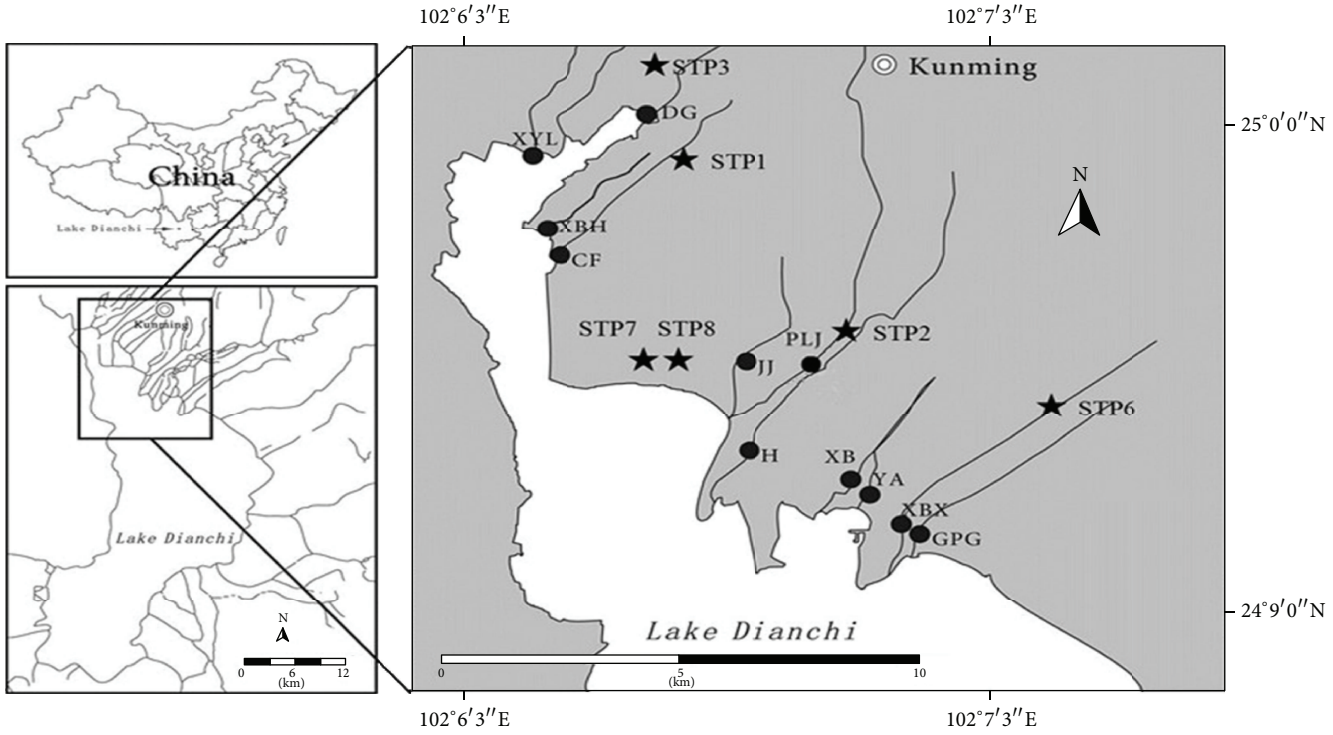

Figure 1: Sampling sites in stream inlets of Dianchi Lake. Black dots (●) are sampling sites; pentagrams (★) are sewage treatment plants (STPs). Stream names: XBX = Xinbaoxiang, H = Haihe, XB = Xiaba, YA = Yaoan, JJ = Jinjia, GPG = Guangpugou, PLJ = Panlongjiang, XBH = Xibahe, CF = Chuangfang, DG = Daguang, and XYL = Xinyunling.

the communities of denitrifiers, which may further lead to changes in the biogeochemical cycling of N in the streams and lake. The results would also provide valuable information on how the abundance and diversities of denitrifiers in various streams responded to the variation of water properties such as nitrogen forms, nitrogen concentration, phosphorus concentration, pH, water temperature, and DO. It was also expected to shed some lights on understanding the variable denitrification potential as well as variable proportion of aquatic N removal that occurred among different streams.

2. Materials and Methods

2.1. Site Description, Sampling, and Water Properties. There are 11 streams around Dianchi Lake located from 24°9′ to 25°0′ latitude and 102°6′ to 102°7′ longitude that were investigated (Figure 1).

Dissolved oxygen (DO), oxidation reduction potential (ORP), pH, and water temperature were measured in situ using portable meter (YSI ProPlus, USA) at all sampling sites. Three replicates of surface water (0–0.5 m) samples were randomly collected at three sampling locations from each sampling site of eleven streams using a cylinder sampler on 25 September 2012. Basically, the three sampling locations at each sampling site were from the upper, middle, and lower sections of a stream. One-liter water samples were reserved at −4°C with addition of Hgcl2/acid solution for chemical analysis, and two-liter water samples were filtered immediately for further molecular DNA extraction after being transported to laboratory. The concentrations of total nitrogen (TN), total phosphorus (TP), nitrate (NO_3^-), and phosphates (PO_4^{3-}) in the water samples were analyzed using a SEAL AutoAnalyzer 3 (SEAL Analytical Co., Hampshire, UK).

2.2. DNA Extraction. All water samples were kept in an ice box, transferred to the laboratory, and filtered through a 5 μm pore size sterilized filter to remove the impurities. The resultant filtrate of each sample (500 mL) was filtered through 0.22 μm Millipore membrane filters using a vacuum air pump and the membranes were stored at −80°C for DNA extraction. The membranes were cut into pieces with sterilized scissors and used immediately for DNA extraction. DNA extractions were performed using an E.Z.N.A. Water DNA Kit (OMEGA Bio-Tek Inc., Doraville, GA, USA) by following the manufacturer's instructions. The DNA samples were stored in a −20°C freezer until use.

2.3. Real-Time Polymerase Chain Reaction Assay. The plasmids containing *nirK*, *nirS*, and *nosZ* fragments from environmental samples were used to create standard curve. The PCR amplified products were cloned into vector pMD19-T using the pMD19-T vector system I kit according to the manufacturer's instructions (Takara, Dalian, China). The recombinant plasmids were inoculated into LB broth with ampicillin and incubated at 37°C overnight. Plasmid DNA was then extracted from the correct insert clones of each

Table 2: Primers and thermal profiles used for the qPCR and DGGE.

Target gene	primers	Thermal profile
qPCR	*nosZ*-F [29] *nosZ*1622R [29]	qPCR: 94°C/2 min; 6 cycles of 94°C/30 s, 57°C/30 s (−1°C/cycle), and 72°C/45 s; 30 cycles of 94°C/30 s, 52°C/30 s, and 72°C/45 s.
DGGE	*nosZ*-F [29] *nosZ*1622-GC* [30]	DGGE: 94°C/2 min; 10 cycles of 94°C/30 s, 58°C/30 s (−0.5°C/cycle), and 72°C/60 s; 30 cycles of 94°C/30 s, 53°C/30 s, and 72°C/60 s; 72°C/10 min.
qPCR	Cd3aF [31] R3cd [31]	q-PCR: 94°C/2 min; 6 cycles of 94°C/30 s, 57°C/30 s (−1°C/cycle), and 72°C/45 s; 30 cycles of 94°C/30 s, 52°C/30 s, and 72°C/45 s.
DGGE	Cd3aF [31] R3cd-GC* [32]	DGGE: 94°C/2 min; 10 cycles of 94°C/30 s, 57°C/30 s (−0.5°C/cycle), and 72°C/45 s; 30 cycles of 94°C/30 s, 52°C/30 s, and 72°C/45 s; 72°C/10 min.
qPCR	F1aCu [33] R3Cu [33]	q-PCR: 95°C/3 min; 6 cycles of 95°C/30 s, 63°C/30 s (−1°C/cycle), and 72°C/30 s; 32 cycles of 95°C/30 s, 58°C/30 s, and 72°C/30 s.
DGGE	F1aCu [33] R3Cu-GC* [33]	DGGE: 95°C/3 min; 32 cycles of 95°C/30 s, 58°C/30 s, and 72°C/45 s; 72°C/10 m.

*(GGCGGCGCGCCGCCCGCCCCGCCCCCGTCGCCC) was attached to the 5′ end of the primers.

target gene using the E.Z.N.A. Plasmid Mini Kit II (OMEGA Bio-Tek Inc., Doraville, GA, USA) according to the manufacturer's instructions. The plasmids DNA concentration was determined by NanoVue spectrophotometer (GE Healthcare Europe, Munich, Germany), and then the copy numbers of target genes were calculated. Tenfold serial dilutions of a known copy number of the plasmid DNA were subjected to real-time PCR assay in triplicate to generate an external standard curve.

The real-time polymerase chain reaction (qPCR) was performed on ABI 7500 real-time system (Life technologies, USA) to assess gene abundance. Amplification was performed in a 20-μL reaction mixture using SYBR Premix Ex Taq as PCR Kit provided by the suppliers (Takara bio, Dalian, China). The DNA diluted template corresponding to 1–10 ng of total DNA extracts was used in each reaction mixture. The primers and procedures used to amplify each target gene when performing real-time PCR were listed in Table 2. Data was analyzed using the 7500 software (version 2.0.6, Life technologies, USA). The parameter Ct (threshold cycle) was determined as the cycle number at which a statistically significant increase in the reporter fluorescence was detected. Standard curves for real-time PCR assays were created according to the method described by Henry et al. [34].

2.4. PCR Amplification Denaturing Gradient Gel Electrophoresis Analysis. The community structures of *nirK*, *nirS,* and *nosZ* genes were analyzed by denaturing gradient gel electrophoresis (DGGE). The amplification was performed in 50-μL reaction mixtures including 1x PCR buffer, 400 μmol/L of each dNTP, and 2.5 U hot star Taq DNA polymerase (Takara Bio, Otsu, Shiga, Japan) plus primers (Table 2).

The amplified products were pooled and resolved on DGGE gels using a Dcode system (Bio-Rad Laboratories Inc. Hercules, USA). PCR samples (50 μL) containing approximately equal amounts of PCR amplicons were loaded onto the 1 mm thick 8% (w/v) polyacrylamide (37.5 : 1, acrylamide : bisacrylamide) gels in 1x TAE buffer (40 mM Tris-acetate and 1 mM EDTA) with denaturing gradients of 50–75% for 15 h (*nirS*), 50–70% for 12 h (*nirK*), and 50–70% (*nosZ*) (100% denaturant contains 7 mol/L urea and 40% (v/v) formamide) for 15 h at 100 V and 60°C, respectively. After being stained with silver nitrate according to the protocol [35], polaroid pictures of the DGGE gels were scanned using an EPSON (Perfection V700 Photo) scanner and stored as TIFF files and digitized and then analyzed with the Quantity One software (version 4.5, Bio-Rad, USA).

2.5. Data Analysis. Three replicates were used in all parameter analysis. Data were presented as the mean values of triplicates and the maximum difference (mean ± SD) among triplicate results was 5%. One way analysis of variance (ANOVA) was performed to test whether there were any significant differences among the means at the 95% confidence level. Potential relationships between all denitrifying bacteria abundance and environmental data sets were tested by Pearson correlation analysis. All data were analysed using SPSS software.

DGGE banding profiles for *nirS*, *nirK,* and *nosZ* communities were digitized after average background subtraction for entire gels. Band position and intensity date for each sample were exported to an excel spreadsheet prior to further statistical analyses. The relative intensity of a specific band was transformed according to the sum of intensities of all bands in a pattern [36]. Redundancy analysis (RDA) for community ordination was conducted using CANOCO (version 4.5, Centre for Biometry, Wageningen, The Netherlands) for Windows using relative band intensity data obtained from the Quantity One analysis [37, 38]. Among all environmental variables, eight parameters, including water temperature, pH, DO, oxidation reduction potential nitrate, total nitrogen, total phosphorus (TP), and phosphates (PO_4^{3-}), were selected to perform RDA by Monte Carlo reduced model tests with 499 unrestricted permutations to statistically evaluate the significance of the first canonical axis and of all canonical axes together. Statistical significance was kept at $p < 0.05$ for all analyses (Table 4).

Table 3: Shannon index (H) and richness (S) values of *nirK*, *nirS*, and *nosZ* genes.

Streams	*nirK*		*nirS*		*nosZ*	
	S	*H*	*S*	*H*	*S*	*H*
XBX	11.00 ± 1.00cd	2.09 ± 0.12b	16.00 ± 1.00b	2.61 ± 0.36ab	14.00 ± 1.00bc	2.56 ± 0.10a
H	13.33 ± 1.53bc	2.33 ± 0.27ab	14.33 ± 0.58b	2.47 ± 0.29ab	11.00 ± 1.00def	1.95 ± 0.19a
XB	11.33 ± 0.58cd	2.20 ± 0.15ab	18.00 ± 1.00a	2.50 ± 0.20a	12.67 ± 0.58cde	2.34 ± 0.22a
YA	11.00 ± 0.00cd	2.10 ± 0.06b	14.33 ± 0.58b	2.42 ± 0.25ab	15.33 ± 1.15ab	2.55 ± 0.21a
JJ	17.33 ± 1.158a	2.64 ± 0.14a	10.00 ± 1.00cd	1.92 ± 0.19b	10.33 ± 0.58ef	2.09 ± 0.25a
GPG	15.00 ± 0.00ab	2.47 ± 0.17ab	15.33 ± 0.58b	2.43 ± 0.31ab	17.33 ± 0.58a	2.60 ± 0.18a
PLJ	13.00 ± 1.00bc	2.22 ± 0.11ab	8.33 ± 1.53d	1.92 ± 0.07ab	9.67 ± 0.58f	1.94 ± 0.29a
XBH	15.00 ± 1.00ab	2.36 ± 0.09ab	15.33 ± 1.15b	2.50 ± 0.40ab	14.67 ± 0.58bc	2.56 ± 0.15a
CF	11.33 ± 1.15cd	2.34 ± 0.19ab	10.33 ± 1.15cd	2.26 ± 0.28ab	13.33 ± 1.15bcd	2.39 ± 0.25a
DG	11.00 ± 1.00cd	2.32 ± 0.33ab	13.67 ± 0.58bc	2.37 ± 0.16ab	12.00 ± 1.00cde	2.43 ± 0.32a
XYL	9.67 ± 1.52d	2.08 ± 0.06b	8.00 ± 0.00cd	1.91 ± 0.07ab	8.67 ± 0.58f	1.89 ± 0.19a

Stream names: XBX = Xinbaoxiang, H = Haihe, XB = Xiaba, YA = Yaoan, JJ = Jinjia, GPG = Guangpugou, PLJ = Panlongjiang, XBH = Xibahe, CF = Chuangfang, DG = Daguang, and XYL = Xinyunliang. The different letters indicate significant differences ($p < 0.05$)

Table 4: Eigen values, F values, and p values obtained from the partial RDAs testing the influence of the significant parameters on the denitrifying bacterial community composition*.

Samples	Environmental variables	Eigen value	% variation explains solely	F value	p value
nirK	PO_4^{3-}	0.21	21	2.37	0.002
	TN	0.19	19	1.32	0.190
	pH	0.10	10	1.12	0.398
	All the above together	0.80			
nirS	pH	0.10	10	1.20	0.298
	Temperature	0.11	11	1.20	0.360
	DO	0.08	8	1.10	0.388
	All the above together	0.77			
nosZ	Temperature	0.17	17	1.83	0.048
	NO_3^-	0.13	13	1.17	0.060
	TP	0.08	8	1.31	0.278
	All the above together	0.83			

*Only keeping the first three significant parameters in models of RDAs based on Monte Carlo permutation ($n = 499$). Sum of all Eigen values for both partial RDAs was 1.000.

3. Results

3.1. Spatial Patterns of Structure and Size of Denitrifier Communities. All digitized data of the three replicates were used in statistics analysis. The Shannon index (H) of *nirK*, *nirS*, and *nosZ* calculated from DGGE gels ranged from 2.08 to 2.64, 1.73 to 2.80, and 1.89 to 2.60, respectively. The significant differences among them were observed statistically ($p < 0.05$). There were relative lower richness and diversity of *nirK*, *nirS*, and *nosZ* in Xinyunliang stream (Table 3), while the highest of the Shannon values and richness of *nirK*, *nirS*, and *nosZ* occurred in Guangpugou stream.

The results of qPCR showed that the abundance of *nirS*, *nirK*, and *nosZ* gene copies per mL water ranged from 2.79×10^3 to 1.20×10^5, 3.23×10^3 to 1.76×10^5, and 8.66×10^2 to 1.90×10^5, respectively. The abundance of *nirK*, *nirS*, and *nosZ* denitrifiers in Xinbaoxiang, Daguan, Chuanfang, and Panlongjiang streams was relatively stable and low. The results of *nirK*, *nirS*, and *nosZ* genes abundance in group Xiaba and Yaoan streams were consistent. The absolute abundance of denitrification genes in the other five streams varied widely (Figure 2). These results indicated that different pollution source would influence the abundance of denitrifiers in streams. The denitrifiers (*nirK*, *nirS*, and *nosZ*) abundance of the water samples in Haihe stream and Guangpugou stream was significantly higher than that in other stream samples ($p < 0.05$). The abundance of *nirK*- and *nosZ*-type denitrifiers had similar trends in the streams, with higher number in Haihe stream and Guangpugou stream and intermediate levels in Xinbaoxiang, Xiaba, Yaoan, Jinjia, Panlongjiang, and Xiaba streams but lower levels in Chuangfang stream, Daguang stream, and Xinyunliang stream. However, the *nirS*-type abundance in all sites did not totally follow this trend and no significant differences were detected in qPCR data among Haihe, Guangpugou, and Daguang streams.

Ratios of *nosZ* abundance to the abundance of *nirK* + *nirS* for all samples varied widely. The highest *nosZ*/(*nirK* + *nirS*) ratio occurred in Haihe stream (0.64), the lowest

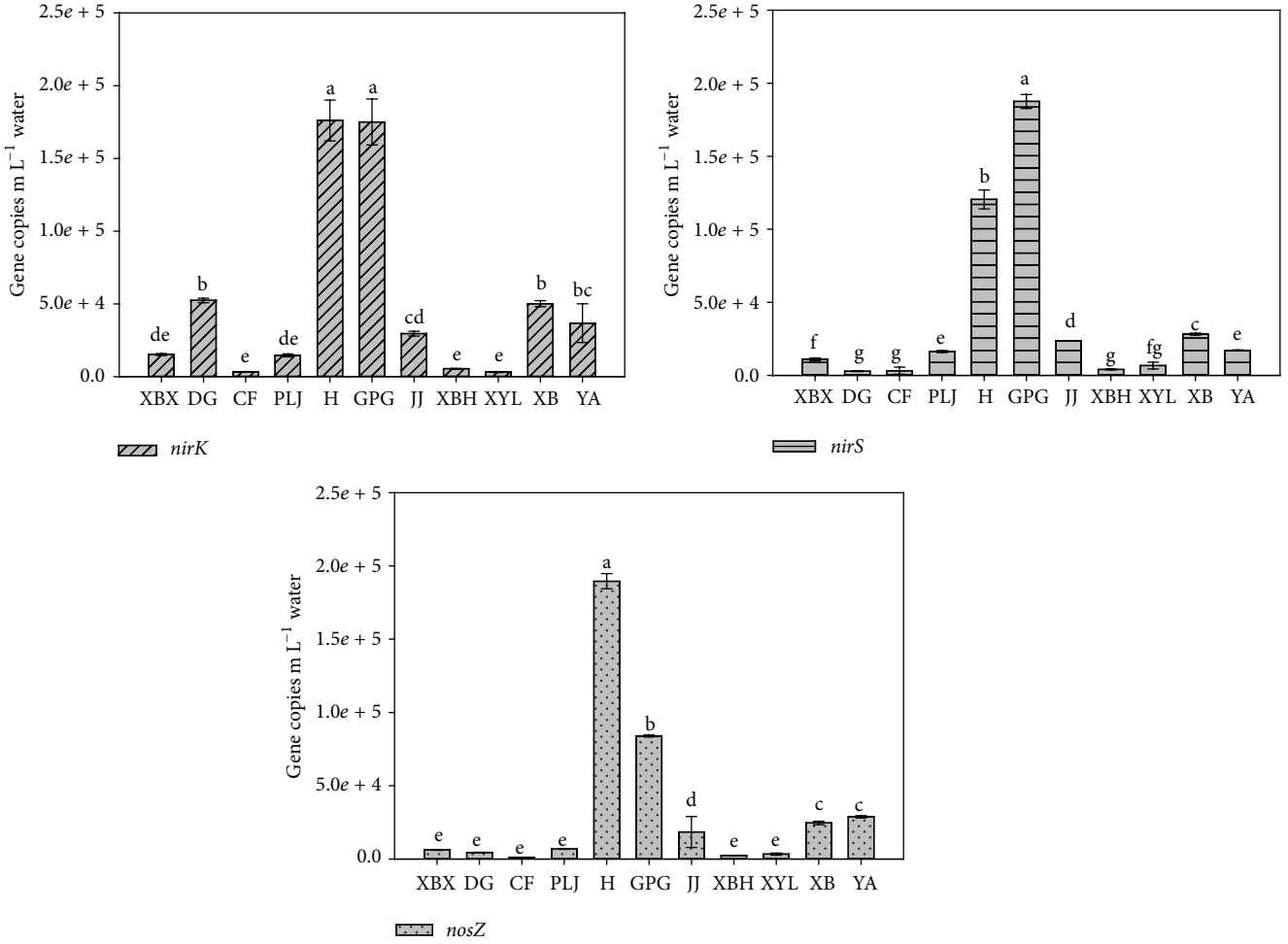

Figure 2: Abundance of *nirS*, *nirK*, and *nosZ* genes in the water samples. Error bars indicate standard deviations ($n = 3$). The different letters indicate significant differences ($p < 0.05$). Stream names: XBX = Xinbaoxiang, H = Haihe, XB = Xiaba, YA = Yaoan, JJ = Jinjia, GPG = Guangpugou, PLJ = Panlongjiang, XBH = Xibahe, CF = Chuangfang, DG = Daguang, and XYL = Xinyunling.

nosZ/(*nirK* + *nirS*) ratio occurred in Daguang stream (0.08), and the *nosZ*/(*nirK* + *nirS*) ratios in the other streams were similar and ranged from 0.13 to 0.35. Ratios of *nirK* abundance *nirK*/*nirS* to *nirS* abundance in different streams were also different. The highest (*nirK*/*nirS*) ratio occurred in Daguang stream (18.79), the lowest (*nirK*/*nirS*) ratios occurred in Xinyunliang stream (0.48), and the (*nirK*/*nirS*) ratios in the other streams were between 0.90 and 2.15. These results implied that the abundance of *nirS* was not always greater than that of *nirK* in stream inlet water column.

3.2. Water Parameters Controlling Denitrifier Communities. In order to determine to what extent the eight environmental properties affected the three types of denitrifying genes on their community compositions, DGGE fingerprints were analyzed by redundancy analysis. The results showed that PO_4^{3-}, pH, and water temperature were the relatively important environmental parameters for denitrifiers (Table 5). For *nirK*-type denitrifier, PO_4^{3-}, TN, and pH explained 50% variations of microbial communities. Variation partitioning analysis showed that PO_4^{3-}, TN, and pH separately explained 21% ($p = 0.002$), 19% ($p = 0.190$), and 10% ($p = 0.398$) of the variation, respectively. The analysis did not reveal significant relationship between *nirS*-type denitrifier communities and any environmental parameters. For *nosZ*-type denitrifier, temperature (17%, $p = 0.048$), NO_3^- (13%, $p = 0.06$), and total P (8%, $p = 0.278$) explained 38% variations of microbial communities.

nirS abundance was significantly and positively correlated with *nirK* and *nosZ* abundance. *nirK* abundance was significantly correlated in a positive direction with *nosZ* abundance. These results suggested that all of three denitrifiers can interact with each other. The abundance diversification of *nirK*, *nirS*, and *nosZ* was strongly and positively associated with TN and PO_4^{3-} ($p < 0.001$). The analysis did not reveal significant relationship between pH and any denitrifying bacteria gene abundance. All relationships between *nirS*, *nirK*, and *nosZ* genes abundance and chemical variables were positively correlated except for DO, ORP, T, and NO_3^-, which were negatively correlated with the copy numbers of *nirS*, *nirK*, and *nosZ* genes. The NO_3^- concentration was a key parameter influencing the ratios of *nirK* abundance of *nirS*.

Table 5: Correlations between abundance and parameters for denitrifying genes in the streams.

	nirK	*nirS*	*nosZ*	*nirK*/*nirS*	*nosZ*/(*nirK* + *nirS*)
nirK	1				
NirS	0.933***	1			
nosZ	0.886***	0.770***	1		
nirK/*nirS*	−0.011	−0. 225	−0. 1743	1	
nosZ/(*nirK* + *nirS*)	0.349*	0.264	0.632***	−0. 396	1
DO	−0.513***	−0.411*	−0.420*	−0.175	−0.333
pH	0.111	0.201	0.244	0.019	0.021
Temp (°C)	−0.507***	−0.543**	−0.459**	0.357*	−0.378*
ORP	−0.582***	−0.649***	−0.525**	0.272	0.337*
NO_3^- (mg L^{-1})	−0.394*	−0.519**	−0.449***	0.665***	−0.047
TN (mg L^{-1})	0.709***	0.698***	0.676***	0.008	0.426**
PO_4^{3-} (mg L^{-1})	0.868***	0.872***	0.875***	0.007	−0.334*
TP (mg L^{-1})	0.560***	0.601***	0.601***	0.283	0.377*

∗ is significant at the 0.05 level (two-tailed); ∗∗ is significant at the 0.01 level (two-tailed); ∗ ∗ ∗ is significant at the 0.001 level (two-tailed).

A significant correlated correlation existed between ratios of *nosZ* abundance to the abundance of *nirK* + *nirS* and the concentration total nitrogen.

4. Discussion

4.1. The Variation of Community Pattern of Denitrifying Bacteria according to Pollution Sources and Effluent Types of Different Streams. Nitrogen cycle in aquatic ecosystems is predominantly controlled by bacteria, and their activities determine the fate of nitrogen compounds. Meanwhile, environmental conditions that regulate the activity of bacteria determine where each nitrogen transformation process occurs and the degree of exchange among various nitrogen pools. Thus, chemical information of different nitrogen species alone is not sufficient to predict rates of nitrogen transformation processes in the environment, and information concerning characteristics of nitrogen cycling bacterial community under various environmental conditions is essential for understanding the related nitrogen cycle process. With regard to the denitrification process, previous studies have shown that it was regulated by various environmental factors such as oxygen and nitrogen concentration, quality, temperature, and pH [5, 39]. However, how the denitrifying bacteria communities were correlated with the environmental factors in streams, receiving massive amount of nutrients and pollutants, remains unclear.

In this study, we evaluated differences in the genetic makeup of the communities by comparing DGGE profiles for denitrification genes encoding nitrite and nitrous oxide reductase (*nirK*, *nirS*, and *nosZ*). It has been suggested that DGGE was a powerful tool for identifying and comparing the dominant of these communities [40, 41]. The DGGE results in this study revealed the significant pairwise differences in the community structure of denitrifying bacteria containing the *nirK*, *nirS*, or *nosZ* genes among the water samples collected from different streams. When comparing the diversities of denitrifier communities from all sites, similar trends emerged with low richness and diversity in the Xinyunliang stream. According to previous studies, Xinyunliang streams run through a historical area of old Kunming city, where there are many industries (such as Yunnan smelter), high population density, and poor sewage networks [42]. This serious industrial pollution could reduce bacterial diversity and damage microbial ecological system [43, 44], although the concentration of NO_3^-, the substrates for denitrification, in Xinyunliang stream was higher than most of other streams with exception of Guangpugou and Haihe streams. Our studied streams differed substantially in the amount of inorganic nutrients which were potentially available to denitrifiers and other microbial populations during the development of microbial community in the water column. The three large streams around Dianchi Lake, Panlongjiang, Daguan, and Chuanfang streams [42], were the important sites receiving effluents from the STPs, with the characteristics of high nitrate concentrations. Nevertheless, the fast-flowing water and irregular discharge of effluents prevented the stream from developing a stable environment for microbial colonization and propagation. Therefore, these streams also represented relatively low diversities of denitrifying bacteria. It has been reported that the high stream flow and nitrate concentration of streams were the major factors controlling the development of planktonic denitrifier populations [45]. On the contrary, the streams of Haihe and Guangpugou were of narrow and slow-flowing, which leading to the long residence time for nitrogen-containing pollutants and well-established hypoxic (~0.2 mg L^{-1} in DO) environment. Therefore, the abundance of denitrifiers was much higher in Haihe and Guangpugou streams than the other streams, which may enhance denitrification in Haihe and Guangpugou streams [46]. This result was consistent with the previous reports that the most transformation of inorganic nitrogen occurred in narrow streams [47]. Simultaneously, an ecological engineering project using *Eichhornia crassipes* for nutrient removal has been conducted in the 11 streams around Dianchi Lake since June 2011. The roots of *E. crassipes* [48, 49] in streams provided a large specific area for denitrifiers to attach, which would benefit the formation

of biofilms and therefore may further change or modify the diversity and abundance of denitrifiers in water [50]. Previous studies suggested that microbial biofilms were highly efficient and successful ecological communities that might also contribute to the influence of the headwater streams on streams, estuaries, and even oceans [51]. Therefore, the slow-moving flows such as Haihe and Guangpugou streams could be considered as living zones of transient storage, where roots and other biofilms bring hydrodynamic retention and biochemical processing into close spatial proximity and influence biogeochemical processes and patterns in streams. All of these results coincided with our hypothesis that the pollution sources and effluent types of different streams would modulate the community composition of denitrifying bacteria to a great extent, although a complex picture of denitrifier community similarity emerged depending on which functional denitrification gene was evaluated.

In this study, we found that the distribution of nir-denitrification genes was much patchier, which was consistent with earlier observations in other streams [52, 53]. Studies of changes in composition and diversity of *nirK* and *nirS* genes communities support the hypothesis of niche differentiation among denitrifying bacteria [54–56]. Meanwhile, this study found the abundance of *nirS* was not consistently greater than that of *nirK* in stream inlet water column, which was different from some of the previously published results [53, 57]. However, in a similar way, some of previous studies also suggested that the spatial distribution of *nirS* and *nirK* genes abundance differs in other types of urban streams, reflecting different habitat preferences [52, 53]. The results of the *nirK*/*nirS* ratios suggested that the *nirK*-type denitrifiers might be more abundant than *nirS*-type denitrifiers in Daguang stream (*nirK*/*nirS* ratio, 18.79), in contrast to Panlongjiang stream (*nirK*/*nirS* ratio, 0.90). However, the concentrations of DO in the two streams were both relatively higher (~2.8 mg L^{-1}) than others. This contradicted with previous studies that *nirK* often prevailed in conditionally O_2-exposed environments [53, 58]. This discrepancy probably was due to other environmental parameters such as nitrogen and phosphorus concentrations [21, 53] which varied significantly in the two streams. Even though the *nirK* and *nirS* are functionally equivalent, denitrifying bacteria harboring either nitrite reductase was likely not under the same community assembly rules [59]. Philippot et al. [60] suggested that the existence of the two types of nitrite reductase (*nir*-gene) was due to differential niche preferences. The different community patterns, together with the spatial distribution of the *nirS*/*nirK* abundance ratio, can suggest habitat selection for the *nirS*- and *nirK*-type denitrifiers [17]. In the present study, the different spatial patterns of *nirK* and *nirS* community diversities, in combination with the spatial distribution of the *nirS*/*nirK* ratio, indicated habitat selection for the two types of denitrifiers. Denitrifying organism includes either *nirS* or *nirK*, but not both of the two-type nitrite reductase genes [61, 62], and experiments have shown the two nitrite reductases to be functionally redundant, as one nir-type gene in denitrifying bacteria can be eliminated and replaced by the other type [63]. This, however, did not necessarily indicate that *nirK*-type denitrifiers contributed more or less in denitrification than *nirK*-type ones. Hence, gene expression analysis is necessary to further investigate which is more important in denitrification in the stream inlet water column around Dianchi Lake.

4.2. Relationship between Water Properties and Spatial Patterns of Denitrifying Bacteria. In the present study, the RDA charts of *nirK*, *nir*S, and *nosZ* genes indicated that diversity of denitrifying populations had varying response to environmental factors, and the concentrations of P (PO_4^{3-} or TP) and N (NO_3^- or TN) were the most important environmental factors causing a significant alteration in the denitrifier community structure among different streams by serving as essential nutrients for microorganisms growth in streams. Meanwhile, abundance of all denitrifiers in this study was, by and large, controlled by the water parameters, especially nutrient (phosphorous and nitrogen) concentration (Table 3). Certainly, microbes need phosphorus for their growth and function. Finlay et al. found increasing phosphorous inputs associated with eutrophication can indirectly promote N losses via enhancing denitrification [64]. Additions of P have been demonstrated to increase N removal in whole-ecosystem experiments in both lakes and streams [65], which provides further support for the role of P as an important control over N cycling and fate in freshwater ecosystems. In addition, different responses of community diversities of *nirS*- and *nirK*-denitrifiers to the changes of phosphorous concentrations agreed with a study suggesting that *nirK*-denitrifiers were most sensitive to alteration of phosphorous concentration [21]. Contrary to previous studies [17, 46], our results implied that variation of phosphorous content in water was positively linked to the abundance of *nirS* and *nirK* genes and resulted in shift of community structure of nir-containing denitrifiers populations. This may further clarify the important function of phosphorous in shaping microorganisms structure in environments [23, 46]. However, the mechanisms concerning how phosphorus would affect growth of denitrifying bacteria in water are still not well understood [21]. Further studies are needed to explain underlying mechanism related to the role of P in regulating the denitrifiers' community, although our results have built some supporting evidence for the related phenomenon. In addition, the water temperature and pH were the main factors driving the changes in the denitrifying bacterial community composition among different streams. The genes *nirS*, *nirK*, and *nosZ* abundance was shown by Pearson correlation coefficient (r) to be mightily influenced by water temperature and oxidation reduction potential (ORP). The quality of inlet water in 11 streams differed with water origin and pollution sources [24, 25, 42]. It has been shown that the changes in denitrifying community structures responded to their habitat conditions like temperature and DO gradient and N forms [12, 13, 66, 67]. The pH was known to generally affect denitrifier community diversity and richness [15]. Generally, the effect of temperature on driving biogeochemical processes is either to alter the functioning bacteria without changing the microbial communities or restructuring communities, thus modifying the fundamental

physiologies [68]. Previous studies suggested that temperature could directly or indirectly affect the communities' diversity and abundance of denitrifying organisms [16, 20, 69–71].

5. Conclusions

The results showed that abundance and diversities of denitrifying genes (*nirK*, *nirS*, and *nosZ*) were variable in the streams of Dianchi Lake. Nutrient concentrations (nitrogen and phosphorous), water temperature, and pH were important environmental factors to alter abundance and community structure of the denitrifiers significantly. The different community patterns, together with the spatial distribution of the *nirS*/*nirK* abundance ratio, suggest habitat selection for the *nirS*- and *nirK*-type denitrifiers.

Conflict of Interests

The authors declare that there is no conflict of interests regarding the publication of this paper.

Authors' Contribution

Neng Yi and Yan Gao contributed equally to this paper.

Acknowledgments

The authors are grateful for the financial support from State Natural Science Foundation of China (no. 41401592), Natural Science Foundation of Jiangsu Province (no. BK20140737), Jiangsu Province Science and Technology Support Plan Project (BE2013436), and Independent Innovation of Agricultural Sciences in Jiangsu Province (no. CX(14)5047).

References

[1] P. J. Mulholland, A. M. Helton, G. C. Poole et al., "Stream denitrification across biomes and its response to anthropogenic nitrate loading," *Nature*, vol. 452, no. 7184, pp. 202–205, 2008.

[2] S. Seitzinger, J. A. Harrison, J. K. Böhlke et al., "Denitrification across landscapes and waterscapes: a synthesis," *Ecological Applications*, vol. 16, no. 6, pp. 2064–2090, 2006.

[3] F. Azam and A. Z. Worden, "Microbes, molecules, and marine ecosystems," *Science*, vol. 303, no. 5664, pp. 1622–1624, 2004.

[4] K. Song, H. Kang, L. Zhang, and W. J. Mitsch, "Seasonal and spatial variations of denitrification and denitrifying bacterial community structure in created riverine wetlands," *Ecological Engineering*, vol. 38, no. 1, pp. 130–134, 2012.

[5] J. Vymazal, "Removal of nutrients in various types of constructed wetlands," *Science of the Total Environment*, vol. 380, no. 1–3, pp. 48–65, 2007.

[6] D. Chèneby, A. Hartmann, C. Hénault, E. Topp, and J. C. Germon, "Diversity of denitrifying microflora and ability to reduce N_2O in two soils," *Biology and Fertility of Soils*, vol. 28, no. 1, pp. 19–26, 1998.

[7] E. Kandeler, T. Brune, E. Enowashu et al., "Response of total and nitrate-dissimilating bacteria to reduced N deposition in a spruce forest soil profile," *FEMS Microbiology Ecology*, vol. 67, no. 3, pp. 444–454, 2009.

[8] S. E. Morales, T. Cosart, and W. E. Holben, "Bacterial gene abundances as indicators of greenhouse gas emission in soils," *The ISME Journal*, vol. 4, no. 6, pp. 799–808, 2010.

[9] D. L. Kirchman, A. I. Dittel, S. E. G. Findlay, and D. Fischer, "Changes in bacterial activity and community structure in response to dissolved organic matter in the Hudson River, New York," *Aquatic Microbial Ecology*, vol. 35, no. 3, pp. 243–257, 2004.

[10] A. Cébron, T. Berthe, and J. Garnier, "Nitrification and nitrifying bacteria in the lower Seine River and estuary (France)," *Applied and Environmental Microbiology*, vol. 69, no. 12, pp. 7091–7100, 2003.

[11] A. Cébron, M. Coci, J. Garnier, and H. J. Laanbroek, "Denaturing gradient gel electrophoretic analysis of ammonia-oxidizing bacterial community structure in the lower seine river: impact of paris wastewater effluents," *Applied and Environmental Microbiology*, vol. 70, no. 11, pp. 6726–6737, 2004.

[12] Z. Liu, S. Huang, G. Sun, Z. Xu, and M. Xu, "Phylogenetic diversity, composition and distribution of bacterioplankton community in the Dongjiang River, China," *FEMS Microbiology Ecology*, vol. 80, no. 1, pp. 30–44, 2012.

[13] B. C. Crump and J. E. Hobbie, "Synchrony and seasonality in bacterioplankton communities of two temperate rivers," *Limnology and Oceanography*, vol. 50, no. 6, pp. 1718–1729, 2005.

[14] K. Enwall, L. Philippot, and S. Hallin, "Activity and composition of the denitrifying bacterial community respond differently to long-term fertilization," *Applied and Environmental Microbiology*, vol. 71, no. 12, pp. 8335–8343, 2005.

[15] S. Hallin, C. M. Jones, M. Schloter, and L. Philippot, "Relationship between N-cycling communities and ecosystem functioning in a 50-year-old fertilization experiment," *The ISME Journal*, vol. 3, no. 5, pp. 597–605, 2009.

[16] M. Wolsing and A. Priemé, "Observation of high seasonal variation in community structure of denitrifying bacteria in arable soil receiving artificial fertilizer and cattle manure by determining T-RFLP of nir gene fragments," *FEMS Microbiology Ecology*, vol. 48, no. 2, pp. 261–271, 2004.

[17] K. Enwall, I. N. Throbäck, M. Stenberg, M. Söderström, and S. Hallin, "Soil resources influence spatial patterns of denitrifying communities at scales compatible with land management," *Applied and Environmental Microbiology*, vol. 76, no. 7, pp. 2243–2250, 2010.

[18] L. Philippot, J. Andert, C. M. Jones, D. Bru, and S. Hallin, "Importance of denitrifiers lacking the genes encoding the nitrous oxide reductase for N_2O emissions from soil," *Global Change Biology*, vol. 17, no. 3, pp. 1497–1504, 2011.

[19] J. Čuhel, M. Šimek, R. J. Laughlin et al., "Insights into the effect of soil pH on N_2O and N_2 emissions and denitrifier community size and activity," *Applied and Environmental Microbiology*, vol. 76, no. 6, pp. 1870–1878, 2010.

[20] J. K. M. Walker, K. N. Egger, and G. H. R. Henry, "Long-term experimental warming alters nitrogen-cycling communities but site factors remain the primary drivers of community structure in high arctic tundra soils," *The ISME Journal*, vol. 2, no. 9, pp. 982–995, 2008.

[21] T. Yan, M. W. Fields, L. Wu, Y. Zu, J. M. Tiedje, and J. Zhou, "Molecular diversity and characterization of nitrite reductase gene fragments (*nirK* and *nirS*) from nitrate-and uranium-contaminated groundwater," *Environmental Microbiology*, vol. 5, no. 1, pp. 13–24, 2003.

[22] K. Hamonts, T. J. Clough, A. Stewart et al., "Effect of nitrogen and waterlogging on denitrifier gene abundance, community structure and activity in the rhizosphere of wheat," *FEMS Microbiology Ecology*, vol. 83, no. 3, pp. 568–584, 2013.

[23] J.-Z. He, Y. Zheng, C.-R. Chen, Y.-Q. He, and L.-M. Zhang, "Microbial composition and diversity of an upland red soil under long-term fertilization treatments as revealed by culture-dependent and culture-independent approaches," *Journal of Soils and Sediments*, vol. 8, no. 5, pp. 349–358, 2008.

[24] Y. Huang, H. Wen, J. Cai, M. Cai, and J. Sun, "Key aquatic environmental factors affecting ecosystem health of streams in the Dianchi Lake Watershed, China," *Procedia Environmental Sciences*, vol. 2, no. 10, pp. 868–880, 2010.

[25] Y. J. Yu, J. Guan, Y. W. Ma, S. Yu, H. Guo, and L. Bao, "Aquatic environmental quality variation in Lake Dianchi watershed," *Procedia Environmental Sciences*, vol. 2, no. 10, pp. 76–81, 2010.

[26] State Environmental Protection Administration, *The National Standard of The People's Republic of China-Surface Water Environmental Quality Standards*, China Environmental Science Press, 2002.

[27] Ncdenr, *Basin Wide Assessment Report: Cape Fear River Basin*, Division of Water Quality, Department of Environment and Natural Resources, Raleigh, NC, USA, 2004.

[28] C. Féray and B. Montuelle, "Chemical and microbial hypotheses explaining the effect of wastewater treatment plant discharges on the nitrifying communities in freshwater sediment," *Chemosphere*, vol. 50, no. 7, pp. 919–928, 2003.

[29] K. Kloos, A. Mergel, C. Rösch, and H. Bothe, "Denitrification within the genus azospirillum and other associative bacteria," *Australian Journal of Plant Physiology*, vol. 28, no. 9, pp. 991–998, 2001.

[30] I. N. Throbäck, K. Enwall, Å. Jarvis, and S. Hallin, "Reassessing PCR primers targeting *nirS*, *nirK* and *nosZ* genes for community surveys of denitrifying bacteria with DGGE," *FEMS Microbiology Ecology*, vol. 49, no. 3, pp. 401–417, 2004.

[31] V. Michotey, V. Méjean, and P. Bonin, "Comparison of methods for quantification of cytochrome cd_1-denitrifying bacteria in environmental marine samples," *Applied and Environmental Microbiology*, vol. 66, no. 4, pp. 1564–1571, 2000.

[32] G. Braker and J. M. Tiedje, "Nitric oxide reductase (*norB*) genes from pure cultures and environmental samples," *Applied and Environmental Microbiology*, vol. 69, no. 6, pp. 3476–3483, 2003.

[33] S. Hallin and P.-E. Lindgren, "PCR detection of genes encoding nitrite reductase in denitrifying bacteria," *Applied and Environmental Microbiology*, vol. 65, no. 4, pp. 1652–1657, 1999.

[34] S. Henry, D. Bru, B. Stres, S. Hallet, and L. Philippot, "Quantitative detection of the nosZ gene, encoding nitrous oxide reductase, and comparison of the abundances of 16S rRNA, narG, nirK, and nosZ genes in soils," *Applied and Environmental Microbiology*, vol. 72, no. 8, pp. 5181–5189, 2006.

[35] D. Radojkovic and J. Kusic, "Silver staining of denaturing gradient gel electrophoresis gels," *Clinical Chemistry*, vol. 46, no. 6, pp. 883–884, 2000.

[36] D. Roesti, R. Gaur, B. N. Johri et al., "Plant growth stage, fertiliser management and bio-inoculation of arbuscular mycorrhizal fungi and plant growth promoting rhizobacteria affect the rhizobacterial community structure in rain-fed wheat fields," *Soil Biology and Biochemistry*, vol. 38, no. 5, pp. 1111–1120, 2006.

[37] J. Lepš and P. Šmilauer, *Multivariate Analysis of Ecological Data using CANOCO*, Cambridge University Press, Cambridge, UK, 2003.

[38] J. Zhang, G. Zeng, Y. Chen et al., "Effects of physico-chemical parameters on the bacterial and fungal communities during agricultural waste composting," *Bioresource Technology*, vol. 102, no. 3, pp. 2950–2956, 2011.

[39] J. L. Faulwetter, V. Gagnon, C. Sundberg et al., "Microbial processes influencing performance of treatment wetlands: a review," *Ecological Engineering*, vol. 35, no. 6, pp. 987–1004, 2009.

[40] Z.-F. Zhou, Y.-M. Zheng, J.-P. Shen, L.-M. Zhang, and J.-Z. He, "Response of denitrification genes nirS, nirK, and nosZ to irrigation water quality in a Chinese agricultural soil," *Environmental Science and Pollution Research*, vol. 18, no. 9, pp. 1644–1652, 2011.

[41] Z. Jin, F.-Y. Ji, X. Xu, X.-Y. Xu, Q.-K. Chen, and Q. Li, "Microbial and metabolic characterization of a denitrifying phosphorus-uptake/side stream phosphorus removal system for treating domestic sewage," *Biodegradation*, vol. 25, no. 6, pp. 777–786, 2014.

[42] B. Wang, B. Huang, W. Jin et al., "Occurrence, distribution, and sources of six phenolic endocrine disrupting chemicals in the 22 river estuaries around Dianchi Lake in China," *Environmental Science and Pollution Research*, vol. 20, no. 5, pp. 3185–3194, 2013.

[43] J. Xiong, Z. He, J. D. Van Nostrand et al., "Assessing the microbial community and functional genes in a vertical soil profile with long-term arsenic contamination," *PLoS ONE*, vol. 7, no. 11, Article ID e50507, 2012.

[44] H. M. A. Mahmoud, R. Goulder, and G. R. Carvalho, "The response of epilithic bacteria to different metals regime in two upland streams: assessed by conventional microbiological methods and PCR-DGGE," *Archiv für Hydrobiologie*, vol. 163, no. 3, pp. 405–427, 2005.

[45] J. K. Böhlke, R. C. Antweiler, J. W. Harvey et al., "Multi-scale measurements and modeling of denitrification in streams with varying flow and nitrate concentration in the upper Mississippi River basin, USA," *Biogeochemistry*, vol. 93, no. 1-2, pp. 117–141, 2009.

[46] C. Yin, F. L. Fan, A. Song, Z. Li, W. Yu, and Y. Liang, "Different denitrification potential of aquic brown soil in Northeast China under inorganic and organic fertilization accompanied by distinct changes of nirS- and nirK-denitrifying bacterial community," *European Journal of Soil Biology*, vol. 65, pp. 47–56, 2014.

[47] B. J. Peterson, W. M. Wollheim, P. J. Mulholland et al., "Control of nitrogen export from watersheds by headwater streams," *Science*, vol. 292, no. 5514, pp. 86–90, 2001.

[48] Y. Gao, N. Yi, Z. Zhang, H. Liu, and S. Yan, "Fate of $^{15}NO_3^-$ and $^{15}NH_4^+$ in the treatment of eutrophic water using the floating macrophyte, *Eichhornia crassipes*," *Journal of Environmental Quality*, vol. 41, no. 5, pp. 1653–1660, 2012.

[49] N. Yi, Y. Gao, X.-H. Long et al., "*Eichhornia crassipes* cleans wetlands by enhancing the nitrogen removal and modulating denitrifying bacteria community," *CLEAN—Soil, Air, Water*, vol. 42, no. 5, pp. 664–673, 2014.

[50] B. Wei, X. Yu, S. Zhang, and L. Gu, "Comparison of the community structures of ammonia-oxidizing bacteria and archaea in rhizoplanes of floating aquatic macrophytes," *Microbiological Research*, vol. 166, no. 6, pp. 468–474, 2011.

[51] T. J. Battin, L. A. Kaplan, J. D. Newbold, and C. M. E. Hansen, "Contributions of microbial biofilms to ecosystem processes in stream mesocosms," *Nature*, vol. 426, no. 6965, pp. 439–442, 2003.

[52] P. M. Groffman, A. M. Dorsey, and P. M. Mayer, "N processing within geomorphic structures in urban streams," *Journal of the North American Benthological Society*, vol. 24, no. 3, pp. 613–625, 2005.

[53] C. W. Knapp, W. K. Dodds, K. C. Wilson, J. M. O'Brien, and D. W. Graham, "Spatial heterogeneity of denitrification genes in a highly homogenous urban stream," *Environmental Science & Technology*, vol. 43, no. 12, pp. 4273–4279, 2009.

[54] S. Hallin, I. N. Throbäck, J. Dicksved, and M. Pell, "Metabolic profiles and genetic diversity of denitrifying communities in activated sludge after addition of methanol or ethanol," *Applied and Environmental Microbiology*, vol. 72, no. 8, pp. 5445–5452, 2006.

[55] B. B. Oakley, C. A. Francis, K. J. Roberts, C. A. Fuchsman, S. Srinivasan, and J. T. Staley, "Analysis of nitrite reductase (nirK and nirS) genes and cultivation reveal depauperate community of denitrifying bacteria in the Black Sea suboxic zone," *Environmental Microbiology*, vol. 9, no. 1, pp. 118–130, 2007.

[56] J. M. Smith and A. Ogram, "Genetic and functional variation in denitrifier populations along a short-term restoration chronosequence," *Applied and Environmental Microbiology*, vol. 74, no. 18, pp. 5615–5620, 2008.

[57] A. García-Lledó, A. Vilar-Sanz, R. Trias, S. Hallin, and L. Bañeras, "Genetic potential for N_2O emissions from the sediment of a free water surface constructed wetland," *Water Research*, vol. 45, no. 17, pp. 5621–5632, 2011.

[58] D. W. Graham, C. Trippett, W. K. Dodds et al., "Correlations between *in situ* denitrification activity and *nir*-gene abundances in pristine and impacted prairie streams," *Environmental Pollution*, vol. 158, no. 10, pp. 3225–3229, 2010.

[59] C. M. Jones and S. Hallin, "Ecological and evolutionary factors underlying global and local assembly of denitrifier communities," *The ISME Journal*, vol. 4, no. 5, pp. 633–641, 2010.

[60] L. Philippot, J. Čuhel, N. P. A. Saby et al., "Mapping field-scale spatial patterns of size and activity of the denitrifier community," *Environmental Microbiology*, vol. 11, no. 6, pp. 1518–1526, 2009.

[61] C. M. Jones, B. Stres, M. Rosenquist, and S. Hallin, "Phylogenetic analysis of nitrite, nitric oxide, and nitrous oxide respiratory enzymes reveal a complex evolutionary history for denitrification," *Molecular Biology and Evolution*, vol. 25, no. 9, pp. 1955–1966, 2008.

[62] W. G. Zumft, "Cell biology and molecular basis of denitrification," *Microbiology and Molecular Biology Reviews*, vol. 61, no. 4, pp. 533–616, 1997.

[63] A. B. Glockner, A. Jüngst, and W. G. Zumft, "Copper-containing nitrite reductase from *Pseudomonas aureofaciens* is functional in a mutationally cytochrome cd_1-free background ($NirS^-$) of *Pseudomonas stutzeri*," *Archives of Microbiology*, vol. 160, no. 1, pp. 18–26, 1993.

[64] J. C. Finlay, G. E. Small, and R. W. Sterner, "Human influences on nitrogen removal in lakes," *Science*, vol. 342, no. 6155, pp. 247–250, 2013.

[65] E. S. Bernhardt, "Cleaner lakes are dirtier lakes," *Science*, vol. 342, no. 6155, pp. 205–206, 2013.

[66] J. J. Rich, R. S. Heichen, P. J. Bottomley, K. Cromack Jr., and D. D. Myrold, "Community composition and functioning of denitrifying bacteria from adjacent meadow and forest soils," *Applied and Environmental Microbiology*, vol. 69, no. 10, pp. 5974–5982, 2003.

[67] M. Castro-González, G. Braker, L. Farías, and O. Ulloa, "Communities of nirS-type denitrifiers in the water column of the oxygen minimum zone in the eastern South Pacific," *Environmental Microbiology*, vol. 7, no. 9, pp. 1298–1306, 2005.

[68] J. P. Schimel and J. Gulledge, "Microbial community structure and global trace gases," *Global Change Biology*, vol. 4, no. 7, pp. 745–758, 1998.

[69] G. Braker, J. Schwarz, and R. Conrad, "Influence of temperature on the composition and activity of denitrifying soil communities," *FEMS Microbiology Ecology*, vol. 73, no. 1, pp. 134–148, 2010.

[70] L. Holtan-Hartwig, P. Dörsch, and L. R. Bakken, "Low temperature control of soil denitrifying communities: kinetics of N_2O production and reduction," *Soil Biology and Biochemistry*, vol. 34, no. 11, pp. 1797–1806, 2002.

[71] L. Zhang, G. Zeng, J. Zhang et al., "Response of denitrifying genes coding for nitrite (*nirK* or *nirS*) and nitrous oxide (*nosZ*) reductases to different physico-chemical parameters during agricultural waste composting," *Applied Microbiology and Biotechnology*, vol. 99, no. 9, pp. 4059–4070, 2015.

Research Article

The *SsDREB* Transcription Factor from the Succulent Halophyte *Suaeda salsa* Enhances Abiotic Stress Tolerance in Transgenic Tobacco

Xu Zhang,[1] Xiaoxue Liu,[1,2] Lei Wu,[1] Guihong Yu,[1] Xiue Wang,[2] and Hongxiang Ma[1]

[1]*Provincial Key Laboratory of Agrobiology, Institute of Biotechnology, Jiangsu Academy of Agricultural Sciences, Nanjing 210014, China*
[2]*National Key Laboratory of Crop Genetics and Germplasm Enhancement, Cytogenetics Institute, Nanjing Agricultural University, Nanjing 210095, China*

Correspondence should be addressed to Hongxiang Ma; hxma@jaas.ac.cn

Received 19 April 2015; Accepted 7 June 2015

Academic Editor: Marián Brestič

Dehydration-responsive element-binding (DREB) transcription factor (TF) plays a key role for abiotic stress tolerance in plants. In this study, a novel cDNA encoding DREB transcription factor, designated *SsDREB*, was isolated from succulent halophyte *Suaeda salsa*. This protein was classified in the A-6 group of DREB subfamily based on multiple sequence alignments and phylogenetic characterization. Yeast one-hybrid assays showed that SsDREB protein specifically binds to the DRE sequence and could activate the expression of reporter genes in yeast, suggesting that the SsDREB protein was a CBF/DREB transcription factor. Real-time RT-PCR showed that *SsDREB* was significantly induced under salinity and drought stress. Overexpression of *SsDREB* cDNA in transgenic tobacco plants exhibited an improved salt and drought stress tolerance in comparison to the nontransformed controls. The transgenic plants revealed better growth, higher chlorophyll content, and net photosynthesis rate, as well as higher level of proline and soluble sugars. The semiquantitative PCR of transgenics showed higher expression of stress-responsive genes. These data suggest that the *SsDREB* transcription factor is involved in the regulation of salt stress tolerance in tobacco by the activation of different downstream gene expression.

1. Introduction

The abiotic stresses like salinity, drought, and low and high temperature negatively affect plant growth and productivity [1]. They are major limiting factors for sustainable food production as they reduce yields by more than 50% in crop plants [2]. To overcome these limitations, plants have generated mechanisms to trigger a cascade of events leading to changes in gene expression and subsequently to biochemical physiological modifications that can enhance their stress tolerance [3]. Molecular and cellular responses to abiotic stresses involve signal perception, transduction of the signal to the cytoplasm and nucleus, alteration of gene expression and, finally, metabolic changes that lead to stress tolerance [4]. Numerous abiotic stress-related genes and transcription factors (TFs) have been isolated from different plant species and overexpressed in homologous and heterologous systems to engineer stress tolerance [5]. The Dehydration-responsive element-binding proteins (DREBs) are members of the APETALA2/ethylene-responsive element-binding factor (AP2/ERF) family of transcription factors in the promoters of stress-inducible genes [6].

Genes included in the DREB subfamily are divided into six small subgroups (A-1 to A-6) based on similarities in the binding domain. The A-1 subgroup, which includes the DREB1/CBF- (C-repeat binding factor-) like genes, are mainly induced by low temperature and activate the expression of many cold stress-responsive genes, whereas the A-2 subgroup, which is comprised of the DREB2 genes, mainly functions in osmotic stress [7]. In addition, multiple research reports indicated that the genes on the CBF/DREB family play very important roles in regulating abiotic stress via ABA-independent/dependent pathway [8–10]. It suggested that CBF/DREB plays distinctive roles in plant response to stress

Table 1: Primers used for RACE-PCR amplification.

Primer name	Oligonucleotides (5′-3′)	Use
DREB-C1	TGGGG KAAR TGGGTYGCHGARAT YCG	AP2/ERF domain
DREB-C2	ACDGADGARTGNAGWGGYT TRTA	AP2/ERF domain
5′AAP	GGCCACGCGTCGACTAGTACGGGIIGGGIIGGGIIG	5′ Universal Primer
5′AUAP	GGCCACGCGTCGACTAGTAC	5′ Universal Primer
5GSP1	TGACCAAACTAGACTCCCTCTAACA	*SsDREB*a 5′ RACE
5GSP2	AGTATTG CTCCGCTCCTAACTCTT	*SsDREB*a 5′ RACE
3′AUAP	GGCCACGCGTCGACTAGTAC	3′ Universal Primer
3GSP1	GA CTACCCAAGAACCGAACCCGGTT	*SsDREB*a 3′ RACE
3GSP2	GGTTATGGCTTGGATCCTTCGATA C	*SsDREB*a 3′ RACE
SsDREB-G1	ATGGCAGCTACAACAA TGGATATG	cDNA
SsDREB-G1	TTAAGATGATGATGATAAGATAGC	cDNA

[11] and that there might also be a crosstalk between drought and cold responsive genes with a DRE element [6]. DREB2 homologous genes have been isolated from a variety of species [12]. Transgenic plants overexpressing either DREB1 or DREB2A genes enhanced tolerance to abiotic stress [13–16].

To date, only few efforts are made in halophytes in response to salt stress. The expression of AhDREB1 from *Atriplex hortensis* was observed in salt stress [17], while AsDREB from *Atriplex halimus* was induced by only dehydration [18]. PpDBF1 from *Physcomitrella patens* was induced under salt, dehydration as well as cold stress [19], while SbDREB2A from *Salicornia brachiata* was induced by NaCl, drought, and heat stress [20].

Suaeda salsa is a native halophyte in China for both industrial application and scientific research [21]. Fresh branches of *S. salsa* are highly valuable as a vegetable, and the seeds can produce edible oil [21]. It can grow both in saline soils and in the intertidal zone where soil salt reaches up to 3%. Treatment of *S. salsa* with 200 mM NaCl could significantly increase its growth and net photosynthetic rate [22]. The high salt tolerance might be partly the result of its efficient antioxidative system [22]. For instance, Mn-SOD and Fe-SOD activities in the leaves of *S. salsa* seedlings were significantly higher under NaCl stress conditions (100 mmol L^{-1}) than those under non-NaCl stress conditions [22]. However, the mechanism of abiotic-stress-tolerance in *S. salsa* is still poorly understood. In the present study, we report the cloning and characterization of the *SsDREB* cDNA. Its expression pattern was investigated in response to exogenous ABA, salt, cold, and drought stress treatments. Overexpression of this cDNA in transgenic tobacco led to enhanced tolerance to salinity and dehydration stresses.

2. Materials and Methods

2.1. Plant Materials and Stress Treatment. Seeds of *S. salsa* were germinated and precultured in pots containing vermiculite with Hoagland nutrient solution in a growth chamber (20/25°C, 16 h light/8 h dark) under 250 mE · m^{-2} · s^{-1} light intensity.

Salinity, dehydration, and ABA stress treatments were performed on *S. salsa* by transferring 3-week-old seedlings in Hoagland nutrient solution supplemented with 250 mM NaCl, 20% PEG6000, and 100 μm/L ABA, respectively. Low temperature treatments were performed by transferring plants to a growth chamber set to 4°C under the light and the photoperiodic conditions described above. Samples were harvested at 0, 0.5, 2, 4, 8, 12, and 24 h after treatment and immediately stored at −80°C for further study. All experiments were repeated in biological triplicates.

2.2. Gene Isolation and Sequencing Analyses. Total RNA was extracted from the leaves of *S. salsa*, treated with 400 mM NaCl for 6 h utilizing SV Total RNA Extraction Kit (Promega, USA) according to the instruction. The conserved AP2/ERF domain of DREB genes in *S. salsa* was amplified by primers DREB-C1 and DREB-C2, designed from the known DREB/CBF genes in the GenBank database. Isolation of the cDNA sequences was carried out using the RNA ligase-mediated rapid amplification of 5′ and 3′ ends (RLM-RACE) method, according to the GeneRacer Kit (Invitrogen, USA). Gene-specific nested primes 5GSP1, 5GSP2, 3GSP1, and 3GSP2 were designed based on the known genomic sequences. Sequences of all relevant primers are listed in Table 1.

The 5′- and 3′-RACE fragments were cloned into separate pGEM-T Easy plasmid vectors (Promega, USA) and sequenced. The cDNA sequences of *SsDREB* were amplified by PCR using the forward primer *SsDREB-G1* and the reverse primer *SsDREB-G2* (Table 1). PCR was performed with a 5-min 94°C denaturation step, followed by 30 cycles of 45 s at 94°C, 45 s annealing at 55°C, a 1-min extension at 72°C, and a final extension period of 10 min.

Sequence analyses were performed using the program BLASTX (National Centre for Biotechnology Information, USA). The ORF of *SsDREB* genes and the properties of protein encoded by them were predicted by DNAStar software. The conserved AP2 domains (Accession number: smart00380) were originally applied as a seed sequence to search the NCBI database (http://www.ncbi.nlm.nih.gov/) and 33 proteins were retrieved with an expected value of

Table 2: Primers used for qRT-PCR amplification.

Primer name	Oligonucleotides (5′-3′)	Use
SsDREB-R1	AGAGGGAGTCTAG TTTGGTCATT	Real-time qRT-PCR
SsDREB-R2	TTTGGAGCCCCTACAATTTC	Real-time qRT-PCR
SsACTIN-R1	ACCGTTCCAATCTATGAGG	Reference gene
SsACTIN-R2	CGTAAGCCAACTTCTCCT	Reference gene

100. Multiple alignments were prepared using ClustalW [23] using default parameters (gap opening penalty = 10, gap extension penalty = 0.2). The resulting alignments of complete protein sequences were used in MEGA (version 5) [24] for the construction of unrooted phylogenetic trees using the neighbor-joining (NJ) method according to Jones-Taylor-Thornton model with uniform rates among sites and complete deletion of gaps data. The reliability of the obtained trees was tested using bootstrapping with 500 replicates.

2.3. DRE Binding and Transcriptional Activity of FeDREB1 in Yeast. The DNA-binding activity of SsDREB protein was measured using a yeast one-hybrid system. Three tandem repeats of the core sequence of the DRE (TACCGACAT) and its mutant (mDRE) sequence (TATTTTCAT) were cloned into the Sac I/Spe I restriction sites of the plasmid pHIS2.1 cloning reporter vector upstream to the HIS3 minimal promoter according to the protocol described by Clontech (Clontech, Mountain View, CA, USA). The entire coding region of *SsDREB* was cloned into the Sma I site of the YepGAP expression vector containing no GAL4 activation domain (AD) [25]. The recombinant YepGAP expression vector containing *SsDREB* cDNA and the pHIS2.1 vector containing three tandem repeats of the DRE or mDRE were cotransformed into the yeast strain Y187. The growth status of the transformed yeast was compared on SD/-Leu-Ura-His+ 10 mM 3-AT plates to test the expression of the HIS reporter gene. Empty YepGAP was used as a negative control.

2.4. Gene Expression Assay by Quantitative Real-Time RT-PCR. Total RNA was extracted from the roots, stem, and leaves using SV Total RNA Extraction Kit (Promega, USA) according to the instruction. First-strand cDNA was produced from 1 μg of RNA using PrimeScript RT reagent Kit (Takara, Dalian, China), according to the manufacturer's protocol. Each sample was amplified in biological and technical triplicate by quantitative real-time RT-PCR using a Roche 2.0 Real-Time PCR Detection System with the SYBR Green Supermix (Takara, Dalian, China). The reaction mixture was cycled as follows: 30 s denaturation at 95°C, then 40 cycles of 5 s at 95°C, 10 s at 60°C, and 20 s at 72°C. The amplification of *S. salsa Actin* gene (FJ587488) was used as the normalization control. The mRNA fold difference was relative to that of untreated samples used as calibrator. The relative quantification value for *SsDREB* was calculated by the $2^{-\Delta\Delta CT}$ method [26]. All relevant primers used in this work are listed in Table 2.

2.5. Generation of Transgenic Tobacco. To generate transgenic plants, *SsDREB* cDNA was amplified using a specific primer pair: forward, 5′-GCCTCTAGAATGGCAGCTACAACAAT GGATATG-3′ (XbaI site underlined) and reverse, 5′-GCCCCCGGGTTAAGATGATGATGAT AAGATAGC-3′ (SmaI site underlined). The PCR product was fused into the binary plant transformation vector pCAMBIA2301 under the control of the CaMV 35S promoter. The constructs were mobilized to *Agrobacterium tumefaciens* strain EHA105. This *Agrobacterium* strain was used for transformation in tobacco leaf discs following the standard protocol [27]. The putative transgenic lines selected on medium containing hygromycin were confirmed by PCR with gene-specific primers.

The seeding of transgenic tobacco plants was selected on solid 1/2 MS medium containing 100 μg/mL kanamycin under long-day condition (16 h light/8 h dark) at 25°C. The transgenic lines of tobacco plants were confirmed by qRT-PCR analysis.

2.6. Salinity and Drought Stress Tolerance Evaluation in Transgenic Plants. Independent homozygous transgenic plants lines and homozygous wild-type transgenic with pCAMBIA2301 empty vector (WT) were precultured in MS liquid medium for 4 days in growth chamber (20/25°C, 16 h light/8 h dark) under 250 mE/m^2/s light intensity. Then, both plants were transferred in an aqueous MS medium supplemented with PEG6000 (0, 5, 10 15, and 20%) or NaCl (0, 50, 100, 150, 200, 250, and 300 mM) for 2 days. Leaves with and without stress treatments were sampled for physiological parameters.

2.7. Measurement of Photosynthetic and Chlorophyll Fluorescence Parameters. Leaf net photosynthetic rate (P_n) was measured using a portable infrared gas analyzer (LI 6400XT portable photosynthetic system, Lincoln, USA). Chlorophyll index was measured using chlorophyll content meter (FMS-2 Pulse Modulated Fluorometer, Hansatech Inc., UK).

2.8. Measurement of Free Proline and Soluble Sugars Content. Fresh leaf material (0.3 g) was extracted with 5 mL of deionized water at 100°C for 10 min, and shaken with 0.03 g of permutit for 5 min. The extract was separated by centrifugation at 3,000 rpm for 10 min, and then the proline content of the aqueous extract was determined using the acid ninhydrin method. The organic phase was determined at 515 nm. The resulting values were compared with a standard curve constructed using known amounts of proline (Sigma).

Fresh leaf material (0.2 g) was extracted with 80% (v/v) ethanol at 70°C for 30 min. The extract was separated by centrifugation at 12,000 rpm for 10 min and diluted with water to 10 mL. Then, the soluble sugar content of the aqueous extract was determined using sulfuric acid anthrone colorimetric method. The resulting values were compared

Table 3: Primers of downstream genes of *SsDREB* for semiquantitative RT-PCR.

Gene (GeneBankID)	Oligonucleotides (5′-3′)
α-tublin (AJ421412)	TAACCATCATAGAAGAGGGTTC
	GCAATCCTTCTTGACAATGAGG
Glutathione S-transferase (D10524)	TTGGCCTTCTACTTCCATCC
	TGTCAACTGCAACCATGAGAG
Cu/ZnSOD (EU123521)	TGTCACGGGACCACATTAC
	CACCAGCATTTCCAGTAGC
Lea5 (AF053076)	GTGCCAGGTGGAGTGAGAGG
	GGGACGTGGTATGGTAACCA
lipid transferase (ltp1) (X62395)	AATAGCTGGGAAAATTGCATG
	CAGTGGAAGGGCTGATCTTG
H^+-ATPase B subunit (AF220611)	TCTTCACCAGTCCAGCCTGAC
	GAAGGAACATCTGGAATTGAC
H^+-ATPase (X66737)	TCAGCAGGAATGATGTCTCC
	TCATGGAAGCTGCTGCTGTC
Peroxidase (AY032675)	AGGGGAAATGTTATTGTCTCC
	CACATTGGGAAGTACCACTAG
TOBPXD (D11396)	GAAATCCTGGCTCCGCTCTG
	TGGAGTTGCCTTGGTAAGAG

with a standard curve constructed using known amounts of sugar.

2.9. Semiquantitative RT-PCR for Expression Analysis of Downstream Genes of SsDREB. Semiquantitative RT-PCR amplification was performed with selected gene primers (Table 3), using the first strand cDNA, synthesized from RNA samples collected from WT and transgenic tobacco seedlings. The reaction mixture was cycled as follows: 3 m denaturation at 95°C, then 35 cycles of 45 s at 94°C, 45 s at 55°C, and 1 m at 72°C. The amplification of *S. salsa* α-tublin gene was used as the normalization control. PCR-amplified products were visualized on ethidium bromide-stained 1.5% agarose gels.

3. Results

3.1. Isolation and Phylogenetic Analysis of SsDREB cDNA. A full length-cDNA sequence, designated as *SsDREB*, was isolated from *S. salsa*. This cDNA is 1095-bp long corresponding to a protein of 364 amino acids. *SsDREB* possesses two regions rich in serine, one region rich in glutamine, and an acidic C-terminal sequence, PSXEIDW, which is known to function in transcriptional activation activity [25, 28]. The putative amino acid sequence showed that the *SsDREB* had a conserved EREBP/AP2 domain of 64 amino acids with valine (V) and leucine (L) at the 14th and 19th residues, respectively (Figure 1(a)). Phylogenic tree analysis of DREB proteins showed that *SsDREB*, together with *Arabidopsis* RAP2.4, ZmDREB1, OsDBF1, and ChDREB2, is attributable to the DREB (A-6) lineage (Figure 1(b)).

3.2. SsDREB Protein Specifically Binds to the DRE Element. To verify the possible binding function between SsDREB protein and DRE element, the recombinant plasmid pAD-SsDREB was separately transformed into yeast strain Y187 containing the reporter genes HIS3 under the control of DRE. As negative controls, pAD-SsDREB was also separately transformed into Y187 harboring the reporter genes HIS3 under the control of a mutant DRE (mDRE) (Figure 2(a)). These results suggested that the DRE::pAD-SsDREB transgenic yeast cells grew well on SD/-His 10 mM 3-AT, whereas the yeast cells harboring mDRE::pAD-SsDREB transgenic yeast cells could not grow on the same medium (Figure 2(b)). These results strongly indicated that the SsDREB can bind the normal DRE element exclusively to drive target gene expression *in vivo*.

3.3. Expression of SsDREB in Response to Various Abiotic Stresses. The expression pattern of *SsDREB* in different organs of *S. salsa* was examined under normal conditions. The expression level of MsDREB2C was highest in leaves followed by roots and stem (Figure 3(a)). Therefore, expression of *SsDREB* in leaf was investigated under different abiotic stresses. Quantitative reverse transcription-PCR (qRT-PCR) revealed that the transcript of *SsDREB* was induced by salt and drought stress. *SsDREB* expression was induced by salt treatment at 0.5 hours after treatment and peaked at 4 h, with the highest abundance of about 16-fold increase (Figure 3(b)). The expression increased slowly from 0.5 h but rapidly peaked at 8 h and then decreased gradually under mimic dehydration stress (Figure 3(b)). Under cold stress (4°C) treatment, *SsDREB* expression was gradually declined and then slightly recovered after 4 h after treatment (Figure 3(c)). Similarly, there was no significant expression change of *SsDREB* after exogenous ABA application, indicating that StDREB1 may function in an ABA-independent signaling pathway (Figure 3(c)).

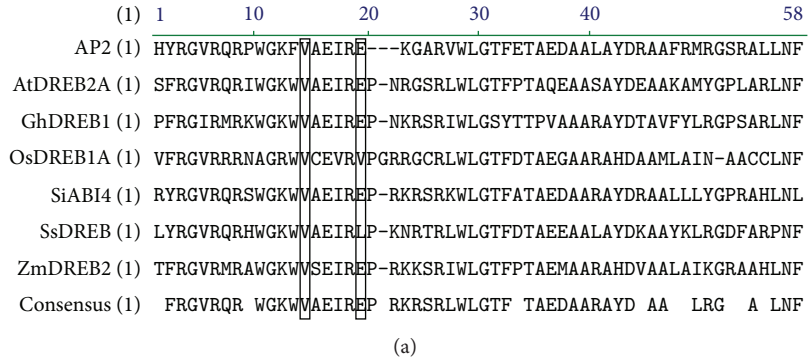

(a)

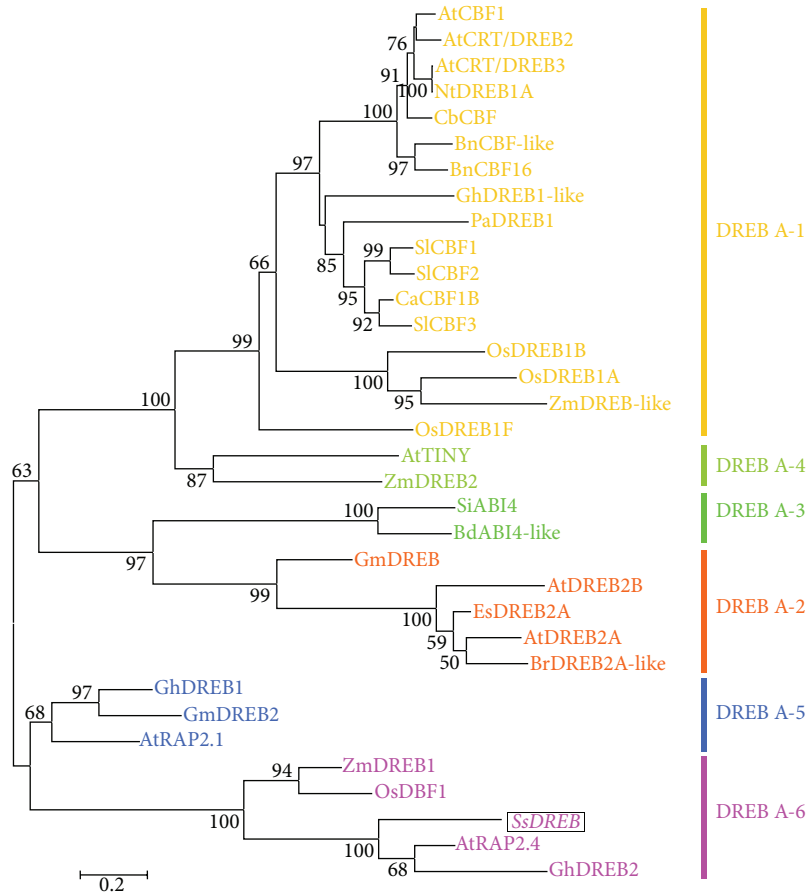

(b)

Figure 1: Conserved domain and phylogenetic analysis of SsDREB protein. (a) SsDREB protein has the same AP2 domain compared with other DREB proteins from *Arabidopsis thaliana*, *Zea mays*, *Gossypium hirsutum*, *Setaria italica*, and *Oryza sativa*. The 14th valine and the 19th leucine acid inside the AP2/ERF domain are presented in boxes. (b) Phylogenetic analysis of proteins from DREB subfamily. The number was the bootstrap value of the clade and low bootstrap values (<50) were removed from the tree. The accession number of each appended protein is as follows: AtCBF1 (AAC49662), AtCRT/DREB2 (AAD15976), AtCRT/DREB3 (AAD15977), NtDREB1A (ABD65969), CbCBF (AAR26658), BnCBF-like (AAL38242), BnCBF16 (AAM18960), GhDREB1-like (ABD65473), SlCBF3 (AAS77819), SlCBF2 (AAS77821), PaDREB1 (BAD27123), CaCBF1B (AAQ88400), OsDREB 1B (AAN02488), OsDREB 1A (AAN02486), ZmDREB2 (AAM80485), ZmDREB-like (AAN76804), AtRAP2.1 (AAC49767), AtRAP2.4 (AAC49770), SlCBF1 (AAK57551), AtTINY (CAA64359), AtDREB2B (BAA33795), AtDREB2A (BAA36705), ZmDREB1 (AAM80486), AtAP2 (AAC39489), ZmERF/AP2 (BAE96012), GmDREB (AAP83131), EsDREB2A (AAS58438), OsDBF1 (AAP56252), GhDREB1 (AAO43165.1), CbCBF25 (AAR35030), GmDREBa (AAT12423), BdABI4-like (XP_003568646), SiABI4-like (XP_004963859), BrDREB2A-like (XP_009125600), BpDREB (ABB89755.1), GmDREB (ABB36645), OsDREB1F (AAX23723), and GhDREB2 (AAT39542).

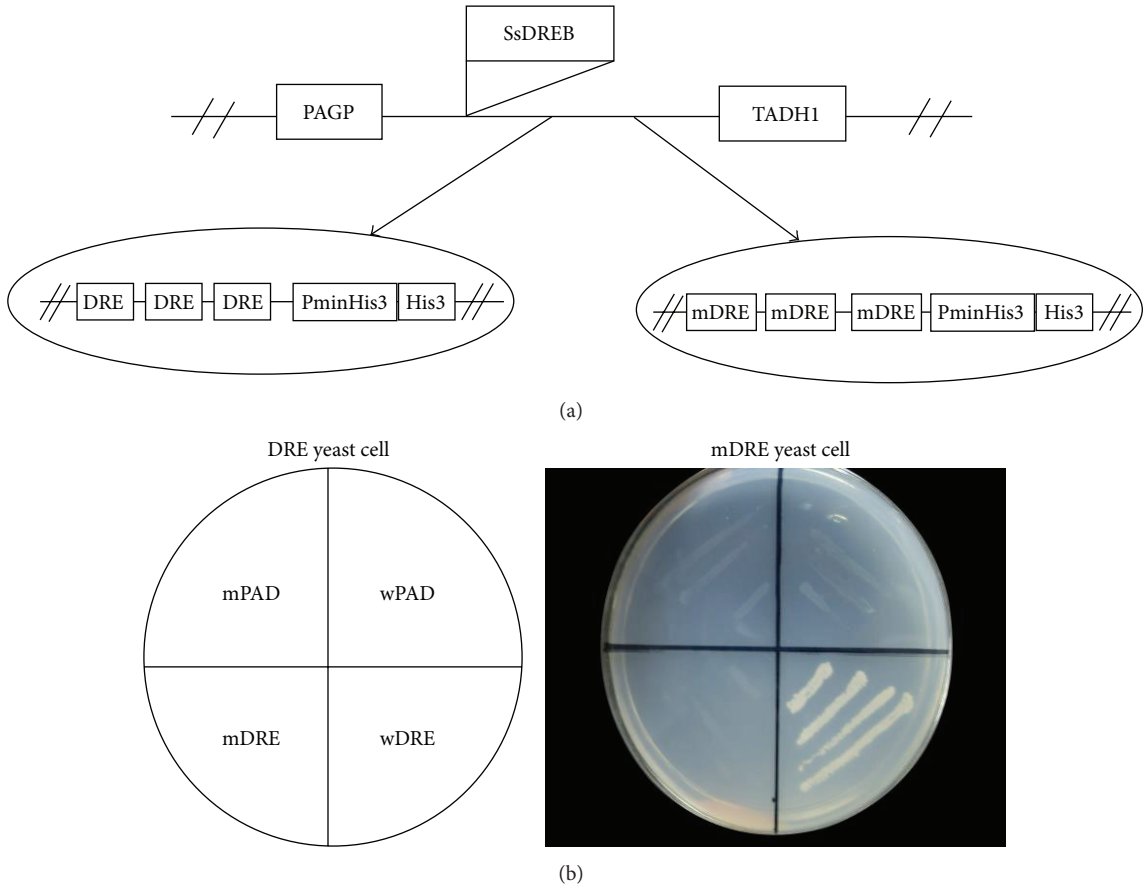

Figure 2: Analysis of SsDREB binding to the DRE element in the yeast one-hybrid system. (a) Construction of the YepGAP-*SsDREB* plasmid. The entire *SsDREB* coding region was fused to the activation domain of GAL4. Recombinant YepGAP-*SsDREB* or plasmid was transformed into yeast cells that are harboring two reporter genes under the control of either wild-type or mutant DRE motifs. PGAP and TADH1 indicate the promoter and terminator of ADH1 gene, respectively. (b) Transformed yeast cells were examined for growth on selective medium (SD−His+10 mM 3-AT) at 30°C (left). Left panel shows the position of each transformed yeast cell. The empty YepGAP (PAD) was used as a control. wDRE and wPAD indicate yeast cells harboring DREB proteins and DRE-controlled reporter genes, while mDRE and mPAD indicate yeast cells harboring DREB proteins and mDRE-controlled reporter genes.

3.4. Confirmation of Putative Transgenic Tobacco Plants Expressing SsDREB. The putative transgenic lines selected on medium containing hygromycin were confirmed by PCR with gene-specific primers using primers the pCAMBIA2301 binary vector corresponding to sequences flanking the *SsDREB* cDNA. As expected, a PCR product of 1095 bp was obtained (Figure 4(a)). PCR-positive plants were successfully transferred to green house for further analysis. Positive transgenic lines also showed expression of *SsDREB* by semiquantitative RT-PCR, whereas expression of *SbDREB* was not observed in WT plants (Figure 4(b)). No phenotypic modification such as dwarfism was noticed in these *SsDREB* transgenic plant lines.

3.5. Tobacco Plants Overexpressing SsDREB Enhance Salinity and Dehydration Tolerance

3.5.1. Morphological Features of Plants. All of the transgenic lines and WT tobacco plants grew well under normal condition (Figure 5(a)). After dehydration and salinity treatment, decrease in leaf size was observed in both transgenic and WT plants. The salt stress proved more detrimental in the WT plants as compared to transgenic seedlings. At 300 mM NaCl, the transgenic plants showed better growth under salt stress with larger leaf area and higher turgor maintenance pressure (Figure 5(b)) as compared to WT. At 20% PEG, the transgenic plants showed significantly better growth under stress with larger leaf area and higher turgor maintenance pressure (Figure 5(c)) as compared to WT.

3.5.2. Photosynthesis and Chlorophyll Fluorescence Parameters. Net photosynthesis rate (P_n) and stomatal conductance (G_s) in WT and transgenic plants were similar under control condition. Net photosynthesis rate (P_n) was 13.8 and 14.0 μmol $CO_2 \cdot m^{-2} \cdot s^{-1}$ in WT and transgenic plants while stomatal conductance was 0.37 and 0.38 μmol $CO_2 \cdot m^{-2} \cdot s^{-1}$ under control condition. Under salinity stress net photosynthesis rate and stomatal conductance reduced drastically as compared to control conditions in WT and transgenic lines. Transgenics showed significantly higher net

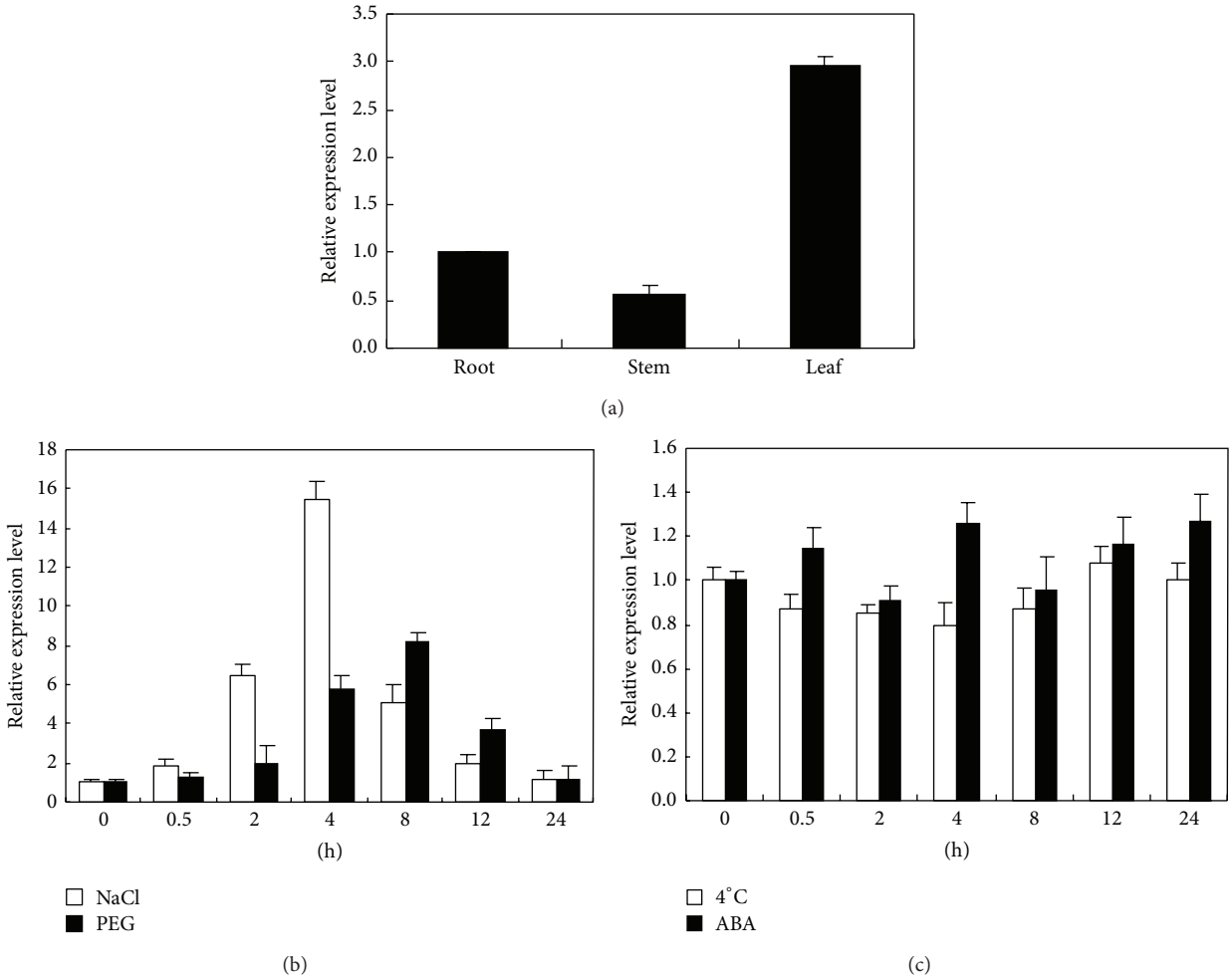

Figure 3: Quantitative real-time PT-PCR analysis of *SsDREB*. (a) Transcript levels of *SsDREB* in the roots, stems, and leaves of untreated plants. (b), (c) The relative expression level of *SsDREB* in *S. salsa* leaves at indicated time points exposed to salinity stress (250 mM NaCl), dehydration stress (20% PEG), low temperature (4°C), and 100 μM ABA, respectively. Columns indicate relative expression levels of *SsDREB* normalized against levels of SsActin as calculated by real-time qRT-PCR (mean ± SE of three biological replicates).

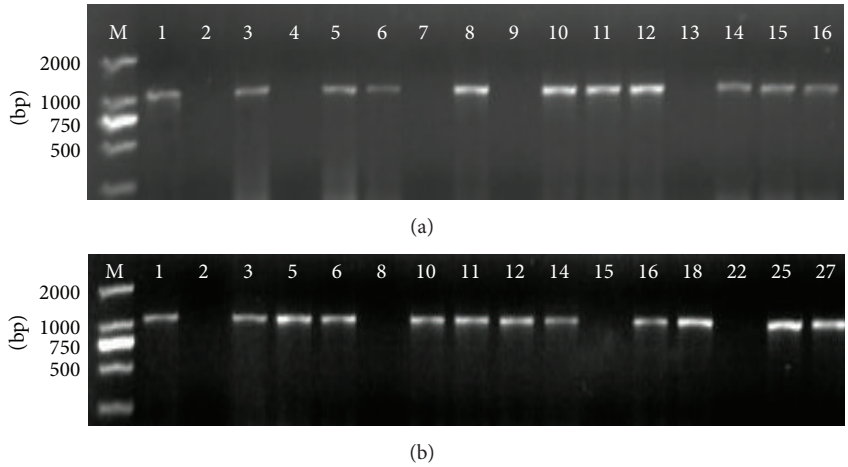

Figure 4: (a) PCR amplification of the specific *SsDREB* gene from genomic DNA of the transgenic lines. (b) RT-PCR analysis of *SsDREB* expression in transgenic lines. (*M* marker DL2000, 1 CK+, 2 WT, 3–27 transgenic lines).

(a) (b) (c)

Figure 5: Phenotype of transgenic tobacco plants under normal and stress condition. (a) Under normal condition. (b) Treated with 300 mM for 2 days. (c) Treated with 20% PEG for 2 days. *Left*: WT plant; *right*: transgenic plan.

photosynthetic rate and stomatal conductance at all five NaCl concentration gradients, compared to WT plants indicating. Net photosynthesis rate was reduced to 12.6, 11.1, 8.7, 6.3, and 2.2 μmol $CO_2 \cdot m^{-2} \cdot s^{-1}$ in WT plants 2 days after 50, 100, 150, 200, and 250 mM NaCl treatment, respectively. But transgenic plants maintained net photosynthesis rate at 13.6, 12.5, 11.6, 10.3, and 8.9 μmol $CO_2 \cdot m^{-2} \cdot s^{-1}$ in the same treatment (Figure 6(a)). In addition, stomatal conductance was reduced to 0.34 and 0.04 mol $H_2O \cdot m^{-2} \cdot s^{-1}$ in WT plants, while transgenic plants maintained around 0.37 and 0.21 $H_2O \cdot m^{-2} \cdot s^{-1}$ days after 50 and 250 mM NaCl treatment, respectively (Figure 6(b)). Similarly, transgenics showed significantly higher net photosynthetic rate and stomatal conductance at all four PEG concentration gradients, compared to WT plants (Figures 6(g)-6(h)). The results showed that *SsDREB* transgenic plants showed higher tolerance to salt stress.

Chlorophyll fluorescence parameters were also investigated. Maximal PS II quantum efficiency (Fv/Fm) and effective PS II quantum yield (YII) in WT and transgenic plants were similar under control condition. Fv/Fm was 0.84 and 0.83 in WT and transgenic plants while Y (II) was 0.78 and 0.77 under control condition. The transgenics showed higher Fv/Fm and Y(II) at all five NaCl concentration gradients, compared to WT plants (Figures 6(c)-6(d)). Fv/Fm was reduced to 0.82, 0.81, 0.78, 0.75, and 0.71 in WT plants 2 days after 50, 100, 150, 200, and 250 mM NaCl treatment, respectively. But transgenic plants maintained Fv/Fm at 0.83 under 50 and 100 mM NaCl stress and then drop slightly to 0.82, 0.81, and 0.80 under 150, 200, and 250 mM NaCl treatment (Figure 6(c)). In addition, Y(II) was reduced to 0.74 and 0.38 in WT plants, while transgenic plants were maintained around 0.76 and 0.59 2 days after 50 and 250 mM NaCl treatment, respectively (Figure 6(d)). Similarly, the transgenics showed higher chlorophyll fluorescence parameters at all four PEG gradients, compared to WT plants (Figures 6(i)-6(j)), indicating that expression of *SsDREB* in transgenic tobacco enhanced abiotic tolerance.

3.5.3. Proline and Soluble Sugar Content. Proline and soluble sugar content accumulate in plants subjected to salinity and dehydration stress conditions to confer stress tolerance in both transgenic and WT plants. The contents of soluble sugar and free proline in transgenic plants were slightly richer than that of the WT plants with all salinity and dehydration stress, demonstrating that the overexpression of *SsDREB* gene could enhance plant salinity and dehydration tolerance in transgenic tobacco (Figures 6(e)-6(f), 6(k)-6(l)).

3.6. Overexpression of StDREB1 Activates the Expression of Stress-Responsive Genes. Given that the *SsDREB* transgenic plants showed enhanced tolerance to salinity and drought and freezing stress, we decided to quantify the molecular responses of eight stress-responsive genes in the transgenic lines to see the level of expression under stress conditions. Semiquantitative RT-PCR analyses of these target genes were performed for the WT and for the *SsDREB* transgenic tobacco plants. An increase in transcription level of these genes was noticed in almost all transgenic plants cultivated under standard growth conditions in comparison to those in WT ones (Figure 7). This most significant increase was in expression of *ltp1*, *Lea5*, and H^+-*ATPase* genes, while expression of *Cu/Zn SOD*, *TOBPXD*, and *GST* was slightly higher in transgenic plants under the same situation. All these findings strongly suggested that *SsDREB* might upregulate the expression of stress-related functional genes.

4. Discussion

This study describes the isolation and characterization of a DREB factor from halophyte *Suaeda salsa*, termed *SsDREB*. To date, only few efforts are made in halophytes in response to salt stress. The AhDREB1 from *Atriplex hortensis* expression was observed in salt stress [17], while AsDREB from *Atriplex halimus* was induced by dehydration but not in salt stress [18]. PpDBF1 from *Physcomitrella patens* was induced under salt, dehydration as well as cold stress [19]. DREB2-type TFs SbDREB2A from halophytic plants *Salicornia brachiata* was induced by NaCl, drought and heat stress [20].

The sequence analysis of *SsDREB* identified an AP2/ERF domain of 64 amino acids that is predicted to fold into a structure containing three anti-parallel β-sheets and one α-helix. *SsDREB* possessed two regions rich of serine, one region rich of glutamine, and an acidic C-terminal sequence, PSXEIDW, which is known to function in transcriptional activation activity [25, 28]. This structure is thought to play a key role in recognizing and binding to specific cis-elements [7]. Sequence alignment and phylogenetic analyses revealed that the *SsDREB* grouped with the DREB (A-6) lineage. In this

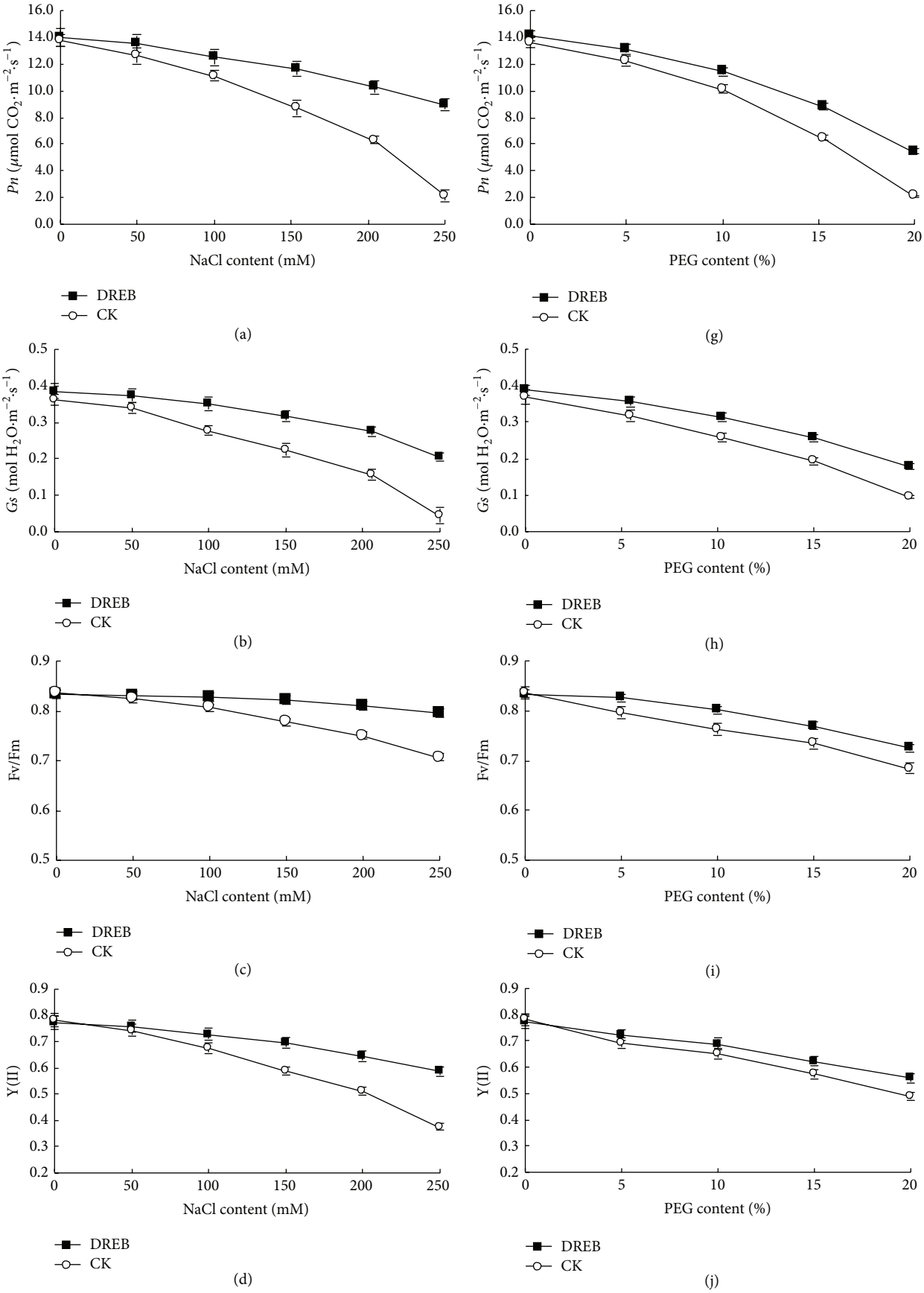

Figure 6: Continued.

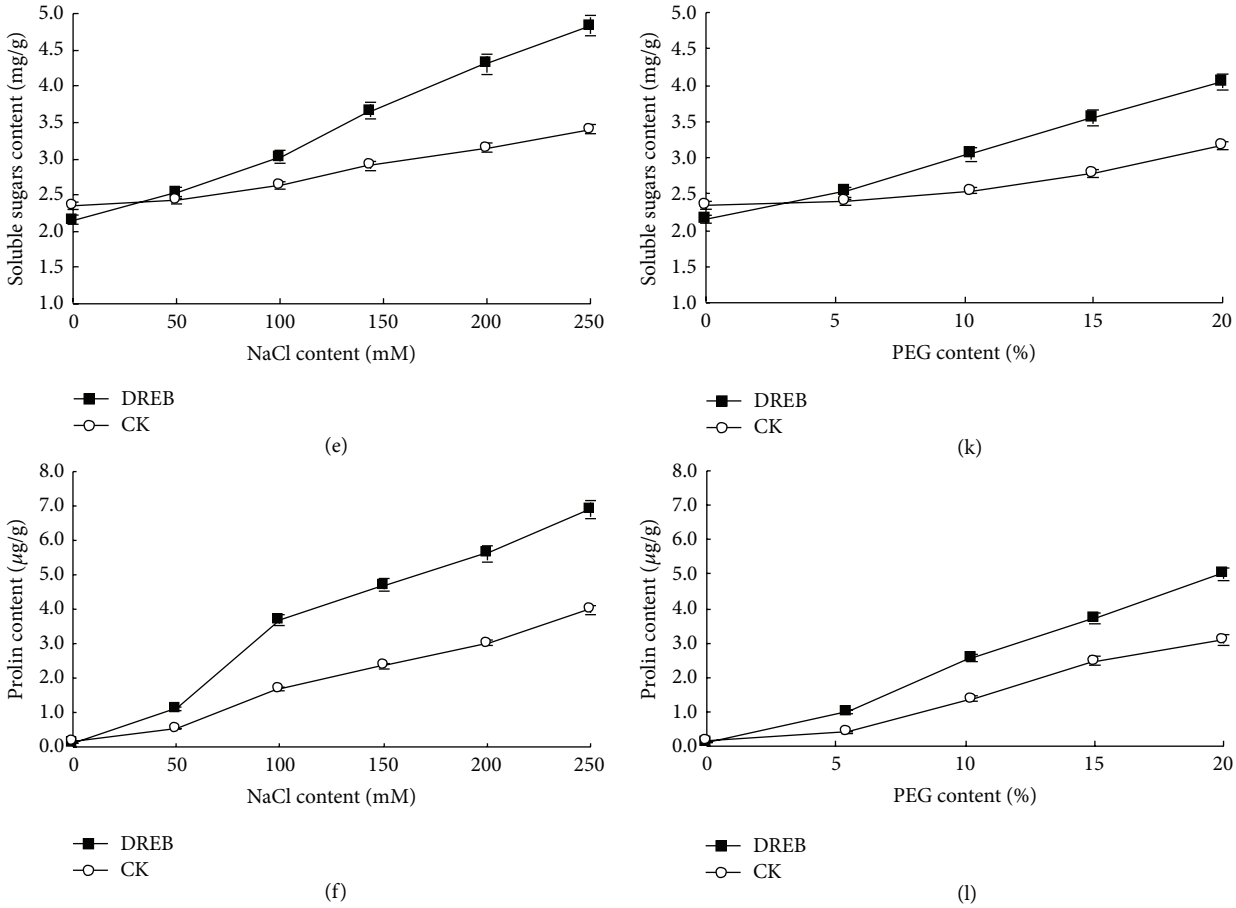

Figure 6: Salinity and dehydration tolerance of transgenic tobacco. (a)–(f) Salinity tolerance of transgenic plants. (g)–(l) Dehydration tolerance of transgenic plants. (a), (g) Net photosynthesis rate (P_n). (b), (h) Stomatal conductance (G_s). (c), (i) Maximal PS II quantum (Fv/Fm). (d), (j) Effective PS II quantum yield (Y II). (e), (k) Soluble sugars content. (f), (l) Proline content. For (a)–(l), each data point is means from three replicates ± SE. Bars indicate SE.

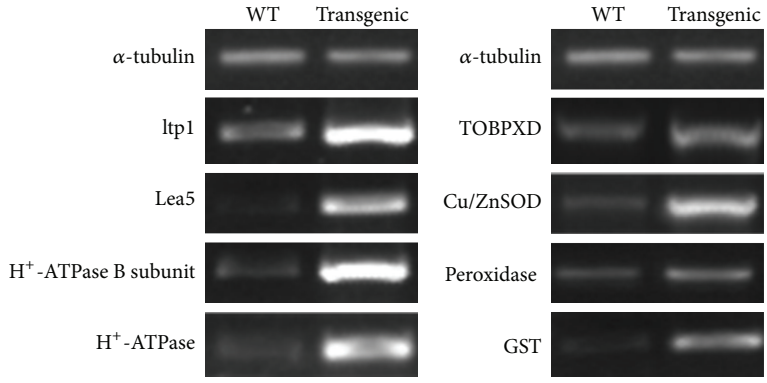

Figure 7: Semiquantitative RT-PCR of stress-responsive genes.

study, the DSAW and LWSY motif, the conserved sequences in A1-subgroup (DREB1) [29], was not found in *SsDREB*.

A number of reports have suggested that Val14 and Glu19 in the AP2/ERF domain are essential for specific binding to DRE [7, 25]. The absolutely conserved 14th valine residue, an important site that acts in DNA binding, has also been found in the AP2/ERF domain of SsDREB protein [7]. However, the 19th glutamic acid residue is replaced by leucine residue in the *SsDREB* (Figure 1(a)). Similar amino acid changes have also been observed in other plant species. In rice, wheat, and barley, the DREB1-type factors harbor a valine residue at position 19 in the AP2/ERF domain [30, 31]. The

Glu (E) 19 is also replaced by Gln (Q) in potato (*Solanum tuberosum* L.) and by His (H) in Buckwheat (*Fagopyrum esculentum*). In *Broussonetia papyrifera*, the 19th glutamic acid residue in BpDREB2 protein was replaced by leucine residue, and the DNA binding assay in the yeast one-hybrid system suggested that the 14th residue is more crucial than the 19th residue in the DRE binding activity of DREB [32]. Other research also reported that mutation in the 19th residue had little effect on DRE binding activity [33]. Our DNA binding assay in the yeast one-hybrid system also suggested that the change in the 19th residue had little effect on DRE binding activity (Figure 3(b)). The mutation of the 19th residue in the AP2/ERF domain indicated that the conserved 14th valine residue may be crucial in the regulation of the DRE binding activity of DREB.

It was reported that the expression of DREB1 (A-1) genes was induced by low temperature, whereas the expression of DREB2 (A-2) genes was attributed to dehydration or salt stress [25]. Quantitative real-time RT-PCR analysis showed that the transcripts of the *SsDREB* were induced by drought and salt stress but not by cold treatment, which is in agreement with previous reports describing the role of DREB factors in plant response to abiotic stress [4, 34]. However, the transcripts of the *SsDREB* were not induced by exogenous ABA application in *S. salsa* (Figure 5). Many studies showed that ABA phytohormone, whether endogenous or exogenous, is involved in several physiologic processes and in the adaptation of plants to different abiotic stresses and plays a crucial role in inducing the expression of some stress-responsive genes [35, 36]. Transcript accumulation of StDREB1 gene from potato (*Solanum tuberosum* L.) was significantly induced by exogenous application of 50 μM ABA, indicating that StDREB1 may function in an ABA-dependent signaling pathway [19]. The transcripts of the FeDREB1 from buckwheat were induced by low-/high-temperature treatment, drought stress, and exogenous ABA application [14]. However, several exceptions regarding this expression pattern have been reported. For instance, *Glycine max* GmDREB2A, a member of the DREB (A-2) group was highly induced not only by dehydration and heat but also by low temperature [37], and PeDREB2 from *Populus euphratica* was induced by drought and salt, as well as cold stress [38]. Moreover, a ZmDBP4, belonging to DREB (A-1) gene, was activated by cold and drought, but not ABA [39]. GmDREB2 and BpDREB2 were also reported not to be responsive to ABA treatment [32, 40]. Our research results indicated that *SsDREB* genes were not responsive to ABA treatment, which suggests that *SsDREB* genes are involved in the dehydration and salinity stress responses through ABA-independent pathways.

Morphological and physiological parameters are actual indicators of stress endurance of transgenic plants. The *SsDREB* transgenic plants imparted both salinity and dehydration tolerance with better morphological growth like larger leaf area and higher turgor maintenance pressure. In contrast to the data reported by Yamaguchi-Shinozaki and Shinozaki [41], the overexpression of StDREB1 gene in transgenic plants did not show any phenotypic changes such as dwarfism. Fluorescence-based photosynthetic activity of leaves plays an important role in adaptation to abiotic stress. Under salinity and dehydration stress, the *SsDREB* transgenic plants kept higher photosynthesis and chlorophyll fluorescence parameters than WT plants, revealing better abiotic stress tolerance.

During stress conditions, proline helps the plant cell by stabilizing subcellular structures such as membranes and proteins, scavenging free radicals and buffering cellular redox potential [42]. Previous studies reported that AtDREB1 could enhance the drought tolerance of transgenic Arabidopsis by activating the expression of downstream genes involved in sugar biosynthesis and proline biosynthesis [43]. Transgenic tobacco overexpressing *SsDREB* accumulated higher free proline and soluble sugar than WT plants under salinity and dehydration stress, revealing the improved salinity and drought tolerance of the transgenic plants. Similarly, overexpression of SbDREB in *Salicornia brachiata* [20] and OsDREB2A in rice [44] also resulted in higher accumulation of proline under salt stress.

The constitutive expression of *SsDREB* conferred improved tolerance to drought and salinity in transgenic plants, possibly because of the overexpression of stress-inducible DREB2-responsive genes. LEA proteins were quite hydrophilic and were believed to protect plant cells from these stresses. Furthermore, the activity of LEA genes was associated with cold stress in plants [45]. In this study, expression level of LEA5 increased significantly in transgenic plants, indicating that SsDREB had activated the expression of downstream genes like LEA5. The expression of glutathioneS-transferase (GST) and superoxide dismutase (SOD) was not high in transgenics, indicating that *SsDREB* was not responsive to oxidative stress.

In conclusion, a novel *SsDREB* transcription factor was cloned from *Suaeda salsa* andclassified in the A-6 group based on phylogenetic characterization. Yeast one-hybrid assays verified that SsDREB protein specifically binds to the DRE element. Real-time RT-PCR showed that *SsDREB* was significantly induced under salinity and drought stress. Overexpression of *SsDREB* cDNA in transgenic tobacco plants exhibited an improved salt and drought stress tolerance, suggesting that the *SsDREB* transcription factor is involved in the regulation of abiotic stress tolerance in tobacco by the activation of different downstream gene expression.

Conflict of Interests

The authors declare that there is no conflict of interests regarding the publication of this paper.

Authors' Contribution

Xu Zhang and Xiaoxue Liu contributed equally to this paper.

Acknowledgments

This work was financially supported by the National Science and Technology Major Project (2014ZX08002-005B), China Agriculture Research System (CARS-03-2-12), and the National Natural Science Foundation of China (31201201).

References

[1] Y. Sakuma, K. Maruyama, Y. Osakabe et al., "Functional analysis of an *Arabidopsis* transcription factor, DREB2A, involved in drought-responsive gene expression," *Plant Cell*, vol. 18, no. 5, pp. 1292–1309, 2006.

[2] E. A. Bray, J. Bailey-Serres, and E. Weretilnyk, "Responses to abiotic stresses," in *Biochemistry and Molecular Biology of Plants*, W. Gruissem, B. Buchannan, and R. Jones, Eds., American Society of Plant Biologists, Rockville, Md, USA, 2000.

[3] S. Ramanjulu and D. Bartels, "Drought- and desiccation-induced modulation of gene expression in plants," *Plant, Cell and Environment*, vol. 25, no. 2, pp. 141–151, 2002.

[4] P. K. Agarwal, P. Agarwal, M. K. Reddy, and S. K. Sopory, "Role of DREB transcription factors in abiotic and biotic stress tolerance in plants," *Plant Cell Reports*, vol. 25, no. 12, pp. 1263–1274, 2006.

[5] P. K. Agarwal, P. S. Shukla, K. Gupta, and B. Jha, "Bioengineering for salinity tolerance in plants: state of the art," *Molecular Biotechnology*, vol. 54, no. 1, pp. 102–123, 2013.

[6] K. Yamaguchi-Shinozaki and K. Shinozaki, "Transcriptional regulatory networks in cellular responses and tolerance to dehydration and cold stresses," *Annual Review of Plant Biology*, vol. 57, pp. 781–803, 2006.

[7] Y. Sakuma, Q. Liu, J. G. Dubouzet, H. Abe, K. Shinozaki, and K. Yamaguchi-Shinozaki, "DNA-binding specificity of the ERF/AP2 domain of *Arabidopsis* DREBs, transcription factors involved in dehydration- and cold-inducible gene expression," *Biochemical and Biophysical Research Communications*, vol. 290, no. 3, pp. 998–1009, 2002.

[8] Q. Wang, Y. Guan, Y. Wu, H. Chen, F. Chen, and C. Chu, "Overexpression of a rice *OsDREB1F* gene increases salt, drought, and low temperature tolerance in both *Arabidopsis* and rice," *Plant Molecular Biology*, vol. 67, no. 6, pp. 589–602, 2008.

[9] C.-T. Wang, Q. Yang, and C. T. Wang, "Isolation and functional characterization of ZmDBP2 encoding a dehydration-responsive element-binding protein in *Zea mays*," *Plant Molecular Biology Reporter*, vol. 29, no. 1, pp. 60–68, 2011.

[10] A. Karaba, S. Dixit, R. Greco et al., "Improvement of water use efficiency in rice by expression of HARDY, an *Arabidopsis* drought and salt tolerance gene," *Proceedings of the National Academy of Sciences of the United States of America*, vol. 104, no. 39, pp. 15270–15275, 2007.

[11] P. Xianjun, M. Xingyong, F. Weihong et al., "Improved drought and salt tolerance of Arabidopsis thaliana by transgenic expression of a novel DREB gene from *Leymus chinensis*," *Plant Cell Reports*, vol. 30, no. 8, pp. 1493–1502, 2011.

[12] C. Lata and M. Prasad, "Role of DREBs in regulation of abiotic stress responses in plants," *Journal of Experimental Botany*, vol. 62, no. 14, pp. 4731–4748, 2011.

[13] S. Matsukura, J. Mizoi, T. Yoshida et al., "Comprehensive analysis of rice DREB2-type genes that encode transcription factors involved in the expression of abiotic stress-responsive genes," *Molecular Genetics and Genomics*, vol. 283, no. 2, pp. 185–196, 2010.

[14] Z. W. Fang, X. H. Zhang, J. F. Gao et al., "A buckwheat (*Fagopyrum esculentum*) DRE-binding transcription factor gene, FeDREB1, enhances freezing and drought tolerance of transgenic Arabidopsis," *Plant Molecular Biology Reporter*, 2015.

[15] A. Sadhukhan, Y. Kobayashi, M. Tokizawa et al., "VuDREB2A, a novel DREB2-type transcription factor in the drought-tolerant legume cowpea, mediates DRE-dependent expression of stress-responsive genes and confers enhanced drought resistance in transgenic *Arabidopsis*," *Planta*, vol. 240, no. 3, pp. 645–664, 2014.

[16] D. Bouaziz, J. Pirrello, M. Charfeddine et al., "Overexpression of StDREB1 transcription factor increases tolerance to salt in transgenic potato plants," *Molecular Biotechnology*, vol. 54, no. 3, pp. 803–817, 2013.

[17] Y.-G. Shen, W.-K. Zhang, S.-J. He, J.-S. Zhang, Q. Liu, and S.-Y. Chen, "An EREBP/AP2-type protein in *Triticum aestivum* was a DRE-binding transcription factor induced by cold, dehydration and ABA stress," *Theoretical and Applied Genetics*, vol. 106, no. 5, pp. 923–930, 2003.

[18] A. H. A. Khedr, M. S. Serag, M. M. Nemat-Alla et al., "A DREB gene from the xero-halophyte *Atriplex halimus* is induced by osmotic but not ionic stress and shows distinct differences from glycophytic homologues," *Plant Cell, Tissue and Organ Culture*, vol. 106, no. 2, pp. 191–206, 2011.

[19] N. Liu, N.-Q. Zhong, G.-L. Wang et al., "Cloning and functional characterization of *PpDBF1* gene encoding a DRE-binding transcription factor from *Physcomitrella patens*," *Planta*, vol. 226, no. 4, pp. 827–838, 2007.

[20] K. Gupta, B. Jha, and P. K. Agarwal, "A dehydration-responsive element binding (DREB) transcription factor from the succulent halophyte *Salicornia brachiata* enhances abiotic stress tolerance in transgenic tobacco," *Marine Biotechnology*, vol. 16, no. 6, pp. 657–673, 2014.

[21] Z. Kefu, F. Hai, and I. A. Ungar, "Survey of halophyte species in China," *Plant Science*, vol. 163, no. 3, pp. 491–498, 2002.

[22] B. Wang, U. Lüttge, and R. Ratajczak, "Specific regulation of SOD isoforms by NaCl and osmotic stress in leaves of the C_3 halophyte *Suaeda salsa* L," *Journal of Plant Physiology*, vol. 161, no. 3, pp. 285–293, 2004.

[23] M. A. Larkin, G. Blackshields, N. P. Brown et al., "Clustal W and Clustal X version 2.0," *Bioinformatics*, vol. 23, no. 21, pp. 2947–2948, 2007.

[24] K. Tamura, D. Peterson, N. Peterson, G. Stecher, M. Nei, and S. Kumar, "MEGA5: molecular evolutionary genetics analysis using maximum likelihood, evolutionary distance, and maximum parsimony methods," *Molecular Biology and Evolution*, vol. 28, no. 10, pp. 2731–2739, 2011.

[25] Q. Liu, M. Kasuga, Y. Sakuma, H. Abe, S. Miura, and K. Yamaguchi-Shinozaki, "Two transcription factors, DREB1 and DREB2, with an EREBP/AP2 DNA binding domain separate two cellular signal transduction pathways in drought- and low-temperature-responsive gene expression, respectively, in Arabidopsis," *Plant Cell*, vol. 10, pp. 1391–1406, 1998.

[26] K. J. Livak and T. D. Schmittgen, "Analysis of relative gene expression data using real-time quantitative PCR and the 2-DDCT method," *Methods*, vol. 25, pp. 402–408, 2001.

[27] R. B. Horsch, J. E. Fry, N. L. Hoffmann, D. Eichholtz, S. G. Rogers, and R. T. Fraley, "A simple and general method for transferring genes into plants," *Science*, vol. 227, no. 4691, pp. 1229–1230, 1985.

[28] M.-L. Zhou, J.-T. Ma, Y.-M. Zhao, Y.-H. Wei, Y.-X. Tang, and Y.-M. Wu, "Improvement of drought and salt tolerance in *Arabidopsis* and *Lotus corniculatus* by overexpression of a novel DREB transcription factor from *Populus euphratica*," *Gene*, vol. 506, no. 1, pp. 10–17, 2012.

[29] K. R. Jaglo, S. Kleff, K. L. Amundsen et al., "Components of the Arabidopsis C-repeat/dehydration-responsive element binding

factor cold-response pathway are conserved in *Brassica napus* and other plant species," *Plant Physiology*, vol. 127, no. 3, pp. 910–917, 2001.

[30] J. G. Dubouzet, Y. Sakuma, Y. Ito et al., "*OsDREB* genes in rice, *Oryza sativa* L., encode transcription activators that function in drought-, high-salt- and cold-responsive gene expression," *Plant Journal*, vol. 33, no. 4, pp. 751–763, 2003.

[31] X. Wang, J. Dong, Y. Liu, and H. Gao, "A novel dehydration-responsive element-binding protein from *Caragana korshinskii* is involved in the response to multiple abiotic stresses and enhances stress tolerance in transgenic tobacco," *Plant Molecular Biology Reporter*, vol. 28, no. 4, pp. 664–675, 2010.

[32] J. Sun, X. Peng, W. Fan, M. Tang, J. Liu, and S. Shen, "Functional analysis of BpDREB2 gene involved in salt and drought response from a woody plant *Broussonetia papyrifera*," *Gene*, vol. 535, no. 2, pp. 140–149, 2014.

[33] Z. F. Cao, J. Li, F. Chen, Y. Q. Li, H.-M. Zhou, and Q. Liu, "Effect of two conserved amino acid residues on DREB1A function," *Biochemistry (Moscow)*, vol. 66, no. 6, pp. 623–627, 2001.

[34] L. Mondini, M. Nachit, E. Porceddu, and M. A. Pagnotta, "Identification of SNP mutations in DREB1, HKT1, and WRKY1 genes involved in drought and salt stress tolerance in durum wheat (*Triticum turgidum L. var durum*)," *OMICS*, vol. 16, no. 4, pp. 178–187, 2012.

[35] P. E. Verslues and J.-K. Zhu, "Before and beyond ABA: upstream sensing and internal signals that determine ABA accumulation and response under abiotic stress," *Biochemical Society Transactions*, vol. 33, no. 2, pp. 375–379, 2005.

[36] T. Hirayama and K. Shinozaki, "Perception and transduction of abscisic acid signals: keys to the function of the versatile plant hormone ABA," *Trends in Plant Science*, vol. 12, no. 8, pp. 343–351, 2007.

[37] J. Mizoi, T. Ohori, T. Moriwaki et al., "GmDREB2A, a canonical dehydration-responsive element binding protein2-type transcription factor in soybean, is post translationally regulated and mediates dehydration-responsive element-dependent gene expression," *Plant Physiology*, vol. 161, pp. 346–361, 2013.

[38] L. Mondini, M. M. Nachit, E. Porceddu, and M. A. Pagnotta, "HRM technology for the identification and characterization of INDEL and SNPs mutations in genes involved in drought and salt tolerance of durum wheat," *Plant Genetic Resources: Characterisation and Utilisation*, vol. 9, no. 2, pp. 166–169, 2011.

[39] C.-T. Wang, Q. Yang, and Y.-M. Yang, "Characterization of the ZmDBP4 gene encoding a CRT/DRE-binding protein responsive to drought and cold stress in maize," *Acta Physiologiae Plantarum*, vol. 33, no. 2, pp. 575–583, 2011.

[40] X.-P. Li, A.-G. Tian, G.-Z. Luo, Z.-Z. Gong, J.-S. Zhang, and S.-Y. Chen, "Soybean DRE-binding transcription factors that are responsive to abiotic stresses," *Theoretical and Applied Genetics*, vol. 110, no. 8, pp. 1355–1362, 2005.

[41] K. Yamaguchi-Shinozaki and K. Shinozaki, "Characterization of the expression of a desiccation-responsive *rd29* gene of *Arabidopsis thaliana* and analysis of its promoter in transgenic plants," *MGG Molecular & General Genetics*, vol. 236, no. 2-3, pp. 331–340, 1993.

[42] M. Ashraf and M. R. Foolad, "Roles of glycine betaine and proline in improving plant abiotic stress resistance," *Environmental and Experimental Botany*, vol. 59, no. 2, pp. 206–216, 2007.

[43] Y. Ito, K. Katsura, K. Maruyama et al., "Functional analysis of rice DREB1/CBF-type transcription factors involved in cold-responsive gene expression in transgenic rice," *Plant and Cell Physiology*, vol. 47, no. 1, pp. 141–153, 2006.

[44] M. Cui, W. Zhang, Q. Zhang et al., "Induced over-expression of the transcription factor OsDREB2A improves drought tolerance in rice," *Plant Physiology and Biochemistry*, vol. 49, no. 12, pp. 1384–1391, 2011.

[45] A. Tunnacliffe and M. J. Wise, "The continuing conundrum of the LEA proteins," *Naturwissenschaften*, vol. 94, no. 10, pp. 791–812, 2007.

Review Article

The Calcium Sensor CBL-CIPK Is Involved in Plant's Response to Abiotic Stresses

S. M. Nuruzzaman Manik,[1,2] Sujuan Shi,[1,3] Jingjing Mao,[1,2] Lianhong Dong,[1,2] Yulong Su,[1,2] Qian Wang,[1] and Haobao Liu[1]

[1]*Key Laboratory of Tobacco Biology and Processing, Tobacco Research Institute of CAAS, Ministry of Agriculture, Qingdao 266101, China*
[2]*Chinese Academy of Agricultural Sciences, Beijing 100081, China*
[3]*Qingdao Agricultural University, Qingdao 266109, China*

Correspondence should be addressed to Qian Wang; wangqian01@caas.cn and Haobao Liu; liuhaobao@caas.cn

Received 18 June 2015; Accepted 3 August 2015

Academic Editor: Marián Brestič

Abiotic stress halts the physiological and developmental process of plant. During stress condition, CBL-CIPK complex is identified as a primary element of calcium sensor to perceive environmental signals. Recent studies established that this complex regulates downstream targets like ion channels and transporters in adverse stages conditions. Crosstalks between the CBL-CIPK complex and different abiotic stresses can extend our research area, which can improve and increase the production of genetically modified crops in response to abiotic stresses. How this complex links with environmental signals and creates adjustable circumstances under unfavorable conditions is now one of the burning issues. Diverse studies are already underway to delineate this signalling mechanism underlying different interactions. Therefore, up to date experimental results should be concisely published, thus paving the way for further research. The present review will concisely recapitulate the recent and ongoing research progress of positive ions (Mg^{2+}, Na^{+}, and K^{+}), negative ions (NO_3^{-}, PO_4^{-}), and hormonal signalling, which are evolving from accumulating results of analyses of CBL and CIPK loss- or gain-of-function experiments in different species along with some progress and perspectives of our works. In a word, this review will give one step forward direction for more functional studies in this area.

1. Introduction

Unlike animals, plants are not mobile organism and cannot go away from adverse environmental conditions. Owing to these reasons, they create special system to adjust themselves in external stress conditions through instant transmit signals. Due to the temporary fluctuations in cytosolic calcium concentration, plant cells receive the signals from external stimuli, so they can accept the signals using their own machineries and decode the signals to secondary messenger [1–4]. Calcium is broadly well known as a ubiquitous secondary messenger because of its diverse functions in plants. Ca^{2+} is encoded in various stimuli of abiotic and biotic stresses. Abiotic stresses caused by high magnesium, high sodium, low potassium, low phosphorus, ABA, and others affect the rate of germination, photosynthesis, seedling growth, leaf expansion, total biomass accumulation, and overall growth effects of plants [5, 6].

In recent decades, Calcineurin B-like (CBL) protein-CBL-interacting protein kinase (CIPK) complex is widely accepted as Ca^{2+} signalling mechanism, which is involved in response to different external stresses signals [5, 7]. In adverse stresses conditions, plants evolve a stress signal that is specifying Ca^{2+} signature [8–10]. The specific Ca^{2+} signatures are received by closely controlled activities of plasma membrane and other organelles channels and transporters [1, 10–12]. In addition, this signature binds to EF hands domains of the CBL proteins. Consequently, the CBL proteins bind the NAF/FISL domain of C-terminal of the CIPK, thus stimulating the kinase [13]. On the other hand, N-terminal of the CBL protein

directs the CBL-CIPK system to an exact cellular target region ensuing in the stimulated CIPK phosphorylating the proper target proteins [11, 14–17].

Bioinformatics and comparative genomic analyses in plants have provided details about the sequence specificity, conservation, function and complexity, and ancestry's history of CBL and CIPK proteins families from lower plants to higher plants. Bioinformatics research reports showed that *Arabidopsis thaliana* has 10 CBLs and 26 CIPKs [13] while in other plants *Populus trichocarpa* has 10 CBLs and 27 CIPKs [18], *Oryza sativa* has 10 CBLs and 31 CIPKs [19], *Zea mays* has 8 CBLs and 43 CIPKs [19], *Vitis vinifera* has 8 CBLs and 21 CIPKs [20], *Sorghum bicolor* has 6 CBLs and 32 CIPKs [20], and *Nicotiana sylvestris* has 12 CBLs and 37 CIPKs (unpublished). Recently some reviewers have focused on functions, structural features, gene expression, and regulation of the CBL-CIPK complex with different pathways [20–24]. Although some reviewers have described the mechanisms, functions, and interaction between the CBL and CIPK, their functional mechanism and regulation with calcium are yet unclear. There is still a huge need to synthesize and understand ongoing findings from current CBL and CIPK studies, so that signalling systems research can be fully harnessed [5, 25–27]. This review will briefly present underlying mechanism of the CBL-CIPK in response to different environmental stresses with emphasis on important pathways. Indeed, it will recap the recent discoveries of these signalling components along with ongoing research progress.

2. CBL-CIPK Signalling System Responses to Environmental Stresses

Mutants studies of *Arabidopsis* have demonstrated that the CBL-CIPK complexes are involved in mediating Ca^{2+} signals elicited by different stresses, such as low magnesium, low potassium, high salt, nitrate, low phosphorus, ABA, high pH, cold, and osmotic stress [4, 14, 15, 28–32]. Crosstalk between the CBL-CIPK network and other pathways can limit the distances of improving the tolerant crops in adverse conditions. Different pathways like Mg^{2+}, Na^{+}, K^{+}, NO_3^{-}, PO_4^{-}, and ABA are now burning issues for abiotic stresses. Overexpressing the CBL/CIPK complex in plants might develop their tolerance to concurrently occurring different abiotic stresses and enhance the yield [33]. This complex can posttranslationally phosphorylate its downstream target proteins like transcriptional factors and nutrient pathway to respond to different external environmental stimuli, and thus plant can adapt to unfavorable condition.

To date, research on the CBL-CIPK system has shown that influx/efflux mechanisms of different ions are involved to create an adjustable condition under unfavorable stages in cell. Next session will briefly discuss the mechanism of different pathways.

2.1. Magnesium Signalling. Maintaining Ca^{2+}/Mg^{2+} homeostasis is not only critical for sufficient supply of mineral nutrients [34] but also important for serpentine-tolerant plants [35].

Recently, a new function has been identified for the CBL-CIPK signalling network in vacuole-mediated detoxification of high external Mg^{2+} [36]. Analysis of double mutant functions of CBL2 and CBL3 (*cbl2-cbl3*) revealed that they are regulating vacuole-mediated Mg^{2+} ion homeostasis in cell [36]. The *cbl2-cbl3* double mutant was hypersensitive to high concentrations of external Mg^{2+} condition, and also ionic profiles analysis showed that a reduced amount of Mg^{2+} accumulation was found in the *cbl2-cbl3* double mutant plants. Tang et al. found that CIPK3/9/23/26 physically interacted with the CBL2/3 on the tonoplast, and the multiple *cipks 3/9/23/26* mutant could fully show hypersensitivity of Mg^{2+}, and a similar ionic profile was found as like as the *cbl2-3* mutant [36, 37]. These results strongly suggested that the CIPK3/9/23/26 work together with the CBL2/3 at the tonoplast to alleviate the toxic effects of external high Mg^{2+} concentrations via vacuolar sequestration, but it is not clear which pairs of CBL-CIPK play a vital role in this pathway (Figure 2) [36].

Transporter family AtMHX was the first identified plant Mg^{2+}/H^{+} antiporter localized on the tonoplast, which apparently contributes to vacuolar Mg^{2+} uptake [38], and also MGT2 and MGT3 are known as Mg^{2+} transporters localized on the tonoplast [39], but mutant results did not show significant phenotypic changes under high Mg^{2+} conditions [36]. Thus there is further identification of the transporters which are activated under Mg^{2+} toxicity conditions, which are a key step to understand the underlying mechanism of this ion detoxification in plants.

2.2. Sodium Signalling. The salt overly sensitive (SOS) pathway is the first identified CBL-CIPK pathway for maintaining ion homeostasis in plant cells [40]. Genetic and biochemical tactics with SOS mutants presented a molecular mechanism in which the CBL-CIPK complex mediates the salt stress-induced Ca^{2+} signal and shows tolerance to salt [41]. Under salt stress situation, this pathway can enhance salt tolerance in plant by multiple ways; for example, it can allow transporter to send back Na^{+} into soil, sequester sodium ion into vacuole, or transport it to the older leaves [24]. The SOS pathway is mainly based on SOS3 (AtCBL4), SOS2 (AtCIPK24), and the plasma membrane Na^{+}/K^{+} antiporter; SOS1, a combined component pathway, plays a vital role in effluxing Na^{+} from the cell through SOS1; thus it can enhance the salt tolerance of plants [40]. In salt stress condition, plants can form SOS3-SOS2 complex in their roots and permit the SOS2 to phosphorylate and activate the SOS1 [40]. If plants are unable to activate SOS1 (such as *sos3* mutants), which can store extra Na^{+} through a reduced efflux capacity, thus they inhibit growth under salty conditions [14].

Different CBLs can interact with the CIPK24 and therefore form a complexity system in response to salt stress. External salt stresses trigger the AtCBL4/SOS3-AtCIPK24/SOS2 complex to stimulate Na^{+}/H^{+} exchange activity of the SOS1 (Figure 1) [42], which can exclude cell from extra Na^{+} [40]. *AtCBL10*, one of the CBL family members, was later included in the salt tolerance pathway. It is thought that tonoplast Na^{+}/H^{+} NHX antiporters are activated by

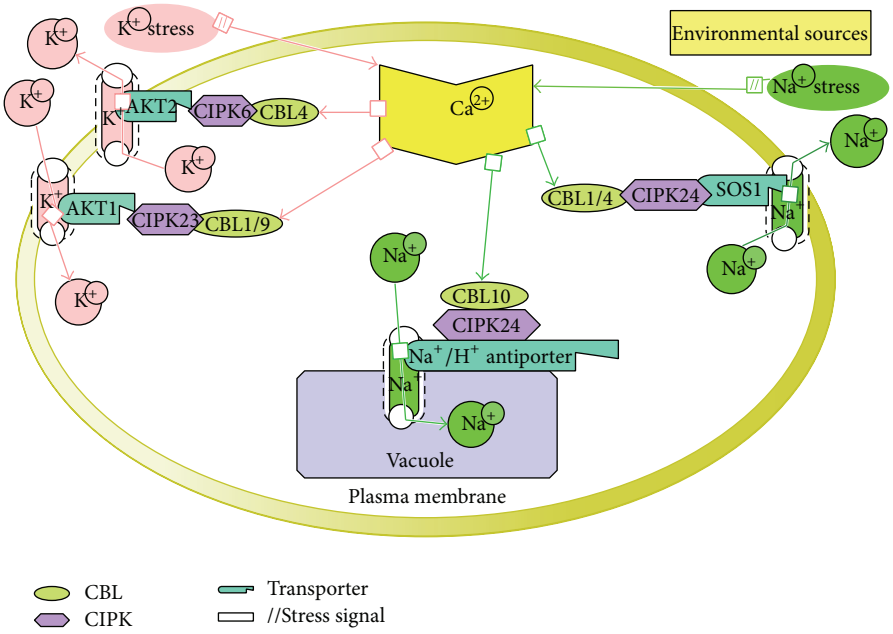

Figure 1: This model represents the identified CBLs-CIPKs interactions process and how they respond to abiotic stresses from environmental sources and maintain homeostasis in cell. All signals are centrally controlled by Ca^{2+}. Different colors indicate different pathways. AKT1: *Arabidopsis* K^+ transporter 1, AKT2: *Arabidopsis* K^+ transporter 2, and SOS1: salt overly sensitive 1. Mechanism in short: environmental stresses trigger Ca^{2+}; Ca^{2+} transmits signal to sensor molecule Calcineurin B-like (CBL) protein-CBL-interacting protein kinase (CIPK) to activate the transporters to create ion homeostasis in cell.

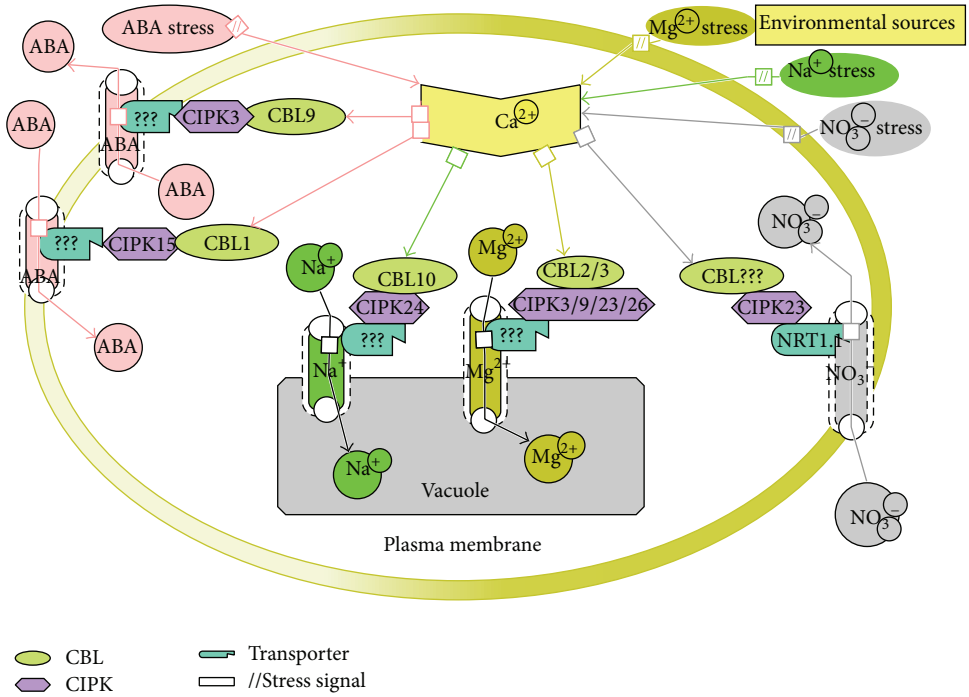

Figure 2: This model represents partially identified CBLs-CIPKs signalling system. Here, question marks (???) indicate that components have not yet been identified. Different colors indicate different pathways. NRT1.1: nitrate transporter 1.1.

the AtCIPK24/SOS2 through a mechanism related to the AtCBL10 to sequester intracellular extra Na^+ in the vacuole (Figure 1) [43]. Moreover, both CBL4/SOS3 and CBL10 are involved in mediating salt tolerance, but they perform their functions in different ways because of their distinct subcellular localizations and expression pattern.

Tissue specific and subcellular localization experiments showed that the CBL4/SOS3 works primarily in the roots and is localized at the plasma membrane, respectively [40]. Thus the CIPK24/SOS2 functions at the same place where it phosphorylates Na^+/H^+ antiporter SOS1, thereby enhancing Na^+ efflux rate [40]. Compared with the CBL10, it is expressed predominantly in the shoots and leaves and localized at the vacuolar membrane (tonoplast) [44]. It is postulated that the CIPK24/SOS2 employed by the CBL10 on the tonoplast may phosphorylate and activate as a yet unknown Na^+ channel or transporter, which is the tonoplast bound and performs a role in transporting cytoplasmic Na^+ into the vacuolar space (Figure 2). That assumption is supported by knockout *Arabidopsis* mutant *cbl10*, which showed the salt-sensitive phenotype specifically in the leaves or shoots and accumulated less Na^+ than the wild type under high salt conditions [44].

Additionally, other studies have shown that a calcium sensor, CBL1, can also interact with the CIPK24 to mediate the regulation of Na^+ in the plant cell (Figure 1) [13]. Thus *cbl1* mutant plants showed less tolerance to salt stress [45]. Subcellular localization assay demonstrated that the CBL1 is localized in the plasma membrane and interacted with the CIPK24/SOS2 as the CBL4/SOS3, and expression pattern analysis showed that it is expressed in the shoots and roots [45]. So, it can be said that Na^+ extrusion mediated by the CIPK24/SOS2-SOS1 system may also occur in the shoots.

Not only do CBLs show the salt sensitivity but also CIPKs are sensitive to salinity conditions. *Arabidopsis cipk6* was described to be more sensitive to salt stress compared to the wild type and it is thought that CIPK6 might be involved in salt tolerance [46]. Interaction between the CIPK6 and the CBL4/SOS3 was proved by yeast two-hybrid system, which indicated the participation of the CIPK6 in this pathway [16]. Possibly, the CBL4/SOS3 also targets the CIPK6 in vivo as well as the CIPK24/SOS2. Further research can shade more light on this complex mechanism involved in response to salt stress.

Apart from the experiments on *Arabidopsis*, recently, researchers have done some experiments on other species and tried to understand the salt pathway clearer. For instance, apple MdCIPK6L-OE conferred tolerance to salt [47] and its ectopic expression could functionally complement *Arabidopsis sos2* mutant, even though it was not homologous to the *Arabidopsis* CIPK24/SOS2 [47]. Besides MdCIPK6L-OE, *MdSOS2* was cloned from apple, which showed the highest similarity to the AtCIPK24/SOS2, and also it positively responds to salt stress and functionally complements the *Arabidopsis sos2* mutant [48]. The structural and functional analysis of BjSOS3 was established in the SOS pathway in *Brassica juncea* [49]. In rice OsCBL4 was the most homologous to the AtCBL4/SOS3 and it was able to functionally complement *sos3-1* mutant in *Arabidopsis*, indicating that it has the same function as the AtCBL4/SOS3 [50]. ZmCBL4 is the most similar to the OsCBL4 and it can also complement the *sos3-1* mutant in *Arabidopsis* [51]. In *Nicotiana sylvestris* CBL10 also showed salt sensitivity in *Arabidopsis*, which demonstrated more tolerance phenotype than wild type Colombia plants under salt stress condition (unpublished). Among the identified CBLs and CIPKs in response to salt stress, only a few have been implicated as negative regulators of salt pathway. For example, AtCBL1 and poplar (*Populus euphratica*) PeCBL1 were found to negatively influence Na^+ efflux from the cell under saline conditions while the mechanisms behind this are still unclear [52].

2.3. Potassium Signalling. Potassium (K^+) is one of the most important mineral nutrients, which participates in various plant physiological processes and governs yield of crop production. Plants recognize external K^+ fluctuations and create preliminary K^+ signal in root cells [53]. Root cell then transfers signals into cytoplasm, which signals are sensed by calcium sensors [53]. Since 1992, AKT1 is called a low affinity inwardly rectifying K^+ channel, which is involved in the cellular uptake of K^+ signal via calcium sensors [15, 31, 32, 55]. The calcium sensor CBL-CIPK acts as a regulator of the AKT1 to maintain the homeostasis of potassium in cell [31, 56].

If the amount of external K^+ became low, one of the CIPKs, CIPK23, is targeted to the plasma membrane, which is concurrently stimulated by CBL1 and CBL9 to phosphorylate the AKT1; thus movement of K^+ will be inwardly into the cells (Figure 1) [15, 31, 32, 56]. Experiments on mutants *cipk23*, *cbl1/cbl9*, and *akt1* showed similar reduced growth and chlorotic leaves under low K^+ conditions [15, 32, 36, 57]. It is hypothesized that the *cbl1/9* are functionally overlapped, because they individually did not show any significant differences. But their tissue specific localization assay demonstrated that they are expressed in root cells and aerial tissues, such as guard cells and vascular cells as like as localization of the AKT1 [15, 32]. Although the AKT1 expressed low level in hydathodes and stomatal guard cells, the AtCIPK23 may be regulated by the AtCBL1 or AtCBL9 in aerial tissue to redistribution of K^+, turgidity of guard cell, and repolarization of cell membrane [55, 58–60]. Instead of mutant experiments, AKT1 overexpressed (OE) *Arabidopsis* plants did not show any significant performance in growth when they were grown in low K^+ conditions, while At/PeCBL1, AtCBL9, and AtCIPK23 OE *Arabidopsis* plants gave comparative tolerance compared to control plants under the same condition [61, 62]. Recently overexpressed AtCIPK23 in potato [63], coexpression of AtCBL9-AtCIPK23-AKT1 in sugarcane [63, 64], OsCBL1-OsCIPK23-OsAKT1 in rice [64], VvCBL1-CIPK4-VvKT1.1 and VvCBL2-CIPK3-VvKT1.2 in grapevine (*Vitis vinifera*) [65] showed improved tolerance under the low potassium conditions. Moreover, the activity of AKT1 can be negatively regulated by a PP2C-type phosphatase AKT1-interacting PP2C1 (AIP1) [56]. Therefore, the CBL1/CBL9-CIPK23 complex can phosphorylate and activate the AKT1, but dephosphorylation by the AIP1 may regulate the deactivation of the AKT1 [56].

Another study showed that CBL4 interacts with CIPK6, so CBL4-CIPK6 complex is controlling the plasma

membrane targeting of the *Arabidopsis* K^+ channel AKT2 by facilitating translocation to the plasma membrane (Figure 1) [16]. In addition, alone the regulatory C-terminal domain of CIPK is sufficient to mediate the CBL4- and Ca^{2+}-dependent channel translocations from the ER membrane to the plasma membrane [66]. This interaction system of the CBL4 is accomplished through a unique targeting pathway that is dependent on the dual site (myristoylation and palmitoylation) [16]. Thus this is a unique system designated as a critical mechanism of ion-channel regulation, in which a calcium sensor controls K^+ channel activity by promoting the translocation of the channel to the plasma membrane [66] that is together in kinase interaction-dependent and phosphorylation-independent manner [16]. These studies suggest that the *Arabidopsis* K^+ channel AKT2 proficiently translocates to the plasma membrane through the CBL4- and Ca^{2+}-dependent targeting pathway that entails the scaffolding task and the kinase activity of the CIPK6. This is consistent with the hypothesis that there are multiple pathways for K^+ channel operating. Besides, CIPK9 responds to various abiotic stresses, such as salinity, osmotic stress, chilling, and cellular injury, and also it plays a critical role in plant tolerance to low K^+ [67]. The knockout T-DNA mutant lines of *cipk9* displayed a hypersensitive response to low K^+ conditions. However, further analysis specified that K^+ uptake and content were not affected in the mutant plants [67]. It has been inferred that the *Arabidopsis* CIPK9 might have a different mode of action than the CIPK23 and CIPK6. It is possible that unknown CBLs interact with the CIPK9 to regulate K^+ homeostasis by activating a vacuolar potassium channel [68]. It can also be hypothesized that the unknown CBLs may interact with different CIPKs to sense Ca^{2+} signals in low K^+ stress conditions [68]. Indeed, there is still needed further research to qualify this assumption.

2.4. Nitrate Signalling. Nitrogen is a key limiting element for crop production and overall plant growth. NO_3^- form of nitrogen, which is the principal nitrogen source of plants [69], research on NO_3^- uptake system, provides a test case to define the nutrient transport system to unravel plant nutrient acquisition signalling pathways. However, the molecular mechanisms of NO_3^- sensing and signalling have just started to be unraveled in *Arabidopsis thaliana*. The members of three nitrate transporter families, such as 53 of AtNRT1, 7 of AtNRT2, and 7 of AtCLC, have been identified in this plant [70–72]. Among the three families, four plasma membrane transporters members of AtNRT1 and AtNRT2 families are occupied in uptake of NO_3^- by root cells [72, 73]. Members of AtNRT2.1 and AtNRT2.2 are engaged in high-affinity uptake that drive either a high affinity (nitrate concentration < 1 mM) or a low affinity (nitrate concentration > 1 mM) [74, 75], and AtNRT1.2 is worked in low-affinity uptake whereas AtNRT1.1 (CHL1) is performed as a dual-affinity transporter involved in both high- and low-affinity uptake of NO_3^- [76, 77].

The CHL1 functions as a high-affinity nitrate transporter when threonine residue 101 (T101) is phosphorylated and as a low-affinity nitrate transporter when this residue is dephosphorylated [78, 79]. The first report of a potential role for the CHL1 in nitrate signalling originated from the studies of loss-of-function mutant (*chl1*) in *Arabidopsis*, which demonstrated that the CHL1 regulates the expression of AtNRT2.1 in response to nitrate stress [77]. In microarray system, it showed that AtCIPK23 was downregulated in the *chl1* mutant (Figure 2). However, the AtCIPK23 is not only the target of the AtNRT1.1-dependent signalling but also a regulator of the AtNRT1.1, which is responsible for its phosphorylation at the T101 residue [78]. The AtCIPK23 therefore governs both transport and signalling activities of AtNRT1.1, which infers that the incidence of retrocontrol loop for the AtNRT1.1-dependent gene acts in response to NO_3^-. Remarkably, the mechanisms leading to the AtCIPK23-mediated phosphorylation of the CHL1 are required to fully understand the possible role of the CHL1 in direct sensing of external nitrate.

In addition, *Arabidopsis* CBL9 is required to activate the AtCIPK23 to mediate the phosphorylation of CHL1 for high-affinity nitrate transportation but the activity of this signalling system remains obscure [80]. Transcriptomic study presented that *Arabidopsis* CIPK8 is involved as a low-affinity nitrate response under stress conditions [81]. Results of continuous experiments on *cipk8* mutant lines showed that the AtCIPK8 is involved in long-term nitrate-regulated root growth and it positively sets the primary nitrate response. In short, the *Arabidopsis* CIPK8 precise regulation of AtNRT1.1 is still unclear and needs further analysis [81].

2.5. Phosphorus Signalling. Phosphorus is known as a secondary macronutrient in plant [82]. Pi (inorganic phosphorus) form of phosphorus is readily absorbed by plants in phosphorous deficient condition [83]. Pi is involved in controlling major enzymatic reactions and switching the metabolic pathways [84]. A report by Chen et al. has published that the CBL-CIPK system is involved during the response to low Pi in *Brassica napus*. Under Pi deficient conditions, BnCBL1 and BnCIPK6 were upregulated and both proteins can interact with each other in yeast two-hybrid screens and split-YFP system [85]. Under low Pi treatment, overexpression of either BnCBL1 or BnCIPK6 showed better plant growth and accumulated more biomass in *Arabidopsis*, mostly found in the lateral roots development [85]. So, the BnCBL1 and BnCIPK6 might control the processes involved in the plant's response to Pi deficiencies, even though the mechanism and pathways are still unknown. It is not clear whether AtCIPK6 is involved in low Pi pathway, though the complementary experiment of the BnCIPK6 with *cipk6* mutant showed that it also responded to low Pi treatment. There is still need for further research in this area [57, 85].

3. Hormonal Signalling

Abscisic acid (ABA) is one of the most essential phytohormones in plants. It performs different roles in plants ranging from seed germination to growth and development as well as responses to abiotic stresses [86]. A specific Ca^{2+} signature responder is found in an early step of the ABA signalling pathways system [87–89], which implies that Ca^{2+} sensors

are involved in this signalling pathway. Moreover, studies on several overexpressed/mutant lines of CBL/CIPK inferred that the CBL-CIPK system is involved in the ABA signalling pathway (Figure 2).

Although the ABA signalling pathways are mainly regulated by two ways, such as ABA-dependent and ABA-independent ways, which are simultaneously controlled stress-responsive genes, ABA-dependent pathway shows a vital role in regulating osmotic stress-responsive genes [90]. The *Arabidopsis* mutant plants lacking CBL9 (*cbl9*) displayed hypersensitivity to ABA in the early developmental stages, such as seed germination and postgermination seedling growth [4]. Experimental results also showed that the *cbl9* accumulated much higher levels of ABA than the control plants under stress conditions [4]. Therefore, the AtCBL9 performs as a negative regulator in abscisic acid signalling [4]. Besides, the expression of AtCIPK3 is induced by cold, high salt, wounding, drought, and ABA. Seed germination analyses of *cipk3* mutants indicated that these lines were more inhibited by the ABA than wild type plants, and results indicated that the AtCIPK3 functions as a negative regulator in ABA signalling during seed germination [91]. It was also demonstrated that the AtCBL9 can form a specific complex with the AtCIPK3 to act together in regulating the ABA responses [92] and suggesting that the AtCBL9-CIPK3 complex negatively regulates the ABA signalling during seed germination (Figure 2) [92].

Furthermore, CBL1 is the most similar isoform of the CBL9 in *Arabidopsis*. Evaluation of the CBL1 function based on loss-of-function mutant showed that (*cbl1*) lines are hypersensitive to abiotic stresses [28, 45]. The *cbl1* did not show significant changes in response to the ABA, but CBL1 and CBL9 mutant lines both displayed less tolerance to drought and salt stress [28, 45]. These results indicated that the CBL1 is not involved in the ABA signalling system dissimilar to the CBL9. Meanwhile, it is remarkable to note that CIPK1 can interact with the CBL1 and CBL9, which mediates ABA responses as well as osmotic stress, drought, and salt responses. Above those factors infer that CBL1-CIPK1 complex is involved in the ABA-dependent way; however CBL9-CIPK1 complex is occupied in the ABA-independent way in *Arabidopsis* [29]. One more research informed that knockdown *cbl1* and *cipk15* generated an ABA-hypersensitive phenotype [93]. Thus CBL1-CIPK15 complex works as a negative regulator in the ABA signalling pathway (Figure 2) [93]. A recent study found that CIPK6 loss-of-function lines (*cipk6*) accumulated high level of ABA in seedlings after treatment, compared to the primary level of expression. This finding implies that the CIPK6 is also involved in responses to ABA [46].

Very few reports have been published of interaction between GA and CBL-CIPK. Research showed that rice CBL gene OsCBL2 was upregulated by gibberellin acid in the aleurone layer in rice [94]. It also showed that this CBL is positively regulating the GA pathway. Using microarray analyses and RNA blots, they have found that the upregulation of the OsCBL2 expression occurs within specific time period after GA treatment [94]. Taken together, these data indicate that CBL-CIPK system plays an important role in the hormonal signalling pathway.

4. Conclusions and Perspectives

Studies on CBLs and CIPKs over the past few years have greatly advanced our knowledge of the function of single proteins in distinct physiological processes. Major advances in our understanding of this signalling system have been made possible by the identification of an increasing number of targets regulated by the CBL-CIPK complexes.

The unraveling of the crosstalk among different pathways will provide more information about the physiological responses of plants, including transpiration, germination of seeds, seedlings growth, and uptake of mineral nutrient under different stress conditions. The progress of the research on the CBL and CIPK families in different plant species other than *Arabidopsis thaliana* is still at an infant stage; in most cases it is limited to interaction studies and expression analyses of these families. Recently, some experiments have been done on the CBL-CIPK complex on poplar, rice, pea, and maize [27]; which experiments indicate an overall participation studies of the research on CBL-CIPK in responses to different abiotic stresses. A few members of the CBLs and CIPKs from above species have been functionally identified, and expression profile has been done in response to stresses, such as salt, drought, cold, and plant hormones [50, 51, 95–98].

Future research should put emphasis on identifying further signalling components over a period generation of mutants by gene knockout approaches and subsequent dissecting of gene functions. Fascinating new insights and prospects are emerging as a result of the increasing number of available genome sequences, which will assist the investigation of the ancestries and functional diversification of these calcium sensors and their interacting protein kinases into the extant complex interaction network. The mechanisms conferring this complex interaction specify the regulatory capabilities to rely on the intermolecular interactions between CBLs and CIPKs [99]. The CBL-CIPK signalling model emphasizes the importance of future research that focuses on the molecular mechanisms underlying the regulation of transporters that allow us to better understand plant's response to abiotic stress and also establish a proficient method of identifying molecular targets for genetically engineered resistant crops with enhanced tolerance to various environmental stresses. Therefore, the most important challenge for future research is not only functional thesis but also the elucidating of the details of synergistic functions in this interaction network and revealing of the molecular mechanisms of the complexes regulating target proteins.

Conflict of Interests

The authors declare that there is no conflict of interests regarding the publication of this paper.

Acknowledgments

The authors thank Professor Guanshan Liu, Professor Yongfeng Guo, Professor Yingzhen Kong, Ali Akhtar, and Marowa Prince (Tobacco Research Institute, Chinese Academy of Agricultural Sciences) for providing them with valuable suggestions. This work was supported by Central Research Institute of Basic Public Welfare Funds of China (2012ZL058) and the National Natural Science Foundation of China (31201489).

References

[1] O. Batistič and J. Kudla, "Analysis of calcium signaling pathways in plants," *Biochimica et Biophysica Acta—General Subjects*, vol. 1820, no. 8, pp. 1283–1293, 2012.

[2] V. Albrecht, O. Ritz, S. Linder, K. Harter, and J. Kudla, "The NAF domain defines a novel protein—protein interaction module conserved in Ca^{2+}-regulated kinases," *The EMBO Journal*, vol. 20, no. 5, pp. 1051–1063, 2001.

[3] J. Shi, K.-N. Kim, O. Ritz et al., "Novel protein kinases associated with calcineurin B-like calcium sensors in Arabidopsis," *The Plant Cell*, vol. 11, no. 12, pp. 2393–2405, 1999.

[4] G. K. Pandey, H. C. Yong, K.-N. Kim et al., "The calcium sensor calcineurin B-like 9 modulates abscisic acid sensitivity and biosynthesis in *Arabidopsis*," *The Plant Cell*, vol. 16, no. 7, pp. 1912–1924, 2004.

[5] J. Zhou, J. Wang, Y. Bi et al., "Overexpression of PtSOS2 enhances salt tolerance in transgenic poplars," *Plant Molecular Biology Reporter*, vol. 32, no. 1, pp. 185–197, 2014.

[6] R. Munns, D. P. Schachtman, and A. G. Condon, "The significance of a two-phase growth response to salinity in wheat and barley," *Australian Journal of Plant Physiology*, vol. 22, no. 4, pp. 561–569, 1995.

[7] Q. Yu, L. An, and W. Li, "The CBL–CIPK network mediates different signaling pathways in plants," *Plant Cell Reports*, vol. 33, no. 2, pp. 203–214, 2014.

[8] J. J. Rudd and V. E. Franklin-Tong, "Unravelling response-specificity in Ca^{2+} signalling pathways in plant cells," *New Phytologist*, vol. 151, no. 1, pp. 7–33, 2001.

[9] D. Sanders, J. Pelloux, C. Brownlee, and J. F. Harper, "Calcium at the crossroads of signaling," *The Plant Cell*, vol. 14, supplement 1, pp. S401–S417, 2002.

[10] A. N. Dodd, J. Kudla, and D. Sanders, "The language of calcium signaling," *Annual Review of Plant Biology*, vol. 61, pp. 593–620, 2010.

[11] O. Batistič, R. Waadt, L. Steinhorst, K. Held, and J. Kudla, "CBL-mediated targeting of CIPKs facilitates the decoding of calcium signals emanating from distinct cellular stores," *The Plant Journal*, vol. 61, no. 2, pp. 211–222, 2010.

[12] D. Sanders, C. Brownlee, and J. F. Harper, "Communicating with calcium," *The Plant Cell*, vol. 11, no. 4, pp. 691–706, 1999.

[13] Ü. Kolukisaoglu, S. Weinl, D. Blazevic, O. Batistic, and J. Kudla, "Calcium sensors and their interacting protein kinases: genomics of the *Arabidopsis* and rice CBL-CIPK signaling networks," *Plant Physiology*, vol. 134, no. 1, pp. 43–58, 2004.

[14] R. Quan, H. Lin, I. Mendoza et al., "SCABP8/CBL10, a putative calcium sensor, interacts with the protein kinase SOS2 to protect *Arabidopsis* shoots from salt stress," *The Plant Cell*, vol. 19, no. 4, pp. 1415–1431, 2007.

[15] Y. H. Cheong, G. K. Pandey, J. J. Grant et al., "Two calcineurin B-like calcium sensors, interacting with protein kinase CIPK23, regulate leaf transpiration and root potassium uptake in *Arabidopsis*," *The Plant Journal*, vol. 52, no. 2, pp. 223–239, 2007.

[16] K. Held, F. Pascaud, C. Eckert et al., "Calcium-dependent modulation and plasma membrane targeting of the AKT2 potassium channel by the CBL4/CIPK6 calcium sensor/protein kinase complex," *Cell Research*, vol. 21, no. 7, pp. 1116–1130, 2011.

[17] M. M. Drerup, K. Schlücking, K. Hashimoto et al., "The calcineurin B-like calcium sensors CBL1 and CBL9 together with their interacting protein kinase CIPK26 regulate the *Arabidopsis* NADPH oxidase RBOHF," *Molecular Plant*, vol. 6, no. 2, pp. 559–569, 2013.

[18] H. Zhang, W. Yin, and X. Xia, "Calcineurin B-like family in *Populus*: comparative genome analysis and expression pattern under cold, drought and salt stress treatment," *Plant Growth Regulation*, vol. 56, no. 2, pp. 129–140, 2008.

[19] X.-F. Chen, Z.-M. Gu, F. Liu, B.-J. Ma, and H.-S. Zhang, "Molecular analysis of rice *CIPKs* involved in both biotic and abiotic stress responses," *Rice Science*, vol. 18, no. 1, pp. 1–9, 2011.

[20] S. Weinl and J. Kudla, "The CBL–CIPK Ca^{2+}-decoding signaling network: function and perspectives," *New Phytologist*, vol. 184, no. 3, pp. 517–528, 2009.

[21] O. Batistič and J. Kudla, "Plant calcineurin B-like proteins and their interacting protein kinases," *Biochimica et Biophysica Acta (BBA)—Molecular Cell Research*, vol. 1793, no. 6, pp. 985–992, 2009.

[22] O. Batistic and J. Kudla, "Integration and channeling of calcium signalling through the CBL calcium sensor/CIPK protein kinase network," *Planta*, vol. 219, no. 6, pp. 915–924, 2004.

[23] R. Li, J. Zhang, J. Wei, H. Wang, Y. Wang, and R. Ma, "Functions and mechanisms of the CBL-CIPK signaling system in plant response to abiotic stress," *Progress in Natural Science*, vol. 19, no. 6, pp. 667–676, 2009.

[24] S. Luan, W. Lan, and S. Chul Lee, "Potassium nutrition, sodium toxicity, and calcium signaling: connections through the CBL–CIPK network," *Current Opinion in Plant Biology*, vol. 12, no. 3, pp. 339–346, 2009.

[25] M. Nagae, A. Nozawa, N. Koizumi et al., "The crystal structure of the novel calcium-binding protein AtCBL2 from *Arabidopsis thaliana*," *The Journal of Biological Chemistry*, vol. 278, no. 43, pp. 42240–42246, 2003.

[26] M. J. Sánchez-Barrena, M. Martínez-Ripoll, J.-K. Zhu, and A. Albert, "The structure of the *Arabidopsis thaliana* SOS3: molecular mechanism of sensing calcium for salt stress response," *Journal of Molecular Biology*, vol. 345, no. 5, pp. 1253–1264, 2005.

[27] M. Akaboshi, H. Hashimoto, H. Ishida et al., "The crystal structure of plant-specific calcium-binding protein AtCBL2 in complex with the regulatory domain of AtCIPK14," *Journal of Molecular Biology*, vol. 377, no. 1, pp. 246–257, 2008.

[28] Y. H. Cheong, K.-N. Kim, G. K. Pandey, R. Gupta, J. J. Grant, and S. Luan, "CBL1, a calcium sensor that differentially regulates salt, drought, and cold responses in *Arabidopsis*," *The Plant Cell*, vol. 15, no. 8, pp. 1833–1845, 2003.

[29] C. D'Angelo, S. Weinl, O. Batistic et al., "Alternative complex formation of the Ca^{2+}-regulated protein kinase CIPK1 controls abscisic acid-dependent and independent stress responses in *Arabidopsis*," *The Plant Journal*, vol. 48, no. 6, pp. 857–872, 2006.

[30] A. T. Fuglsang, Y. Guo, T. A. Cuin et al., "*Arabidopsis* protein kinase PKS5 inhibits the plasma membrane H^+-ATPase by preventing interaction with 14-3-3 protein," *The Plant Cell*, vol. 19, no. 5, pp. 1617–1634, 2007.

[31] L. Li, B.-G. Kim, Y. H. Cheong, G. K. Pandey, and S. Luan, "A Ca^{2+} signaling pathway regulates a K^+ channel for low-K response in Arabidopsis," *Proceedings of the National Academy of Sciences of the United States of America*, vol. 103, no. 33, pp. 12625–12630, 2006.

[32] J. Xu, H.-D. Li, L.-Q. Chen et al., "A protein kinase, interacting with two calcineurin B-like proteins, regulates K^+ transporter AKT1 in *Arabidopsis*," *Cell*, vol. 125, no. 7, pp. 1347–1360, 2006.

[33] G. Thapa, M. Dey, L. Sahoo, and S. K. Panda, "An insight into the drought stress induced alterations in plants," *Biologia Plantarum*, vol. 55, no. 4, pp. 603–613, 2011.

[34] T. Yamanaka, Y. Nakagawa, K. Mori et al., "MCA1 and MCA2 that mediate Ca^{2+} uptake have distinct and overlapping roles in *Arabidopsis*," *Plant Physiology*, vol. 152, no. 3, pp. 1284–1296, 2010.

[35] H. D. Bradshaw Jr., "Mutations in CAX1 produce phenotypes characteristic of plants tolerant to serpentine soils," *New Phytologist*, vol. 167, no. 1, pp. 81–88, 2005.

[36] R. J. Tang, F. Zhao, V. J. Garcia et al., "Tonoplast CBL–CIPK calcium signaling network regulates magnesium homeostasis in *Arabidopsis*," *Proceedings of the National Academy of Sciences*, vol. 112, no. 10, pp. 3134–3139, 2015.

[37] C. Gao, Q. Zhao, and L. Jiang, "Vacuoles protect plants from high magnesium stress," *Proceedings of the National Academy of Sciences*, vol. 112, no. 10, pp. 2931–2932, 2015.

[38] O. Shaul, D. W. Hilgemann, J. de-Almeida-Engler, M. van Montagu, D. Inzé, and G. Galili, "Cloning and characterization of a novel Mg^{2+}/H^+ exchanger," *The EMBO Journal*, vol. 18, no. 14, pp. 3973–3980, 1999.

[39] S. J. Conn, V. Conn, S. D. Tyerman, B. N. Kaiser, R. A. Leigh, and M. Gilliham, "Magnesium transporters, MGT2/MRS2-1 and MGT3/MRS2-5, are important for magnesium partitioning within *Arabidopsis thaliana* mesophyll vacuoles," *New Phytologist*, vol. 190, no. 3, pp. 583–594, 2011.

[40] Q.-S. Qiu, Y. Guo, M. A. Dietrich, K. S. Schumaker, and J.-K. Zhu, "Regulation of SOS1, a plasma membrane Na^+/H^+ exchanger in *Arabidopsis thaliana*, by SOS2 and SOS3," *Proceedings of the National Academy of Sciences of the United States of America*, vol. 99, no. 12, pp. 8436–8441, 2002.

[41] Z.-M. Pel, Y. Murata, G. Benning et al., "Calcium channels activated by hydrogen peroxide mediate abscisic acid signalling in guard cells," *Nature*, vol. 406, no. 6797, pp. 731–734, 2000.

[42] J.-K. Zhu, "Salt and drought stress signal transduction in plants," *Annual Review of Plant Biology*, vol. 53, pp. 247–273, 2002.

[43] N.-H. Cheng, J. K. Pittman, J. K. Zhu, and K. D. Hirschi, "The protein kinase SOS2 activates the Arabidopsis H^+/Ca^{2+} antiporter CAX1 to integrate calcium transport and salt tolerance," *The Journal of Biological Chemistry*, vol. 279, no. 4, pp. 2922–2926, 2004.

[44] B.-G. Kim, R. Waadt, Y. H. Cheong et al., "The calcium sensor CBL10 mediates salt tolerance by regulating ion homeostasis in Arabidopsis," *The Plant Journal*, vol. 52, no. 3, pp. 473–484, 2007.

[45] V. Albrecht, S. Weinl, D. Blazevic et al., "The calcium sensor CBL1 integrates plant responses to abiotic stresses," *The Plant Journal*, vol. 36, no. 4, pp. 457–470, 2003.

[46] L. Chen, Q.-Q. Wang, L. Zhou, F. Ren, D.-D. Li, and X.-B. Li, "Arabidopsis CBL-interacting protein kinase (CIPK6) is involved in plant response to salt/osmotic stress and ABA," *Molecular Biology Reports*, vol. 40, no. 8, pp. 4759–4767, 2013.

[47] R.-K. Wang, L.-L. Li, Z.-H. Cao et al., "Molecular cloning and functional characterization of a novel apple MdCIPK6L gene reveals its involvement in multiple abiotic stress tolerance in transgenic plants," *Plant Molecular Biology*, vol. 79, no. 1-2, pp. 123–135, 2012.

[48] D.-G. Hu, M. Li, H. Luo et al., "Molecular cloning and functional characterization of MdSOS2 reveals its involvement in salt tolerance in apple callus and Arabidopsis," *Plant Cell Reports*, vol. 31, no. 4, pp. 713–722, 2012.

[49] H. R. Kushwaha, G. Kumar, P. K. Verma, S. L. Singla-Pareek, and A. Pareek, "Analysis of a salinity induced BjSOS3 protein from *Brassica* indicate it to be structurally and functionally related to its ortholog from *Arabidopsis*," *Plant Physiology and Biochemistry*, vol. 49, no. 9, pp. 996–1004, 2011.

[50] J. Martínez-Atienza, X. Jiang, B. Garciadeblas et al., "Conservation of the salt overly sensitive pathway in rice," *Plant Physiology*, vol. 143, no. 2, pp. 1001–1012, 2007.

[51] M. Wang, D. Gu, T. Liu et al., "Overexpression of a putative maize calcineurin B-like protein in *Arabidopsis* confers salt tolerance," *Plant Molecular Biology*, vol. 65, no. 6, pp. 733–746, 2007.

[52] J.-L. Zhang, T. J. Flowers, and S.-M. Wang, "Mechanisms of sodium uptake by roots of higher plants," *Plant and Soil*, vol. 326, no. 1-2, pp. 45–60, 2010.

[53] Y. Wang and W.-H. Wu, "Potassium transport and signaling in higher plants," *Annual Review of Plant Biology*, vol. 64, pp. 451–476, 2013.

[54] E. Kiegle, C. A. Moore, J. Haseloff, M. A. Tester, and M. R. Knight, "Cell-type-specific calcium responses to drought, salt and cold in the Arabidopsis root," *Plant Journal*, vol. 23, no. 2, pp. 267–278, 2000.

[55] M. Nieves-Cordones, F. Caballero, V. Martínez, and F. Rubio, "Disruption of the *Arabidopsis thaliana* inward-rectifier K^+ channel AKT1 improves plant responses to water stress," *Plant and Cell Physiology*, vol. 53, no. 2, pp. 423–432, 2012.

[56] S. C. Lee, W.-Z. Lan, B.-G. Kim et al., "A protein phosphorylation/dephosphorylation network regulates a plant potassium channel," *Proceedings of the National Academy of Sciences of the United States of America*, vol. 104, no. 40, pp. 15959–15964, 2007.

[57] E. L. Thoday-Kennedy, A. K. Jacobs, and S. J. Roy, "The role of the CBL–CIPK calcium signalling network in regulating ion transport in response to abiotic stress," *Plant Growth Regulation*, vol. 76, no. 1, pp. 3–12, 2015.

[58] J. I. Schroeder, J. M. Ward, and W. Gassmann, "Perspectives on the physiology and structure of inward-rectifying K^+ channels in higher plants: biophysical implications for K^+ uptake," *Annual Review of Biophysics and Biomolecular Structure*, vol. 23, no. 1, pp. 441–471, 1994.

[59] A. Szyroki, N. Ivashikina, P. Dietrich et al., "KAT1 is not essential for stomatal opening," *Proceedings of the National Academy of Sciences of the United States of America*, vol. 98, no. 5, pp. 2917–2921, 2001.

[60] K. L. Dennison, W. R. Robertson, B. D. Lewis, R. E. Hirsch, M. R. Sussman, and E. P. Spalding, "Functions of AKT1 and AKT2 potassium channels determined by studies of single and double mutants of *Arabidopsis*," *Plant Physiology*, vol. 127, no. 3, pp. 1012–1019, 2001.

[61] G. Pilot, F. Gaymard, K. Mouline, I. Chérel, and H. Sentenac, "Regulated expression of Arabidopsis Shaker K^+ channel genes involved in K^+ uptake and distribution in the plant," *Plant Molecular Biology*, vol. 51, no. 5, pp. 773–787, 2003.

[62] H. Zhang, F. Lv, X. Han, X. Xia, and W. Yin, "The calcium sensor PeCBL1, interacting with PeCIPK24/25 and PeCIPK26,

regulates Na^+/K^+ homeostasis in *Populus euphratica*," *Plant Cell Reports*, vol. 32, no. 5, pp. 611–621, 2013.

[63] X. Wang, J. Li, X. Zou et al., "Ectopic expression of AtCIPK23 enhances tolerance against low-K^+ stress in transgenic potato," *American Journal of Potato Research*, vol. 88, no. 2, pp. 153–159, 2011.

[64] J. Li, L. Yu, G.-N. Qi et al., "The Os-AKT1 channel is critical for K^+ uptake in rice roots and is modulated by the rice CBL1-CIPK23 complex," *The Plant Cell*, vol. 26, no. 8, pp. 3387–3402, 2014.

[65] T. Cuéllar, F. Azeem, M. Andrianteranagna et al., "Potassium transport in developing fleshy fruits: the grapevine inward K^+ channel VvK1.2 is activated by CIPK-CBL complexes and induced in ripening berry flesh cells," *The Plant Journal*, vol. 73, no. 6, pp. 1006–1018, 2013.

[66] G. A. Tuskan, S. DiFazio, S. Jansson et al., "The genome of black cottonwood, *Populus trichocarpa* (Torr. & Gray)," *Science*, vol. 313, no. 5793, pp. 1596–1604, 2006.

[67] G. K. Pandey, Y. H. Cheong, B.-G. Kim, J. J. Grant, L. Li, and S. Luan, "CIPK9: a calcium sensor-interacting protein kinase required for low-potassium tolerance in *Arabidopsis*," *Cell Research*, vol. 17, no. 5, pp. 411–421, 2007.

[68] A. Amtmann and P. Armengaud, "The role of calcium sensor-interacting protein kinases in plant adaptation to potassium-deficiency: new answers to old questions," *Cell Research*, vol. 17, no. 6, pp. 483–485, 2007.

[69] N. M. Crawford, "Nitrate: nutrient and signal for plant growth," *The Plant Cell*, vol. 7, no. 7, pp. 859–868, 1995.

[70] A. D. Angeli, D. Monachello, G. Ephritikhine et al., "CLC-mediated anion transport in plant cells," *Philosophical Transactions of the Royal Society B: Biological Sciences*, vol. 364, no. 1514, pp. 195–201, 2009.

[71] B. G. Forde, "Nitrate transporters in plants: structure, function and regulation," *Biochimica et Biophysica Acta—Biomembranes*, vol. 1465, no. 1-2, pp. 219–235, 2000.

[72] Y.-F. Tsay, J. I. Schroeder, K. A. Feldmann, and N. M. Crawford, "The herbicide sensitivity gene CHL1 of *Arabidopsis* encodes a nitrate-inducible nitrate transporter," *Cell*, vol. 72, no. 5, pp. 705–713, 1993.

[73] A. Gojon, P. Nacry, and J.-C. Davidian, "Root uptake regulation: a central process for NPS homeostasis in plants," *Current Opinion in Plant Biology*, vol. 12, no. 3, pp. 328–338, 2009.

[74] W. Li, Y. Wang, M. Okamoto, N. M. Crawford, M. Y. Siddiqi, and A. D. M. Glass, "Dissection of the *AtNRT*2. 1: *AtNRT*2. 2 inducible high-affinity nitrate transporter gene cluster," *Plant Physiology*, vol. 143, no. 1, pp. 425–433, 2007.

[75] D. Y. Little, H. Rao, S. Oliva, F. Daniel-Vedele, A. Krapp, and J. E. Malamy, "The putative high-affinity nitrate transporter NRT2.1 represses lateral root initiation in response to nutritional cues," *Proceedings of the National Academy of Sciences of the United States of America*, vol. 102, no. 38, pp. 13693–13698, 2005.

[76] K.-H. Liu, C.-Y. Huang, and Y.-F. Tsay, "CHL1 is a dual-affinity nitrate transporter of Arabidopsis involved in multiple phases of nitrate uptake," *Plant Cell*, vol. 11, no. 5, pp. 865–874, 1999.

[77] R. Wang, D. Liu, and N. M. Crawford, "The Arabidopsis CHL1 protein plays a major role in high-affinity nitrate uptake," *Proceedings of the National Academy of Sciences of the United States of America*, vol. 95, no. 25, pp. 15134–15139, 1998.

[78] C.-H. Ho, S.-H. Lin, H.-C. Hu, and Y.-F. Tsay, "CHL1 functions as a nitrate sensor in plants," *Cell*, vol. 138, no. 6, pp. 1184–1194, 2009.

[79] K.-H. Liu and Y.-F. Tsay, "Switching between the two action modes of the dual-affinity nitrate transporter CHL1 by phosphorylation," *The EMBO Journal*, vol. 22, no. 5, pp. 1005–1013, 2003.

[80] G. Vert and J. Chory, "A toggle switch in plant nitrate uptake," *Cell*, vol. 138, no. 6, pp. 1064–1066, 2009.

[81] H.-C. Hu, Y.-Y. Wang, and Y.-F. Tsay, "AtCIPK8, a CBL-interacting protein kinase, regulates the low-affinity phase of the primary nitrate response," *The Plant Journal*, vol. 57, no. 2, pp. 264–278, 2009.

[82] D. P. Schachtman, R. J. Reid, and S. M. Ayling, "Phosphorus uptake by plants: from soil to cell," *Plant Physiology*, vol. 116, no. 2, pp. 447–453, 1998.

[83] R. L. Bieleski, "Phosphate pools, phosphate transport, and phosphate availability," *Annual Review of Plant Physiology*, vol. 24, no. 1, pp. 225–252, 1973.

[84] M. E. Theodorou and W. C. Plaxton, "Metabolic adaptations of plant respiration to nutritional phosphate deprivation," *Plant Physiology*, vol. 101, no. 2, pp. 339–344, 1993.

[85] L. Chen, F. Ren, L. Zhou, Q.-Q. Wang, H. Zhong, and X.-B. Li, "The Brassica napus Calcineurin B-Like 1/CBL-interacting protein kinase 6 (CBL1/CIPK6) component is involved in the plant response to abiotic stress and ABA signalling," *Journal of Experimental Botany*, vol. 63, no. 17, pp. 6211–6222, 2012.

[86] K. Nakashima and K. Yamaguchi-Shinozaki, "ABA signaling in stress-response and seed development," *Plant Cell Reports*, vol. 32, no. 7, pp. 959–970, 2013.

[87] G. J. Allen, S. P. Chu, C. L. Harrington et al., "A defined range of guard cell calcium oscillation parameters encodes stomatal movements," *Nature*, vol. 411, no. 6841, pp. 1053–1057, 2001.

[88] G. J. Allen, S. P. Chu, K. Schumacher et al., "Alteration of stimulus-specific guard cell calcium oscillations and stomatal closing in *Arabidopsis* det3 mutant," *Science*, vol. 289, no. 5488, pp. 2338–2342, 2000.

[89] J. Leung and J. Giraudat, "Abscisic acid signal transduction," *Annual Review of Plant Biology*, vol. 49, no. 1, pp. 199–222, 1998.

[90] V. Chinnusamy, K. Schumaker, and J.-K. Zhu, "Molecular genetic perspectives on cross-talk and specificity in abiotic stress signalling in plants," *Journal of Experimental Botany*, vol. 55, no. 395, pp. 225–236, 2004.

[91] K.-N. Kim, Y. H. Cheong, J. J. Grant, G. K. Pandey, and S. Luan, "CIPK3, a calcium sensor-associated protein kinase that regulates abscisic acid and cold signal transduction in *Arabidopsis*," *Plant Cell*, vol. 15, no. 2, pp. 411–423, 2003.

[92] G. K. Pandey, J. J. Grant, Y. H. Cheong, B.-G. Kim, L. G. Li, and S. Luan, "Calcineurin-B-like protein CBL9 interacts with target kinase CIPK3 in the regulation of ABA response in seed germination," *Molecular Plant*, vol. 1, no. 2, pp. 238–248, 2008.

[93] Y. Guo, L. Xiong, C.-P. Song, D. Gong, U. Halfter, and J.-K. Zhu, "A calcium sensor and its interacting protein kinase are global regulators of abscisic acid signaling in *Arabidopsis*," *Developmental Cell*, vol. 3, no. 2, pp. 233–244, 2002.

[94] Y.-S. Hwang, P. C. Bethke, H. C. Yong, H.-S. Chang, T. Zhu, and R. L. Jones, "A gibberellin-regulated calcineurin B in rice localizes to the tonoplast and is implicated in vacuole function," *Plant Physiology*, vol. 138, no. 3, pp. 1347–1358, 2005.

[95] S. Mahajan, S. K. Sopory, and N. Tuteja, "Cloning and characterization of CBL-CIPK signalling components from a legume (*Pisum sativum*)," *The FEBS Journal*, vol. 273, no. 5, pp. 907–925, 2006.

[96] Y. Xiang, Y. Huang, and L. Xiong, "Characterization of stress-responsive CIPK genes in rice for stress tolerance improvement," *Plant Physiology*, vol. 144, no. 3, pp. 1416–1428, 2007.

[97] Y. Yu, X. Xia, W. Yin, and H. Zhang, "Comparative genomic analysis of CIPK gene family in Arabidopsis and Populus," *Plant Growth Regulation*, vol. 52, no. 2, pp. 101–110, 2007.

[98] Z. Gu, B. Ma, Y. Jiang, Z. Chen, X. Su, and H. Zhang, "Expression analysis of the calcineurin B-like gene family in rice (*Oryza sativa* L.) under environmental stresses," *Gene*, vol. 415, no. 1-2, pp. 1–12, 2008.

[99] M. J. Sánchez-Barrena, M. Martínez-Ripoll, and A. Albert, "Structural biology of a major signaling network that regulates plant abiotic stress: the CBL-CIPK mediated pathway," *International Journal of Molecular Sciences*, vol. 14, no. 3, pp. 5734–5749, 2013.

Research Article

Changes in the Physiological Parameters of *SbPIP1*-Transformed Wheat Plants under Salt Stress

G. H. Yu, X. Zhang, and H. X. Ma

Provincial Key Laboratory of Agrobiology, Jiangsu Academy of Agricultural Sciences, Nanjing 210014, China

Correspondence should be addressed to H. X. Ma; hxma@jaas.ac.cn

Received 14 April 2015; Revised 24 June 2015; Accepted 25 June 2015

Academic Editor: Marián Brestič

The SbPIP1 gene is a new member of the plasma membrane major intrinsic gene family cloned from the euhalophyte *Salicornia bigelovii* Torr. In order to understand the physiological responses in plants that are mediated by the SbPIP1 gene, SbPIP1-overexpressing wheat lines and WT plants of the wheat cv. Ningmai 13 were treated with salt stress. Several physiological parameters, such as the proline content, the malondialdehyde (MDA) content, and the content of soluble sugars and proteins, were compared between SbPIP1-transformed lines and WT plants under normal growth or salt stress conditions. The results indicate that overexpression of the SbPIP1 gene can increase the accumulation of the osmolyte proline, decrease the MDA content, and enhance the soluble sugar biosynthesis in the early period but has no influence on the regulation of soluble protein biosynthesis in wheat. The results suggest that SbPIP1 contributes to salt tolerance by facilitating the accumulation of the osmolyte proline, increasing the antioxidant response, and increasing the biosynthesis of soluble sugar in the early period. These results indicate SbPIP1 plays an important role in the salt stress response. Overexpression of SbPIP1 might be used to improve the salt tolerance of important crop plants.

1. Introduction

Water uptake is a vital function of terrestrial plant roots for survival. The growth of terrestrial plants will be seriously inhibited when water uptake through the roots is reduced by water-related stress such as drought and salt stress. Aquaporins are involved in plant response to water-related stress [1–5]. Aquaporins are membrane intrinsic proteins with a molecular mass of approximately 30 kDa. Aquaporins belong to a major intrinsic protein (MIP) super family with six transmembrane helices that facilitate the permeation of water through biomembranes [6]. Plant aquaporins are mainly divided into two types according to their subcellular localization: plasma membrane intrinsic proteins (PIPs) and tonoplast membrane intrinsic proteins (TIPs) [7].

Overexpression of the *Arabidopsis* plasma membrane aquaporin (PIP1b) in transgenic tobacco plants increased the plant growth rate, transpiration rate, stomatal density, and photosynthetic efficiency under favorable growth conditions, whereas PIP1b overexpression had no beneficial effect under salt stress and even a negative effect during drought stress, causing faster wilting [8]. Yu et al. showed that overexpression of BnPIP1 from *Brassica napus* in transgenic tobacco plants resulted in an increased tolerance to water stress [9]. The aquaporin RWC3 was upregulated during a water deficit in upland rice and RWC3-transformed lowland rice plants showed an improved water status during a water deficit [10]. Gao et al. reported that the overexpression of a putative aquaporin gene from wheat, TaNIP, enhanced salt tolerance in transgenic *Arabidopsis* [11]. Zhou et al. reported that constitutive overexpression of the soybean plasma membrane intrinsic protein GmPIP1;6 confers salt tolerance [12]. Xu et al. reported that overexpression of MaPIP1;1 from banana in transgenic *Arabidopsis* plants confers drought and salt stress tolerance by maintaining osmotic balance, improving ion distribution, and reducing membrane injury [13]. Overexpression of MusaPIP2;6 enhanced the salt tolerance in transgenic banana plants and MusaPIP2;6-overexpressing banana plants displayed better photosynthetic efficiency and lower membrane damage under salt stress conditions [14].

Despite the increase in the number of reports demonstrating the roles of aquaporins in plant response to

environmental stresses, most studies have focused on the research of aquaporin function in glycophytes. Research on aquaporin function in halophytes is limited. Yamada et al. reported that the transcript accumulation of McMipA and McMipC (members of a family of MIP-related genes) was correlated with turgor recovery following salt-induced water stress in the ice plant (*Mesembryanthemum crystallinum*, moderate salt-tolerant) which is a halophyte; McMipA- and McMipB-encoded proteins expressed in *Xenopus* oocytes led to increased water permeability [15]. Decreases in the photosynthetic rate and stomatal conductance were less significant in McMIPB-overexpressing tobacco plants than in control plants when plants were grown under the soil water deficit condition [16].

Salicornia bigelovii Torr. is a euhalophyte that requires sodium (100 to 400 mM NaCl) for optimal growth. *S. bigelovii* can grow well with seawater irrigation, indicating that it has developed good molecular and physiological systems for adaptation to salt stress conditions. Therefore, *S. bigelovii* is a valuable model plant to characterize the genes responsible for water-related stress tolerance in plants. A new member of the plasma membrane major intrinsic gene family (*SbPIP1*) was cloned from *S. bigelovii* [17]. The *SbPIP1* gene was transformed into the wheat genome of cv. Ningmai 13 and the salt tolerance analysis of the transgenic lines during the germination period showed that the salt tolerance of the *SbPIP1*-transformed lines was better than that of Ningmai 13 [18]. We hypothesize that *SbPIP1* plays an important role under salt stress conditions.

The purpose of this study was to reveal the mechanism of enhanced salt tolerance mediated by the *SbPIP1* gene in plants. *SbPIP1*-overexpressing wheat lines and WT plants (Ningmai 13) were subjected to salt stress. Various physiological parameters, such as the proline content, the MDA content, and the contents of soluble sugars and soluble proteins, were compared between *SbPIP1*-transformed lines and WT plants under normal growth or salt stress conditions. Our results provide mechanistic details of salt tolerance conferred by the *SbPIP1* gene in correlation with the physiological changes observed. This study is the first report to explain the mechanism of enhanced salt tolerance in wheat, which is an important worldwide crop, mediated by an aquaporin gene from a halophyte.

2. Materials and Methods

2.1. Plant Material and Salt Stress Condition. Seeds from four transformed wheat lines (variety Ningmai 13) harboring the *SbPIP1* gene [18] were sown and raised inside a net house. Seedlings of the four transformed lines were tested using Basta spray for the selection of true transgenic plants and were raised for two months in the net house, after which they were transferred from pots to glass tubes (containing 40 mL of Hoagland's nutrient solution) and cultured in an incubator for 7 days under controlled conditions of 70%–75% relative humidity, 16 h of light, and an average temperature of 25°C. Seedlings of the Ningmai 13 variety (WT, wild type) were raised and cultured as the transgenic lines at the same time. In the salt stress treatment, Hoagland's nutrient solution was replaced with Hoagland's nutrient solution containing 250 mM NaCl in the glass tubes. The leaves from the WT and transgenic wheat plants were collected at 0, 1, 2, and 3 days and used for the experiments. In each treatment, the leaves of 3 seedlings were mixed and used for analysis. All the tests were carried out in triplicate.

2.2. Assay of Proline Content. The proline content in wheat leaves was estimated according to Shah and Dubey [19]. Fresh leaf samples (0.2 g) were homogenized in 5 mL of 3% aqueous sulphosalicylic acid and then centrifuged at 12,000 rpm for 10 min. Acid ninhydrin (2 mL) and glacial acetic acid (2 mL) were added to 2 mL of supernatant. The mixture was boiled in a water bath at 100°C for 1 h and then extracted with 4 mL of toluene. The absorbance of chromophore was measured at 520 nm using toluene as a blank. L-Proline (Merck) was used to construct the standard curve. The proline concentration (μg/g FW) was calculated as follows: proline content (μg) × extraction solution volume (mL)/sample volume (mL) × fresh leaf sample weight (g).

2.3. Measurement of MDA Content. Fresh leaf samples (0.2 g) were homogenized in 10 mL of 10% trichloroacetic acid and centrifuged at 12000 rpm for 10 min. The supernatant (2 mL) was added to 2 mL of 0.6% thiobarbituric acid (TBA) and incubated in a water bath at 100°C for 15 min. The mixture was centrifuged at 12,000 rpm for 10 min after it had cooled. The supernatant was measured at 532, 600, and 450 nm. The MDA content was calculated as follows: MDA content (uM) = 6.45 (OD532−OD600) − 0.56 OD 450.

2.4. Measurement of Soluble Protein Concentration. A standard curve for protein concentration was determined using the absorbance values of known concentrations of bovine serum albumin (0, 20, 40, 60, 80, and 100 μg) at 595 nm. Fresh leaf samples (0.2 g) were homogenized in 4.0 mL phosphate buffer (0.01 M, pH = 7.0), and centrifuged at 12,000 rpm for 10 min. 4 mL Coomassie brilliant blue G250 solution was added to the supernatant (2 mL). The light absorbance of the mixture was measured at 595 nm, and the protein concentration was calculated using the standard curve. The soluble protein concentration (mg/g FW) was calculated as follows: protein content (mg) × extraction solution volume (mL)/sample volume (mL) × fresh leaf sample weight (g).

2.5. Soluble Sugar Content Assay. A standard curve for sugar mass was created by using absorbance values of known concentrations of glucose (0, 20, 40, 60, 80, and 100 μg) at 620 nm. Fresh leaf samples (0.2 g) were homogenized in 4 mL of water, boiled in a water bath at 100°C for 30 min, and centrifuged at 12,000 rpm for 10 min. The supernatant was diluted with water to 10 mL, and a 0.2 mL aliquot of anthrone solution (0.5 g anthrone dissolved in 500 mL of 80% sulfuric acid solution) was added and then incubated at 100°C for 10 min. The absorbance values were measured at 620 nm and the sugar content was calculated using the standard curve. The soluble sugar concentration (%) was calculated as follows:

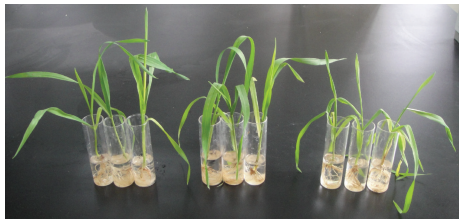

Figure 1: The influence of salt stress on transgenic lines and WT plants. 1: WT plants without stress; 2: transgenic lines D1 after 3 days of salt stress; 3: WT plants after 3 days of salt stress. WT represents the untransformed wheat variety Ningmai 13.

Table 1: Proline content in the WT plants and *SbPIP1* gene transgenic lines after 3 days of 250 mM NaCl treatment.

Lines	Proline content (μg/g)	5% level	1% level
WT	448.333	c	C
D1	1109.39	a	A
D2	920.067	b	B
D3	1095.407	a	A
D4	876.037	b	B

sugar content (μg) × extraction solution volume (mL) × dilute fold × 100/sample volume (mL) × fresh leaf sample weight (g) × 10^6.

3. Results

3.1. Assessment of Salt Tolerance. The growth of the transgenic lines and WT plants were compared following exposure to 250 mM NaCl stress. The growth of *SbPIP1*-transformed lines was generally not affected by salt treatment. There were almost no differences between the growth of transgenic plants after 3 days of salt stress and the growth of WT plants without stress. However, the growth of the WT plants was remarkably affected by salt treatment. The leaves of WT plants had clearly wilted after 3 days of salt stress (Figure 1). These results indicate that *SbPIP1* transgenic lines retain a salt-tolerant phenotype.

3.2. Accumulation of Proline Content under Salt Stress. The proline content in all transgenic wheat lines increased with an increase in the duration of the salt stress (Figure 2). The proline content in WT plants increased during the first two days of salt stress and then dropped slightly by the 3rd day. Overall, the proline contents in the plants overexpressing the *SbPIP1* gene were significantly ($P < 0.01$) higher than those in the WT plants after 3 days of stress treatment (Table 1).

3.3. MDA Content Assay. The MDA content in the transgenic lines and WT plants was analyzed (Figure 3). During salt stress treatment with NaCl, the MDA contents changed in all of the treatment groups, that is, the transgenic lines and the WT plants. The MDA content in the WT plants decreased during the first two days and then increased on the 3rd day.

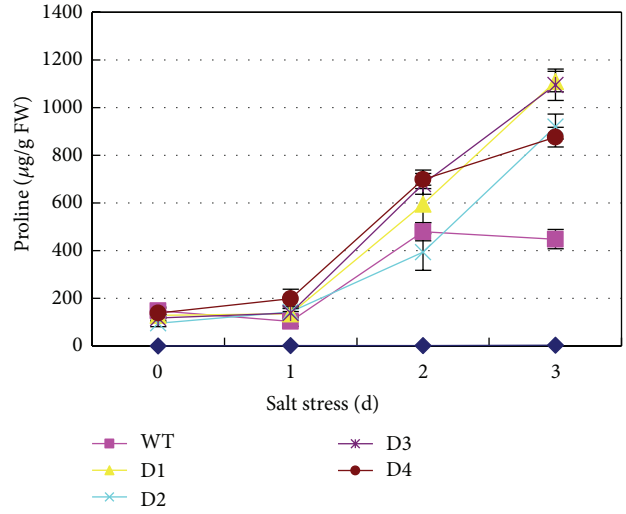

Figure 2: Proline content in WT plants and *SbPIP1* gene transgenic lines. D1, D2, D3, and D4 represent the transgenic lines D1, D2, D3, and D4, respectively; WT represents the untransformed wheat variety Ningmai 13.

The MDA contents in all of the transgenic lines except the transgenic line D3 exhibited a declining trend during the three days of salt stress; the MDA content in the transgenic line D3 decreased after 1 day of stress treatment and then increased slightly over the subsequent days of treatment. Overall, the MDA contents in plants overexpressing the *SbPIP1* gene were significantly ($P < 0.05$) lower than those in the WT plants after 3 days of stress treatment, indicating that lipid peroxidation was lower in the *SbPIP1*-transformed lines than in the WT plants. These results suggest that the *SbPIP1* gene might contribute to decreased lipid peroxidation in wheat.

3.4. Soluble Protein Content Assay. The soluble protein content was measured in the *SbPIP1*-transformed lines and the WT plants (Figure 4). An almost identical change trend was exhibited in all the treated groups, that is, the transgenic wheat lines and the WT plants, during the salt stress treatment. The soluble protein content increased approximately 0.5-fold after 1 day of stress treatment, followed by a slight decrease after 2 days of stress treatment, and then remained fairly constant after exposure to salt stress for 3 days.

3.5. Soluble Sugar Content Assay. The soluble sugar content was analyzed in both the transgenic wheat plants and the WT plants (Figure 5). Under salt stress conditions (250 mM NaCl treatment), the soluble sugar contents changed in all treatment groups; however, there were distinct differences in the soluble sugar content between the *SbPIP1*-transformed plants and the WT plants. The soluble sugar content increased 0.5-fold in WT plants after 1 day of stress treatment and then decreased slowly over the subsequent days of treatment. In the *SbPIP1*-transformed plants, the soluble sugar content increased greatly (approximately 1-fold) after 1 day of stress

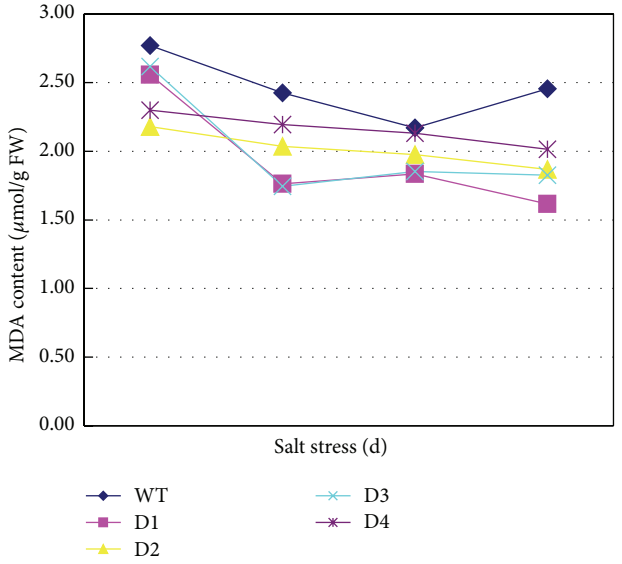

Figure 3: MDA content in the WT plants and *SbPIP1* gene transgenic lines. D1, D2, D3, and D4 represent the transgenic lines D1, D2, D3, and D4, respectively; WT represents the untransformed wheat variety Ningmai 13.

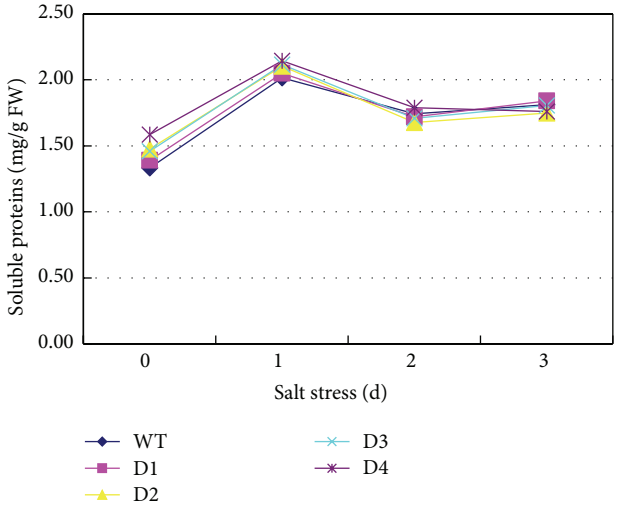

Figure 4: Soluble protein content in the WT plants and *SbPIP1* gene transgenic lines. D1, D2, D3, and D4 represent the transgenic lines D1, D2, D3, and D4, respectively; WT represents the untransformed wheat variety Ningmai 13.

treatment and then decreased dramatically over the subsequent days of treatment. As shown in Figure 5, the soluble sugar levels in all transgenic plant groups dropped to the same level as the WT plants after 3 days of salt stress treatment. Although the soluble sugar content differed among the three transgenic plant lines, a similar change trend was exhibited in all transgenic plant lines during the salt stress treatment. Overall, the soluble sugar content changes observed in the *SbPIP1*-transformed plants differed from those observed in

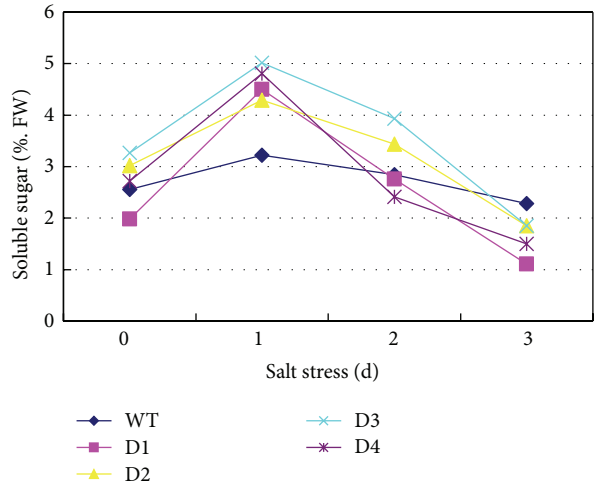

Figure 5: Soluble sugar content in the WT plants and *SbPIP1* gene transgenic lines. D1, D2, D3, and D4 represent the transgenic lines D1, D2, D3, and D4, respectively; WT represents the untransformed wheat variety Ningmai 13.

the WT plants, suggesting that the *SbPIP1* gene plays a role in the regulation of soluble sugar biosynthesis in wheat.

4. Discussion

It is known that proline has various functions in plants under stress conditions. This amino acid can serve as an eliminator of free radicals, a mediator of osmotic adjustment, a buffer of redox potential, a stabilizer of inserted subcellular structures, and an important component of cell wall proteins [20, 21]. The proline content accumulates considerably in plants subjected to salt and drought stress due to its increased synthesis or decreased degradation [22–24]. Therefore, the proline content in plants under salt stress can be a vital criterion for evaluating salt tolerance. Gao et al. reported that TaNIP-overexpressing *Arabidopsis* accumulated more proline than the wild-type plants [11]. In addition, MaPIP1;1-overexpressing transgenic *Arabidopsis* plants maintained higher levels of proline compared with WT plants subjected to a similar drought treatment [13]. In the current study, a significant increase in proline accumulation was observed in transgenic wheat plants after salt stress treatment, and this was correlated with enhanced tolerance to salt stress.

Key enzymes in the lipid metabolic pathways in plants are affected by salt stress [25]. Lipid peroxidation is considered the most damaging process in living organisms. Since MDA is one of the end-products of lipid peroxidation in biomembranes, the MDA content is usually used to represent the level of lipid peroxidation and membrane injury. The MDA content is an important criterion in evaluating the stress tolerance of plants under stress conditions. MaPIP1;1-overexpressing *Arabidopsis* exhibited a reduced MDA content under salt or drought conditions [13]. In addition, TaAQP7- (a PIP2 subgroup aquaporin gene) overexpressing tobacco plants and TaAQP8- (a PIP1 subgroup aquaporin gene) overexpressing tobacco plants had lower levels of MDA

than the WT plants under salt stress [26, 27]. The MDA levels were lower in transgenic banana plants overexpressing MusaPIP2;6 than in the untransformed plants under salt stress condition [14]. In this study, the MDA levels in plants overexpressing the *SbPIP1* gene were significantly ($P < 0.05$) lower than those in the WT plants after 3 days of stress treatment. This result showed that overexpression of the *SbPIP1* gene may significantly reduce lipid peroxidation in transgenic wheat plants.

The soluble protein content in different plant species changes in different ways under salt stress. In salt-tolerant plant species such as rice, barley, and sunflower [28], the soluble protein content increases under salt stress. In mulberry cultivars, the soluble protein content increased at a low salinity level but decreased at a high salinity level [29]. The overexpression of GmCLC1 (a vacuolar Cl^- transporter protein gene) in poplar led to an increase in the soluble protein content during salt stress [30]. The soluble protein content in transgenic tobacco (overexpressing a bZIP transcription factor gene from *Medicago sativa* L.) increased compared with nontransgenic tobacco under salt or drought stress [31]. In the current study, the soluble protein levels in the transgenic lines and WT wheat plants exhibited an almost identical change trend. We hypothesize that overexpression of the *SbPIP1* gene has no influence on the regulation of soluble protein biosynthesis in wheat.

Under abiotic stress conditions, plant cells accumulate different types of osmolytes to adjust the intracellular osmotic potential and avoid cell injury. Among many different kinds of osmolytes, soluble sugars are the major types of osmolytes. The major role played by soluble sugars in stress mitigation involves osmoprotection, carbon storage, and scavenging of reactive oxygen species [32]. The overexpression of GhAnn1 (a cotton annexin gene) in transgenic cotton plants conferred enhanced salt tolerance with higher levels of soluble sugars compared with the wild-type plants [33]. The overexpression of OsDREB2A in soybean enhanced salt tolerance, which was accompanied with an accumulation of soluble sugars [23]. In the current study, we examined the soluble sugar content in transgenic wheat plants overexpressing the *SbPIP1* gene and found that the soluble sugar levels were significantly ($P < 0.05$) higher than those in the WT plants after 1 day of salt stress treatment (Figure 5), after which the soluble sugar content decreased more dramatically than that in the WT plants. Based on these data, we hypothesize that the *SbPIP1* gene may contribute to the synthesis of soluble sugars during the early period (1 day) of salt stress treatment.

The overexpression of several PIP1 genes such as BnPIP1, NtAQP1, TaAQP8, OsPIP1;1, MusaPIP1;2, and MaPIP1;1 enhanced the hydraulic conductance and tolerance of transgenic plants in response to water stress [9, 13, 27, 34–36]. Aharon et al. (2003) reported that AtPIP1b overexpression in transgenic tobacco plants had no beneficial effect under salt stress and even a negative effect during drought stress, causing faster wilting [8]. Zhou et al. (2014) reported that transgenic soybean overexpressing GmPIP1;6 exhibited higher growth and greater yield under salt treatment compared with the WT plants [12]. However, the mechanism of how some PIP1 genes can increase the tolerance to water stress is largely unknown. Maintaining osmotic balance, improving ion distribution, reducing membrane injury, and enhancing the activities of antioxidants were mentioned with respect to the overexpression of the PIP1 genes [13, 26, 27]. In this study, the overexpression of *SbPIP1* led to increases in the accumulation of proline and the synthesis of soluble sugars and reduced lipid peroxidation. From the results in this study, we confirmed that *SbPIP1* plays an important role in the salt stress response in halophytes and glycophytes. The overexpression of *SbPIP1* in plants might be used to improve the salt tolerance of important crop plants.

Conflict of Interests

The authors declare that there is no conflict of interests regarding the publication of this paper.

Acknowledgments

This project was supported by the Jiangsu Agriculture Science and Technology Innovation Fund (CX(11)4034) and the GMO Cultivation of New Varieties Project of China (2014ZX0800205B).

References

[1] W. Kammerloher, U. Fischer, G. P. Piechottka, and A. R. Schäffner, "Water channels in the plant plasma membrane cloned by immunoselection from a mammalian expression system," *Plant Journal*, vol. 6, no. 2, pp. 187–199, 1994.

[2] R. G. Fray, A. Wallace, D. Grierson, and G. W. Lycett, "Nucleotide sequence and expression of a ripening and water stress-related cDNA from tomato with homology to the MIP class of membrane channel proteins," *Plant Molecular Biology*, vol. 24, no. 3, pp. 539–543, 1994.

[3] X. Sarda, D. Tousch, K. Ferrare et al., "Two TIP-like genes encoding aquaporins are expressed in sunflower guard cells," *Plant Journal*, vol. 12, no. 5, pp. 1103–1111, 1997.

[4] J.-B. Mariaux, C. Bockel, F. Salamini, and D. Bartels, "Desiccation- and abscisic acid-responsive genes encoding major intrinsic proteins (MIPs) from the resurrection plant Craterostigma plantagineum," *Plant Molecular Biology*, vol. 38, no. 6, pp. 1089–1099, 1998.

[5] M. Ayadi, D. Cavez, N. Miled, F. Chaumont, and K. Masmoudi, "Identification and characterization of two plasma membrane aquaporins in durum wheat (*Triticum turgidum* L. subsp. *durum*) and their role in abiotic stress tolerance," *Plant Physiology and Biochemistry*, vol. 49, no. 9, pp. 1029–1039, 2011.

[6] T. Walz, T. Hirai, K. Murata et al., "The three-dimensional structure of aquaporin-1," *Nature*, vol. 387, no. 6633, pp. 624–627, 1997.

[7] A. R. Schäffner, "Aquaporin function, structure, and expression: are there more surprises to surface in water relations?" *Planta*, vol. 204, no. 2, pp. 131–139, 1998.

[8] R. Aharon, Y. Shahak, S. Wininger, R. Bendov, Y. Kapulnik, and G. Galili, "Overexpression of a plasma membrane aquaporin in transgenic tobacco improves plant vigor under favorable growth conditions but not under drought or salt stress," *Plant Cell*, vol. 15, no. 2, pp. 439–447, 2003.

[9] Q. Yu, Y. Hu, J. Li, Q. Wu, and Z. Lin, "Sense and antisense expression of plasma membrane aquaporin *BnPIP1* from *Brassica* napus in tobacco and its effects on plant drought resistance," *Plant Science*, vol. 169, no. 4, pp. 647–656, 2005.

[10] H. L. Lian, X. Yu, Q. Ye et al., "The role of aquaporin RWC3 in drought avoidance in rice," *Plant and Cell Physiology*, vol. 45, pp. 481–489, 2004.

[11] Z. X. Gao, X. L. He, B. C. Zhao et al., "Overexpressing a putative aquaporin gene from wheat, TaNIP, enhances salt tolerance in transgenic *Arabidopsis*," *Plant and Cell Physiology*, vol. 51, no. 5, pp. 767–775, 2010.

[12] L. Zhou, C. Wang, R. Liu et al., "Constitutive overexpression of soybean plasma membrane intrinsic protein GmPIP1;6 confers salt tolerance," *BMC Plant Biology*, vol. 14, article 181, 2014.

[13] Y. Xu, W. Hu, J. Liu et al., "A banana aquaporin gene, MaPIP1;1, is involved in tolerance to drought and salt stresses," *BMC Plant Biology*, vol. 14, no. 1, article 59, 2014.

[14] S. Sreedharan, U. K. S. Shekhawat, and T. R. Ganapathi, "Constitutive and stress-inducible overexpression of a native aquaporin gene (*MusaPIP2;6*) in transgenic banana plants signals its pivotal role in salt tolerance," *Plant Molecular Biology*, vol. 88, no. 1-2, pp. 41–52, 2015.

[15] S. Yamada, M. Katsuhara, W. B. Kelly, C. B. Michalowski, and H. J. Bohnert, "A family of transcripts encoding water channel proteins: tissue-specific expression in the common ice plant," *Plant Cell*, vol. 7, no. 8, pp. 1129–1142, 1995.

[16] M. Kawase, Y. T. Hanba, and M. Katsuhara, "The photosynthetic response of tobacco plants overexpressing ice plant aquaporin McMIPB to a soil water deficit and high vapor pressure deficit," *Journal of Plant Research*, vol. 126, no. 4, pp. 517–527, 2013.

[17] D. D. Zhang, *Differential salt-tolerant gene expression of Salicornia bigeloii Torr. and several genes analysis [Ph.D. dissertation]*, Nanjing University, Supervisor: Y. H. Yang, and H. X. Ma, 2007 (Chinese).

[18] G. H. Yu, X. B. Sun, X. Zhang et al., "Obtaining of transgenic wheat plants with SbPIP1 gene and preliminary assay of salt tolerance," *Molecular Plant Breeding*, vol. 10, no. 4, pp. 398–403, 2012 (Chinese).

[19] K. Shah and R. S. Dubey, "Effect of cadmium on proline accumulation and ribonuclease activity in rice seedlings: role of proline as a possible enzyme protectant," *Biologia Plantarum*, vol. 40, no. 1, pp. 121–130, 1997.

[20] P. D. Hare and W. A. Cress, "Metabolic implications of stress-induced proline accumulation in plants," *Plant Growth Regulation*, vol. 21, no. 2, pp. 79–102, 1997.

[21] T. Nanjo, M. Kobayashi, Y. Yoshiba et al., "Biological functions of proline in morphogenesis and osmotolerance revealed in antisense transgenic *Arabidopsis* thaliana," *The Plant Journal*, vol. 18, no. 2, pp. 185–193, 1999.

[22] F. Zhang, S. F. Li, S. M. Yang, L. Wang, and W. Guo, "Overexpression of a cotton annexin gene, *GhAnn1*, enhances drought and salt stress tolerance in transgenic cotton," *Plant Molecular Biology*, vol. 87, no. 1-2, pp. 47–67, 2015.

[23] X.-X. Zhang, Y.-J. Tang, Q.-B. Ma et al., "OsDREB2A, a rice transcription factor, significantly affects salt tolerance in transgenic soybean," *PLoS ONE*, vol. 8, no. 12, Article ID e83011, 2013.

[24] S. S. Gill and N. Tuteja, "Reactive oxygen species and antioxidant machinery in abiotic stress tolerance in crop plants," *Plant Physiology and Biochemistry*, vol. 48, no. 12, pp. 909–930, 2010.

[25] R. H. Gao, K. Duan, G. M. Guo et al., "Comparative transcriptional profiling of two contrasting barley genotypes under salinity stress during the seedling stage," *International Journal of Genomics*, vol. 2013, Article ID 972852, 19 pages, 2013.

[26] S. Y. Zhou, W. Hu, X. M. Deng et al., "Overexpression of the wheat aquaporin gene, TaAQP7, enhances drought tolerance in transgenic tobacco," *PLoS ONE*, vol. 7, no. 12, Article ID e52439, 2012.

[27] W. Hu, Q. Yuan, Y. Wang et al., "Overexpression of a wheat aquaporin gene, *TaAQP8*, enhances salt stress tolerance in transgenic tobacco," *Plant and Cell Physiology*, vol. 53, no. 12, pp. 2127–2141, 2012.

[28] A. Parvaiz and S. Satyawati, "Salt stress and phyto-biochemical responses of plants—a review," *Plant, Soil and Environment*, vol. 54, no. 3, pp. 89–99, 2008.

[29] P. Agastian, S. J. Kingsley, and M. Vivekanandan, "Effect of salinity on photosynthesis and biochemical characteristics in mulberry genotypes," *Photosynthetica*, vol. 38, no. 2, pp. 287–290, 2000.

[30] W. B. Sun, D. X. Deng, L. H. Yang et al., "Overexpression of the chloride channel gene (GmCLC1) from soybean increases salt tolerance in transgenic *Populus deltoides* × *P. euramericana* 'Nanlin 895'," *Plant Omics*, vol. 6, no. 5, pp. 347–354, 2013.

[31] Y. Li, Y. Sun, Q. C. Yang, F. Fang, J. Kang, and T. Zhang, "Isolation and characterization of a gene from *Medicago sativa* L., encoding a bZIP transcription factor," *Molecular Biology Reports*, vol. 40, no. 2, pp. 1227–1239, 2013.

[32] B. Gupta and B. Huang, "Mechanism of salinity tolerance in plants: physiological, biochemical, and molecular characterization," *International Journal of Genomics*, vol. 2014, Article ID 701596, 18 pages, 2014.

[33] F. Zhang, S. F. Li, S. M. Yang, L. Wang, and W. Guo, "Overexpression of a cotton annexin gene, GhAnn1, enhances drought and salt stress tolerance in transgenic cotton," *Plant Molecular Biology*, vol. 87, pp. 47–67, 2015.

[34] N. Sade, M. Gebretsadik, R. Seligmann, A. Schwartz, R. Wallach, and M. Moshelion, "The role of tobacco Aquaporin1 in improving water use efficiency, hydraulic conductivity, and yield production under salt stress," *Plant Physiology*, vol. 152, no. 1, pp. 245–254, 2010.

[35] C. W. Liu, T. Fukumoto, T. Matsumoto et al., "Aquaporin OsPIP1;1 promotes rice salt resistance and seed germination," *Plant Physiology and Biochemistry*, vol. 63, pp. 151–158, 2013.

[36] S. Sreedharan, U. K. S. Shekhawat, and T. R. Ganapathi, "Transgenic banana plants overexpressing a native plasma membrane aquaporin MusaPIP1;2 display high tolerance levels to different abiotic stresses," *Plant Biotechnology Journal*, vol. 11, no. 8, pp. 942–952, 2013.

Research Article

Water Properties Influencing the Abundance and Diversity of Denitrifiers on *Eichhornia crassipes* Roots: A Comparative Study from Different Effluents around Dianchi Lake, China

Neng Yi, Yan Gao, Zhenhua Zhang, Hongbo Shao, and Shaohua Yan

Institute of Agricultural Resources and Environment and Institute of Agro-biotechnology, Jiangsu Academy of Agricultural Sciences, Nanjing 210014, China

Correspondence should be addressed to Hongbo Shao; shaohongbochu@126.com and Shaohua Yan; shyan@jaas.ac.cn

Received 20 December 2014; Revised 1 April 2015; Accepted 1 April 2015

Academic Editor: Ferenc Olasz

To evaluate effects of environmental conditions on the abundance and communities of three denitrifying genes coding for nitrite (*nirK, nirS*) reductase and nitrous oxide (*nosZ*) reductase on the roots of *Eichhornia crassipes* from 11 rivers flowing into the northern part of Dianchi Lake. The results showed that the abundance and community composition of denitrifying genes on *E. crassipes* root varied with different rivers. The *nirK* gene copies abundance was always greater than that of *nirS* gene on the roots of *E. crassipes*, suggesting that the surface of *E. crassipes* roots growth in Dianchi Lake was more suitable for the growth of *nirK*-type denitrifying bacteria. The DGGE results showed significant differences in diversity of denitrifying genes on the roots of *E. crassipes* among the 11 rivers. Using redundancy analysis (RDA), the correlations of denitrifying microbial community compositions with environmental factors revealed that water temperature (T), dissolved oxygen (DO), and pH were relatively important environmental factors to modifying the community structure of the denitrifying genes attached to the root of *E. crassipes*. The results indicated that the specific environmental conditions related to different source of rivers would have a stronger impact on the development of denitrifier communities on *E. crassipes* roots.

1. Introduction

Phytoremediation technology using floating macrophytes (*Eichhornia crassipes*) performed very well in remediation eutrophic water body since *E. crassipes* is capable of assimilating large amount of nutrients efficiently [1–3]. During 2010–2012, large-scale confined growth of *E. crassipes* was used to remove pollutants (mainly N and P) from Dianchi Lake as well as the rivers connecting to the lake. Dianchi Lake is the sixth largest freshwater lake in China. There are more than 31 rivers, which carried wastewater discharged from different types of sewage treatment plants (STPs), agriculture, and domestic source, flowing into the lake. The macrophytes significantly improved water quality in both inflow rivers and Dianchi Lake [4].

To evaluate the contributions of water hyacinth to the removal of nitrogen from the lake, both assimilation and stimulated denitrification by the macrophyte are important since N-15 tracing experiment in labs indicated that the values of N-15 at.% excess of N_2-N production were significantly ($p < 0.05$) higher with the growth of *E. crassipes* than that without [5, 6]. The presence of *E. crassipes* roots has positive effect on stimulating the activity, abundance, and diversity of denitrifiers. Studies have reported that plant rhizosphere enhanced bacterial abundance, activity, and diversity [7]. Previous studies also suggested that the root system of floating macrophyte could support the attachment of microorganism and enhance the growth and activity of bacteria for removing organic matter and nutrients [8].

Environmental conditions are also critically important in mediating the activity, abundance, and diversity of bacteria [9, 10]. The abundance and diversity of denitrifiers on *E. crassipes* roots grown in the rivers receiving wastewater with different water properties may vary with the variation of environmental factors. The abundance of the functional genes and community compositions of denitrifiers can be affected by many factors, such as water temperature, pH, DO, and nutrient concentrations. In the rivers with different sources of

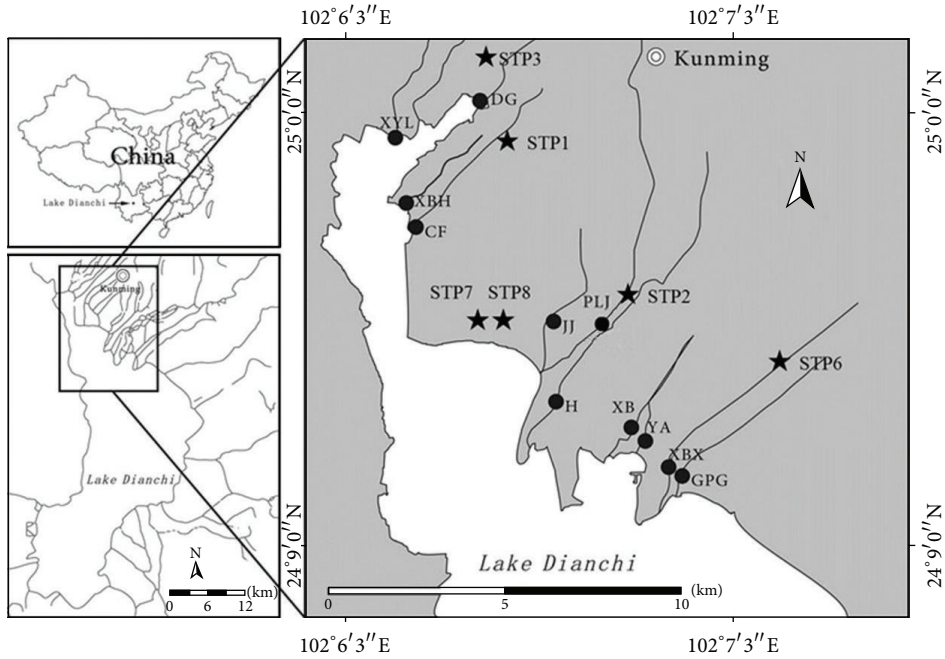

Figure 1: Sampling sites in rivers of Dianchi Lake. Black dot (●) is sampling site, and Pentagram (★) is sewage treatment plants (STP).

condensed pollutants and diverse physiochemical properties, the abundance and diversity of denitrifiers on the *E. crassipes* roots may be modified in various patterns.

Hence, in the present study, we investigated the abundance and diversity of denitrifying bacteria on *E. crassipes* roots in 11 rivers with different pollution sources in the north side of Dianchi Lake. It put an emphasis on understanding the interactions between the changes of environmental factors and the abundance and diversity of denitrifying bacteria attached to *E. crassipes* roots. It was expected that the results would shed some insight on how environmental factors and cultivation of *E. crassipes* mediate denitrification process in different eutrophic rivers flowing into the Dianchi Lake.

2. Materials and Methods

2.1. Site Description, Sampling, and Water Properties. A total of 11 rivers around Dianchi Lake located from 24°9′ to 25°0′ latitude and 102°6′ to 102°7′ longitude were investigated (Figure 1). As shown in Figure 1, Xinbaoxiang (XBX), Daguan (DG), Chuanfang (CF), and Panlongjiang (PLJ) rivers receive effluents from sewage treatment plants (STPs). Haihe (H), Guangpugou (GPG), Jinjia (JJ), Xibahe (XBH), and Xinyunliang (XYL) rivers receive raw sewage from industrial, domestic, and agricultural sources. Xiaba (XB) and Yaoan (YA) rivers represent the same sewage origin from the same upstream (not sampled due to water hyacinth not being grown) but different tributaries separated at water treatment wetland named Wujia (not sampled due to water hyacinth not grown).

Water temperature, pH, and dissolved oxygen (DO) were measured *in situ* using portable meter (YSI ProPlus, USA). One-liter water samples were collected from each site with three replicates at 0–0.5 m of the water column of the eleven rivers using cylinder sampler in September 25, 2012. Total nitrogen (TN), ammonium (NH_4^+), nitrate (NO_3^-), nitrite (NO_2^-), and total soluble nitrogen (TSN) were analyzed using a SEAL AutoAnalyzer 3 (SEAL Analytical Co., Hampshire, UK). Mixed root samples were collected randomly with three replicates at each sampling site using sterile scissors and forceps and then stored in an ice box and taken back to the laboratory. Fresh roots (2 g) of *E. crassipes* were transferred into 200 mL sterile water. Bacteria attached to *E. crassipes* roots were detached by vigorous shaking for 30 min (18.3 Hz, Thermomixer Eppendorf) and filtered through a 0.45 μm sterile filter. The resultant filtrates were filtered through 0.22 μm Millipore membrane filters using a vacuum air pump and the membranes stored at −80°C for DNA extraction [5].

2.2. DNA Extraction. All the abovementioned membranes were cut into pieces with sterile scissors and used immediately for DNA extraction, which was performed using an E.Z.N.A. Water DNA Kit (OMEGA Bio-Tek Inc., Doraville, GA, USA) by following the manufacturer's instructions. The extracted DNA was stored in a −20°C freezer [5].

2.3. Real-Time Polymerase Chain Reaction (qPCR) Assay. Real-time quantitative PCR was performed to estimate the denitrifying bacteria abundance using the primers listed in Table 1. Real-time polymerase chain reaction (qPCR) was performed on ABI 7500 real-time System (Life Technologies, USA). Amplification was performed in triplicate in a total volume of 20 μL reaction mixtures by using SYBR Premix Ex TaqTM (TIiRNaseH Plus) qPCR Kit as described by the suppliers (Takara Bio, Dalian, China). For each assay, three different PCR conditions were performed separately

Table 1: Primers used for the qPCR and DGGE.

Gene		Primers	Thermal profile
nosZ	for qPCR for DGGE	*nosZ*-F [45]	CGYTGTTCMTCGACAGCCAG
		*nosZ*1622R [45]	CGSACCTTSTTGCCSTYGCG
		*nosZ*1622R-GC [46]	GGCGGCGCGCCGCCCGCCCCGCCCCCGTCGCCC-CGSACCTTSTTGCCSTYGCG
nirS	for qPCR for DGGE	*nirS*-Cd3Af [47]	GTSAACGTSAAGGARACSGG
		nirS-R3cd [47]	GASTTCGGRTGSGTCTTGA
		nirS-R3cd-GC [48]	GGCGGCGCGCCGCCCGCCCCGCCCCCGTCGCCC-GASTTCGGRTGSGTCTTGA
nirK	for qPCR for DGGE	*nirK* F1aCu [49]	ATCATGGTSCTGCCGCG
		nirK R3Cu [49]	GCCTCGATCAGRTTGTGGTT
		nirK R3Cu-GC [49]	GGCGGCGCGCCGCCCGCCCCGCCCCCGTCGCCC-GCCTCGATCAGRTTGTGGTT

for the same sample by varying annealing temperature at either 54°C (*nirS*- Cd3Af/*nirS*-R3cd *and nosZ*-F/*nosZ*-1622R) or 58°C (*nirK*-F1aCu/*nirK*-R3Cu). The qPCR amplification was performed as follows: initial denaturation at 95°C for 2 min, followed by 35 cycles consisting of denaturation step at 95°C for 5 s, varying annealing temperature for 30 s, and elongation at 72°C for 30 s. The data were collected during the 72°C for 30 s step. Data was analyzed using the ABI 7500 software (Version 2.0.6, Life Technologies, USA). The parameter Ct (threshold cycle) was determined as the cycle number at which a statistically significant increase in the reporter fluorescence was detected. The standard curves for real-time PCR assays were developed as previously described [5].

2.4. PCR Amplification Denaturing Gradient Gel Electrophoresis (DGGE) Analysis. For denaturing gradient gel electrophoresis (DGGE) analysis, the PCR was performed in reaction mixtures including 1 μL of template DNA, 5 μL of 10 × PCR buffer, 1 μL of dNTPs (10 mM each), 1 μL of each primer (20 μM) (Table 1), and 2 U of Taq polymerase (Takara Bio, Dalian, China) and adjusted to a final volume of 50 μL with sterile deionized water. The reaction was performed in a Bio-Rad C1000 thermal cycler (Bio-Rad, USA) using different cycling conditions. The *nirK* gene (F1aCu/R3Cu-GC) PCR program was carried out with an initial denaturation at 94°C for 3 min, followed by 32 cycles of 94°C for 30 s, 58°C for 30 s, and 72°C for 45 s, followed by 72°C for 10 min, and ended at 10°C. The touchdown PCR amplification of *nirS* (Cd3Af/R3cd-GC) and *nosZ* (*nosZ*-F/*nosZ*1622R-GC) was performed as follows: 94°C for 2 min, followed by 10 cycles, 94°C for 30 s, and 57°C for 30 s in the initial cycle and at decreasing temperatures by 0.5°C/cycle until a temperature of 52°C was reached in the subsequent cycles. The extension step was performed at 72°C for 1 min. After the touchdown program, 30 cycles at 94°C for 30 s, 53°C for 30 s, and 72°C for 1 min, followed by 72°C for 10 min, and ended at 10°C.

The amplified products were pooled and resolved on DGGE gels using a Dcode system (Bio-Rad Laboratories, Hercules, USA). The purified PCR products (30 μL) of *nirS*, *nirK*, and *nosZ* containing approximately equal amounts of PCR amplicons were loaded onto the 1 mm-thich 6% (w/v) polyacrylamide (37.5 : 1, acrylamide : bisacrylamide) gels with denaturing gradients of 50–75% for 15 h (*nirS*), 50–70% for 12 h (*nirK*), and 50–70% for 15 h (*nosZ*) (100% denaturant contains 7 mol/L urea and 40% (v/v) formamide). The gels were run in 1 × TAE (40 mM Tris-acetate and 1 mM EDTA) at 100 V and 60°C. The gel was silver-stained using protocol [11]. Polaroid pictures of the DGGE gels were scanned using an Epson Perfection V700 Photo scanner (Seiko Epson Corporation, Nagano, Japan). DGGE profiles were digitized after average background subtraction for the entire gel using Quantity One software (Version 4.5, Bio-Rad, USA) as previously described [5]. Digitized information from the DGGE banding profiles was used to calculate the diversity indices such as richness (S), which was determined from the number of bands in each lane, and Shannon-Wiener Index (H), which was calculated from $H = -\sum P_i \times \ln P_i$ [12], where P_i is the importance probability of the bands in a gel lane, calculated as $P_i = n_i/N$, where n_i is the intensity of a band and N is the sum of intensities of all bands.

2.5. Data Analysis. Three replicates were used in all parameter analyses. Data presented as mean values ± SD. One way analysis of variance (ANOVA) followed by *S-N-K*-test was performed to check for quantitative differences between samples; $P < 0.005$ was considered to be statistically significant. All statistical analyses were done using SPSS software.

The relative intensity of a specific band was transformed according to the sum of intensities of all bands in a pattern [13]. Redundancy analysis (RDA) for community ordination was conducted using CANOCO (version 4.5, Centre for Biometry, Wageningen, Netherlands) for Windows using relative band intensity data obtained from the Quantity One analysis [14]. Eight environmental parameters, including water temperature, pH, DO, ammonia, nitrate, nitrite, total nitrogen, and total soluble nitrogen, were selected to perform RDA-based variance inflation factor (VIF) analysis with 499 unrestricted permutations to statistically evaluate the significance of the first canonical axis and of all canonical axes together. Statistical significance was kept at $P < 0.05$ for all analyses.

3. Results

3.1. Water Properties. The corresponding environmental parameters (Table 2) of the eleven rivers represented their own properties of different pollution sources. The water from STP sites was characterized by relatively high concentrations of nitrate (4.79–12 mg L^{-1}) and low concentrations of ammonia nitrogen (0.06–1.98 mg L^{-1}) and organic matter, which had contrary properties comparing to those rivers receiving raw sewage from industrial, domestic, and agricultural sources. The XB and YA rivers had similar characteristics to those rivers receiving water from STP but lower dissolved oxygen and higher ammonia nitrogen.

3.2. Quantification of Denitrifying Genes (nirK, nirS, nosZ). The results showed that the abundance of *nirK*, *nirS*, and *nosZ* gene copies per gram fresh root ranged from 4.13×10^7 to 6.11×10^8, 1.45×10^8 to 1.99×10^8, and 2.20×10^8 to 2.20×10^{10}, respectively (Figure 2). The *nirK* and *nirS* abundance on the roots of *E. crassipes* in YA river and XB river were significantly higher than those in other rivers ($P < 0.05$). The highest abundance of *nosZ* was observed on the root sample in JJ river. The lowest abundance of *nirK* and *nosZ* type denitrifiers were determined on the root sample from DG river. The *nirK*, *nirS*, and *nosZ* copy abundance varied between sites indicated that different pollution source would influence the abundance of denitrifiers in rivers.

The highest abundance ratio (125.34) of *nosZ*/(*nirK* + *nirS*) occurred in JJ river, followed by GPG (39.75), while the lowest ratio was in XYL river (1.43), and the ratios in other rivers were similar, ranging from 3.26 to 8.38. However, the *nirK*/*nirS* ratio in all samples ranged from 1.70 to 6.60.

To explain the relationship between environmental factors and the abundance of *nirK*, *nirS*, and *nosZ*, the gene copy numbers of three denitrifiers and eight parameters were explored by redundancy analysis (Figure 3). The gray circle area implies a positive correlation and the white circle area implies a negative correlation. The larger the circle area, the greater the impact corresponding to the changes in environmental factors that would have influenced the denitrifiers. Denitrifier lines at the end in the gray circle had positive regression coefficients for that environmental variable with the corresponding *t*-value larger than 2.0. The results showed that the temperature, pH, and nitrate circle areas were larger than other environmental factors, which indicated that temperature, pH, and nitrate circle greatly affected the *nirS*, *nirK*, and *nosZ* abundance than other factors.

The abundance of *nirK* and *nirS* was positively correlated with water temperature, nitrate, and nitrite concentrations and was negatively correlated with the other factors (pH, DO, DTN, TN, and ammonium). The abundance of *nosZ* was negatively correlated with water temperature and was positively correlated with the pH and DO, while there were no significant correlations with other factors.

3.3. DGGE Fingerprints of nirK, nirS, and nosZ Genes. Only one of the three replicates of DGGE profiles was listed for each gene type to illustrate resolution. However, all the three replicates of the profiles were digitized and were used in statistics analysis.

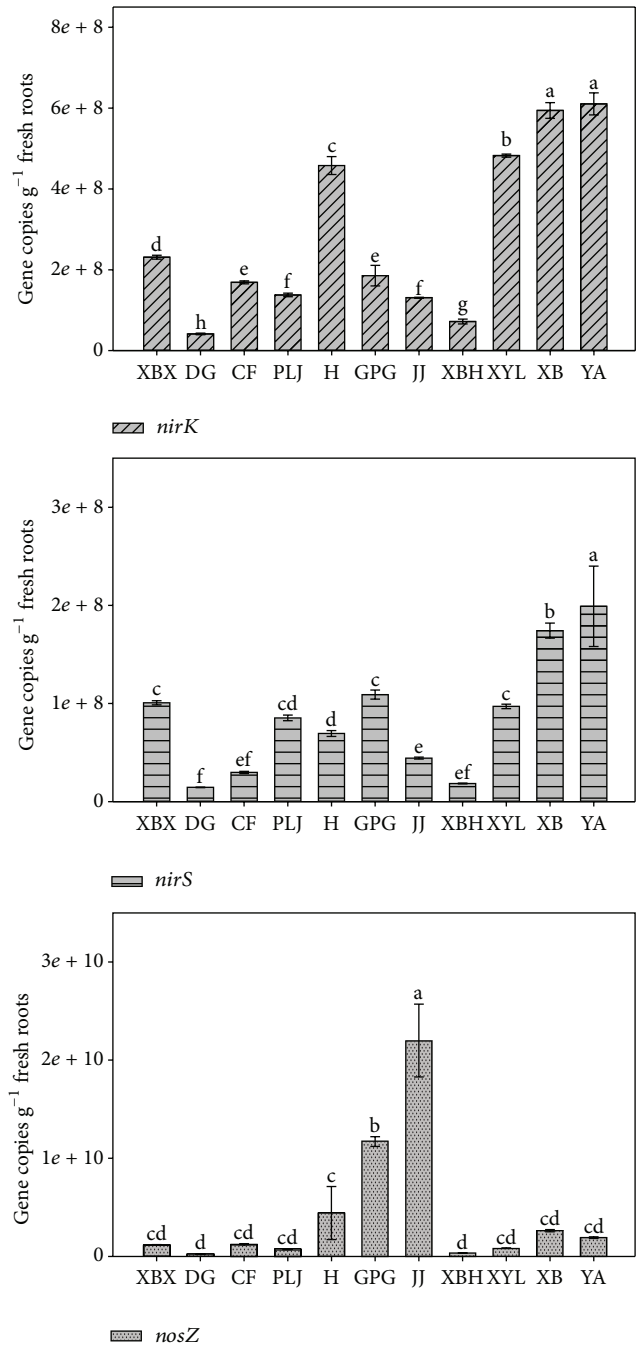

Figure 2: Abundance of *nirS*, *nirK*, and *nosZ* genes on the root of *E. crassipes*. Error bars indicate standard deviations ($n = 3$). The different letters indicate significant differences ($P < 0.05$).

3.4. Richness and Diversity of nirK, nirS, and nosZ on the Root of E. crassipes. The Shannon indices (H) calculated from DGGE gels ranged from 2.23 to 2.90 for *nirK*, 2.08 to 2.69 for *nirS*, and 2.11 to 2.73 for *nosZ*, which showed that high diversity of denitrifier (*nirK*, *nirS*, and *nosZ*) genes on the root

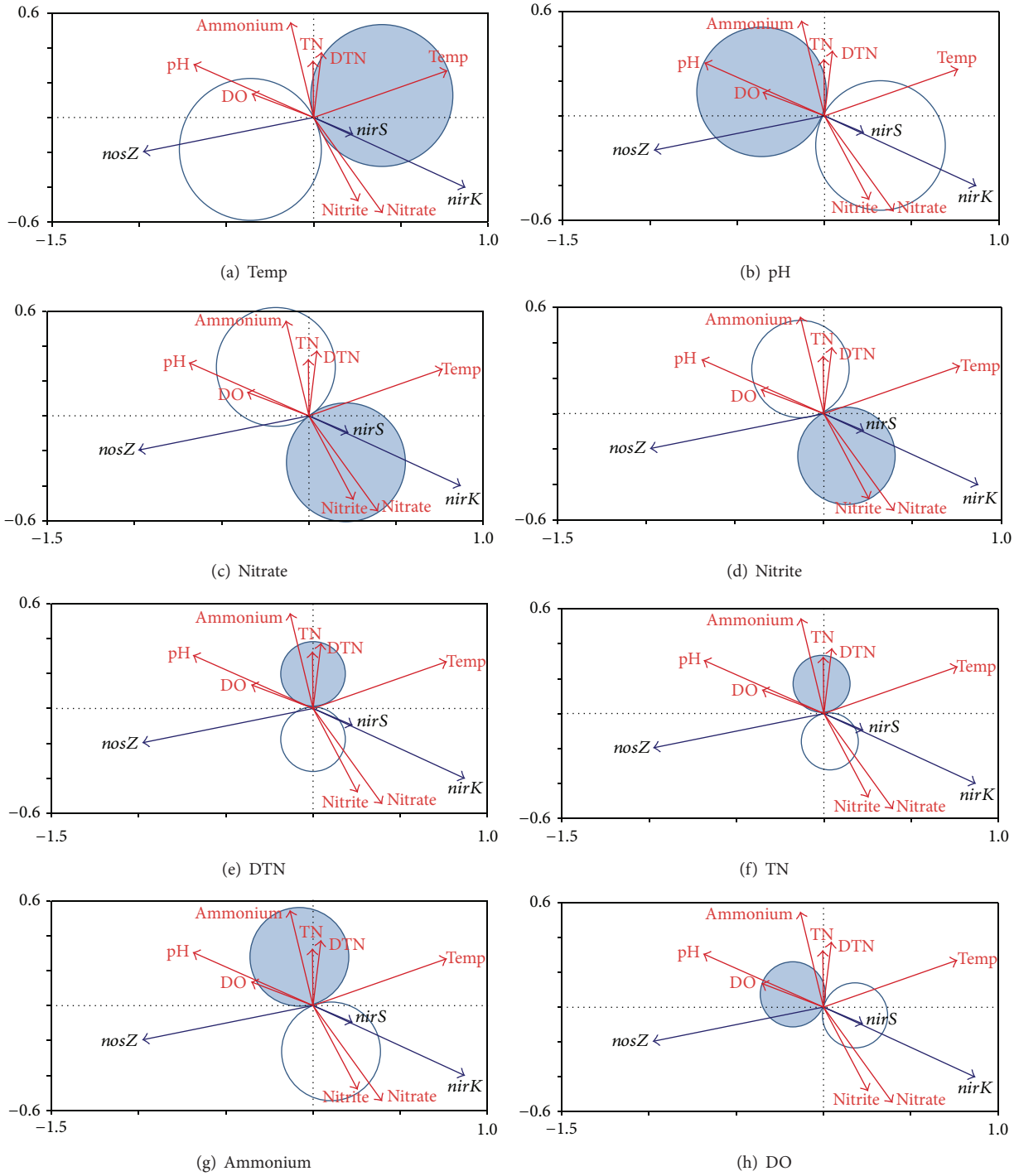

Figure 3: Redundancy analysis t-value biplots of environmental factors Temp, pH, nitrate, nitrite, DTN, TN, DO, and ammonium and abundance of *nirK*, *nirS*, and *nosZ* genes.

of *E. crassipes* (Table 3). The significant differences among them were observed statistically ($P < 0.05$). With respect to the richness and diversity of denitrifier communities in all sites, similar trends emerged with low richness and diversity of *nirK* and *nirS* genes in XBX and DG rivers, which mainly received effluent from STPs. Next trends were in the H, JJ, and XBH rivers with relatively higher richness and diversity of *nirK* and *nirS* genes, which were less impacted by the effluent from STPs. The highest richness and diversity of *nirK* showed in the XB and YA rivers, which received wastewater after flowing through a wetland incubation on the water way. The richness and diversity of *nosZ*, which was mainly impacted by temperature, gave a similar trend for all rivers due to the fact that temperature did not vary too much in all sites.

Table 2: Water properties of the rivers at Dianchi Lake (mean ± SD).

Rivers	NO_3^- (mg L^{-1})	NO_2^- (mg L^{-1})	NH_4^+ (mg L^{-1})	TN (mg L^{-1})	TSN (mg L^{-1})	DO (mg L^{-1})	pH	T (°C)
XBX	4.79 ± 0.39	0.25 ± 0.02	0.69 ± 0.07	7.44 ± 0.19	6.54 ± 0.32	2.15 ± 0.15	7.83 ± 0.06	19.60 ± 0.00
DG	12.00 ± 0.67	0.46 ± 0.00	0.10 ± 0.02	12.91 ± 0.62	12.26 ± 0.42	2.70 ± 0.13	7.56 ± 0.04	22.15 ± 0.05
CF	5.09 ± 0.03	0.62 ± 0.02	1.98 ± 0.02	8.63 ± 0.10	7.57 ± 0.06	3.80 ± 0.10	7.90 ± 0.06	21.75 ± 0.05
PLJ	5.86 ± 0.01	0.10 ± 0.00	0.06 ± 0.02	8.08 ± 0.19	6.45 ± 0.08	2.80 ± 0.00	8.03 ± 0.00	19.70 ± 0.00
H	0.16 ± 0.02	0.09 ± 0.00	18.48 ± 2.30	23.69 ± 0.79	19.84 ± 1.91	0.20 ± 0.10	7.90 ± 0.01	18.80 ± 0.00
GPG	0.08 ± 0.02	0.04 ± 0.01	19.54 ± 0.19	23.66 ± 0.16	21.27 ± 0.07	0.20 ± 0.10	7.83 ± 0.00	17.90 ± 0.00
JJ	0.43 ± 0.02	0.15 ± 0.00	5.12 ± 0.50	8.14 ± 0.54	6.86 ± 0.37	1.30 ± 0.10	7.90 ± 0.01	19.50 ± 0.00
XBH	5.92 ± 0.25	0.70 ± 0.00	0.78 ± 0.20	8.60 ± 0.19	6.96 ± 0.58	0.60 ± 0.00	7.77 ± 0.00	21.60 ± 0.00
XYL	0.08 ± 0.02	0.05 ± 0.00	18.72 ± 3.31	21.40 ± 2.78	19.95 ± 3.55	0.45 ± 0.05	7.78 ± 0.02	21.55 ± 0.05
XB	0.56 ± 0.14	0.17 ± 0.04	3.03 ± 0.52	6.35 ± 1.21	5.60 ± 0.64	0.55 ± 0.25	7.78 ± 0.06	17.95 ± 0.05
YA	8.99 ± 0.00	0.62 ± 0.01	2.49 ± 0.27	15.08 ± 0.50	11.97 ± 0.56	1.05 ± 0.35	7.85 ± 0.07	17.60 ± 0.10

Table 3: Shannon (H) and richness (S) values of *nirK*, *nirS*, and *nosZ* genes.

Rivers	*nirK*		*nirS*		*nosZ*	
	S	H	S	H	S	H
XBX	11.00 ± 1.00	2.25 ± 0.20	11.67 ± 0.58	2.18 ± 0.06	10.67 ± 0.58	2.11 ± 0.10
DG	13.67 ± 1.15	2.23 ± 0.21	11.67 ± 1.53	2.15 ± 0.07	15.67 ± 0.58	2.56 ± 0.20
CF	16.67 ± 0.58	2.48 ± 0.17	15.33 ± 0.58	2.57 ± 0.30	17.33 ± 0.58	2.65 ± 0.25
PLJ	16.67 ± 1.15	2.54 ± 0.41	18.67 ± 1.15	2.65 ± 0.21	18.00 ± 1.00	2.73 ± 0.26
H	17.00 ± 0.00	2.53 ± 0.45	17.67 ± 1.53	2.69 ± 0.31	11.00 ± 0.00	2.18 ± 0.16
GPG	14.33 ± 1.53	2.36 ± 0.37	17.00 ± 0.00	2.66 ± 0.34	16.33 ± 0.58	2.44 ± 0.34
JJ	18.66 ± 058	2.59 ± 0.04	10.33 ± 1.53	2.08 ± 0.35	12.33 ± 0.58	2.25 ± 0.21
XBH	17.67 ± 0.58	2.71 ± 0.19	13.33 ± 0.58	2.26 ± 0.19	14.67 ± 0.58	2.45 ± 0.32
XYL	14.33 ± 1.15	2.38 ± 0.16	13.00 ± 0.00	2.56 ± 0.22	16.33 ± 0.58	2.64 ± 0.24
XB	21.00 ± 1.00	2.61 ± 0.20	17.00 ± 0.00	2.64 ± 0.39	14.67 ± 1.15	2.35 ± 0.31
YA	22.33 ± 0.58	2.90 ± 0.56	15.33 ± 0.00	2.54 ± 0.11	13.00 ± 0.00	2.29 ± 0.15

3.5. Relationship between Environment Matrices and Denitrifier Diversity. To determine to what extent the eight environmental properties affected the three types of denitrifier community compositions, *nirK*, *nirS*, and *nosZ* DGGE fingerprints were evaluated by redundancy analysis (Table 4). The first axis explained 26.9% of the *nirK*-type denitrifier diversity, and the second axis explained 21.8% of the diversity. For *nirS*-type denitrifier, the first two canonical axes explained 29.5% and 11.5% of the variation, respectively. For *nosZ*-type denitrifier, 37.8% and 13.7% of the variation were explained by the first two canonical axes (Table 4).

Of the parameters, total N, DO, pH, and water temperature appeared to be the relatively important environmental factors for denitrifiers (Table 5). For *nirK*-type denitrifier, water temperature, DO, and total N explained 46% variations of microbial communities, leaving 54% of the variation unexplained. Variation partitioning analysis showed that water temperature, DO, and total N separately explained 19% ($P = 0.020$), 13% ($P = 0.054$), and 14% ($P = 0.240$) of the variation, respectively. For *nirS*-type denitrifier, water temperature (18%, $P = 0.066$), pH (10%, $P = 0.304$), and DO (8%, $P = 0.038$) explained 36% variations of microbial communities, leaving 64% of the variation unexplained. Compared to *nirS*, the total N rather than DO was relatively important for *nosZ*-type denitrifier (Table 5).

The relationships of microbial patterns to environmental variables were summarized in RDA ordination plots (Figures 4(b), 5(b), and 6(b)). The RDA charts (Figure 4(b)) of *nirK* gene showed four rivers (PLJ, XYL, DG, and CF) grouped into one type, while other four rivers (XBH, XBX, H, and YA) clustered together. Other rivers were located independently; they did not belong to either group. For *nirS* gene, PLJ, JJ, and CF rivers were similar and grouped into one type, while other three rivers (XBH, XYL, and XBX) clustered together. Other rivers were not similar and did not belong to either group (Figure 5(b)). According to the RDA chart (Figure 6(b)) of *nosZ* gene, DG, H, GPG, and XBH rivers were located independently and did not cluster with any group. However, PLJ, XYL, JJ, and CF rivers clustered into one group, while other three rivers (XB, XBX, and YA) clustered together.

4. Discussion

The activity of denitrifying microorganisms leads to significant net removal of dissolved nitrogen from the water,

Table 4: Redundancy analysis results of *nirK*, *nirS*, and *nosZ* DGGE profiles.

Axis	Eigenvalue	Denitrifier-environment correlation	Cumulative% variation of denitrifier	Cumulative% variation of denitrifier-environment	Sum of all canonical eigenvalues
			nirK RDA		
Axis 1	0.269	0.987	26.9	31.0	0.867
Axis 2	0.218	0.954	48.7	56.2	
Axis 3	0.141	0.944	62.8	72.5	
Axis 4	0.075	0.990	70.3	81.1	
			nirS RDA		
Axis 1	0.295	0.965	29.5	42.6	0.693
Axis 2	0.114	0.895	41.0	59.1	
Axis 3	0.099	0.780	50.8	73.3	
Axis 4	0.072	0.861	58.0	83.8	
			nosZ RDA		
Axis 1	0.378	0.996	37.8	48.1	0.786
Axis 2	0.136	0.973	51.5	65.5	
Axis 3	0.097	0.682	61.2	77.9	
Axis 4	0.071	0.971	68.4	87.0	

Table 5: Eigenvalues, *F* values, and *P* values obtained from the partial RDAs testing the influence of the significant water properties on the denitrifying bacterial community composition.

Samples	Environmental variables	Eigenvalue	% variation explains solely	*F* value	*P* value
nirK	Temp	0.19	19	2.08	0.020
	DO	0.13	13	1.46	0.054
	Total *N*	0.14	14	1.54	0.240
	All the above together	0.92	92		
nirS	Temp	0.18	18	1.93	0.066
	pH	0.10	10	1.19	0.304
	DO	0.08	8	0.96	0.038
	All the above together	0.69	69		
nosZ	Temp	0.22	22	2.50	0.032
	pH	0.11	11	1.41	0.082
	Total *N*	0.13	13	1.39	0.260
	All the above together	0.79	79		

Partial RDAs based on Monte Carlo permutation ($n = 499$) kept only the significant water properties in the models. For each partial model, the other significant water properties were used as covariables. *F* and *P* values were estimated using Monte Carlo permutations. Sum of all eigenvalues for both partial RDAs was 1.000.

resulting in considerable improvement of water quality in aquatic ecosystem [15]. Denitrifiers play an important role in buffering of the excessive load of nitrogen from upstream to downstream [16]. In aquatic ecosystems, mats of macrophytes are important sites for microbial mediated biogeochemical processes, as accrual of biomass and increases in mat density reduce the degree of external factors to influence internal processes [17]. The suspended root system of *E. crassipes* could provide a large surface area, approximately 2.5 to 8.0 $m^2\,kg^{-1}$ on a dry weight basis, for microbial attachment [5, 18]. Releasing of oxygen and dissolved organic carbon from roots of *E. crassipes* would support an appropriate microenvironment for nitrification and/or denitrification [19, 20].

Process of denitrification is driven by the denitrifying microorganisms under the influence of environmental conditions. Water properties in different rivers in the present study were shown altering the abundance and diversity of denitrifiers on *E. crassipes* roots.

4.1. Differential Characteristics of Different Rivers Impact the Abundance of Denitrifier on the Roots. The abundance of *nirK*, *nirS*, and *nosZ* denitrifiers on the root of macrophytes varied with the variation of environmental parameters in different rivers, which seemed depending on the nitrogen concentrations, water temperature [21], water turbulence, and pretreatment of wastewater using wetland.

The abundance of *nirK*, *nirS*, and *nosZ* denitrifiers on root samples from XBX, DG, CF, and PLJ rivers was relatively stable and low. These rivers were larger than other rivers around Dianchi Lake [22], which were important sites receiving effluent from the STPs. The fast-flowing water

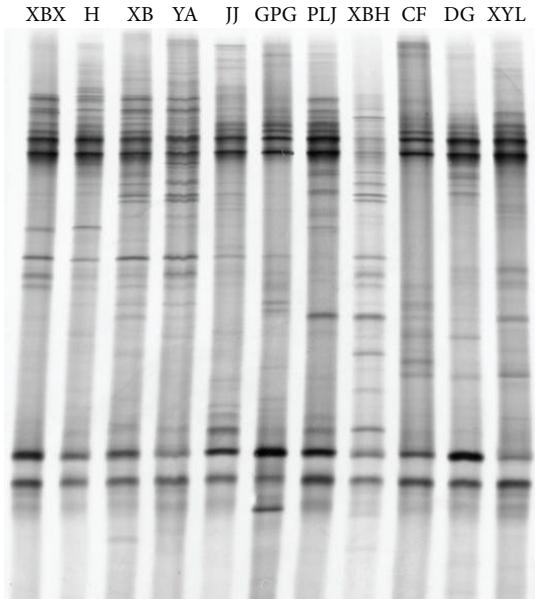

(a)

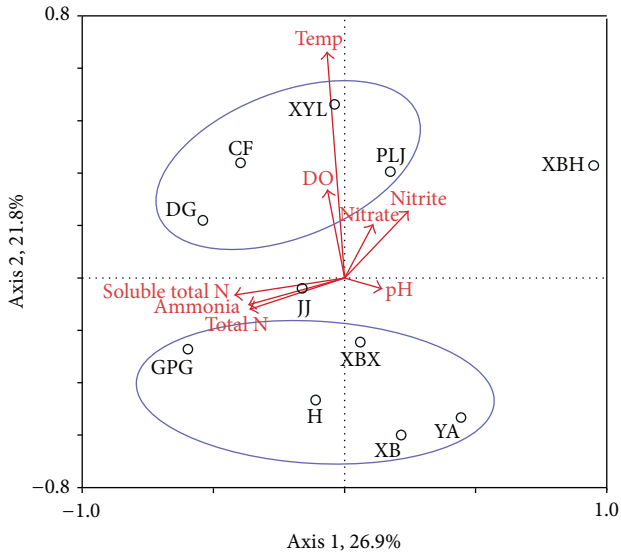

(b)

Figure 4: DGGE fingerprints and the redundancy analysis of DGGE band data of *nirK* gene. Arrows represent quantitative variables of environmental variables and small circles with letters represent the name of sample rivers; river names: XBX = Xinbaoxiang, DG = Daguang, CF = Chuangfang, PLJ = Panlongjiang, H = Haiheriver, GPG = Guangpugou, JJ = Jinjia, XBH = Xibahe, XYL = Xinyunling, XB = Xiaba, and YA = Yaoan.

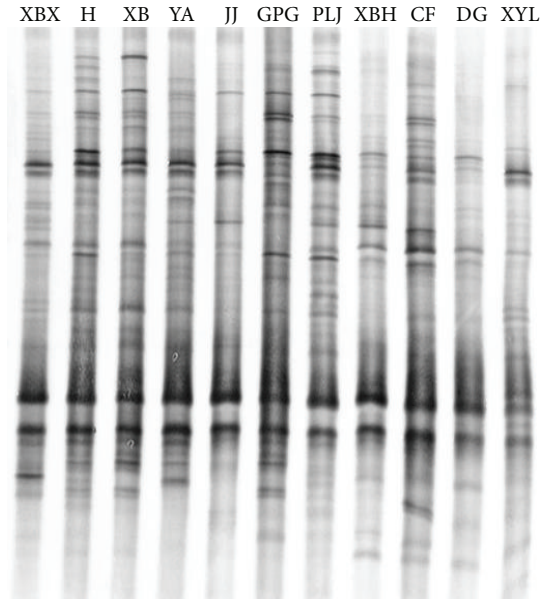

(a)

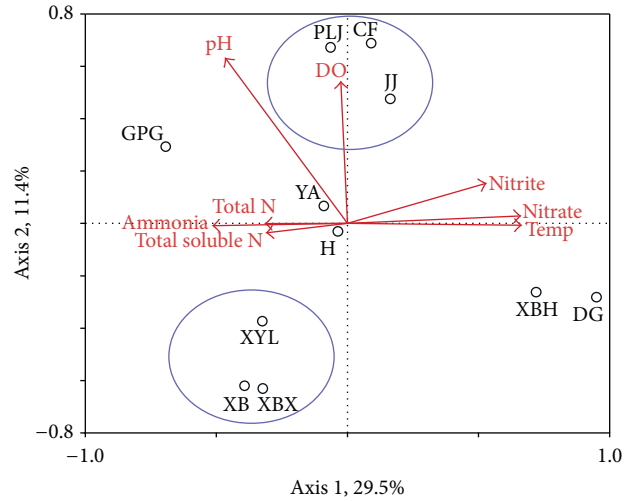

(b)

Figure 5: DGGE fingerprints and the redundancy analysis of DGGE band data of *nirS* gene. Arrows represent quantitative variables of environmental variables and small circles with letters represent the name of sample rivers; river names: XBX = Xinbaoxiang, DG = Daguang, CF = Chuangfang, PLJ = Panlongjiang, H = Haiheriver, GPG = Guangpugou, JJ = Jinjia, XBH = Xibahe, XYL = Xinyunling, XB = Xiaba, and YA = Yaoan.

and irregular discharge of effluent of these rivers [22] may prevent development of the stable environment properties from microbial attachment and propagate. Contrarily, the abundance of denitrifiers genes on roots samples in XB and YA rivers (Xiaba and Yaoan rivers) was higher than that in other rivers. The XB river received both the wastewater from industrial and residential areas and the tidal water from Dianchi Lake, when water level increased in rainy seasons (May to October) [23]. The water merged at Wujia wetland, and then part of it was pumped into YA river after 45 days of retention in Wujia wetland. This implies that a combination of wetland and growth of water hyacinth may further promote denitrification processes in eutrophic water.

The abundance of *nirK* gene was always greater than that of *nirS* gene on the roots of *E. crassipes*, suggesting that the fresh water of Dianchi lake was more suitable for the growth of *nirK*-type denitrifying bacteria. This was different from the previous reports [24]. The *nirS* gene of cytochrome *cd1* type has also been found more often in anoxic locations, where DO

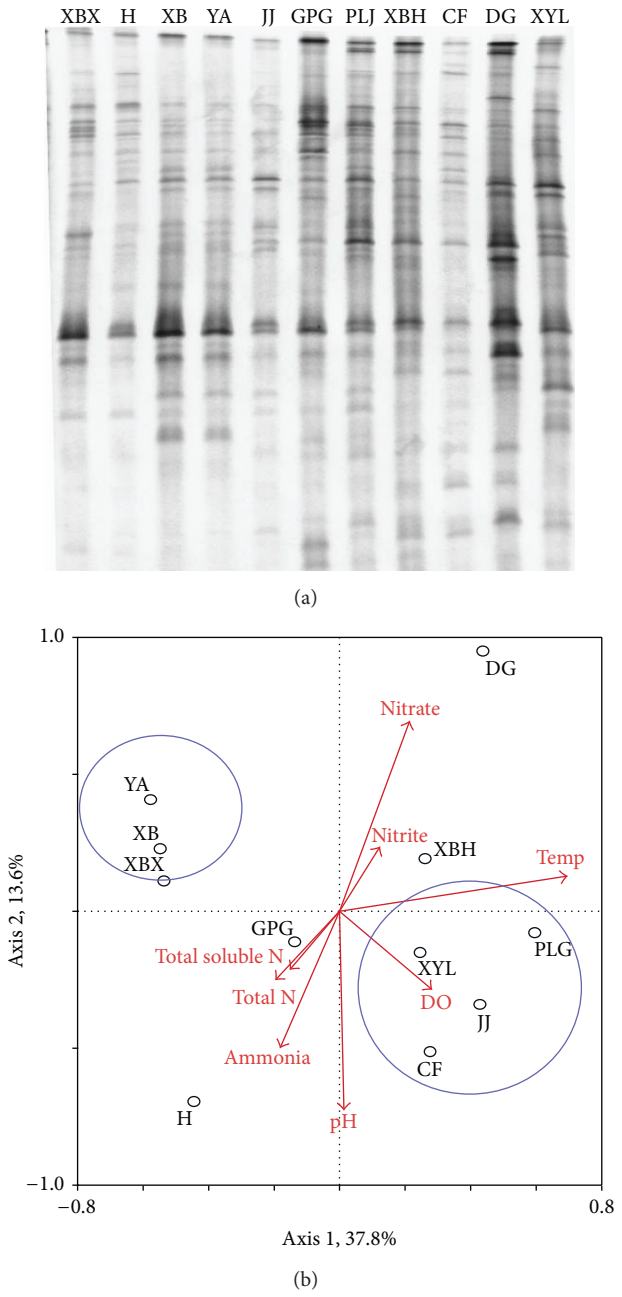

Figure 6: DGGE fingerprints and the redundancy analysis of DGGE band data of *nosZ* gene. Arrows represent quantitative variables of environmental variables and small circles with letters represent the name of sample rivers; river names: XBX = Xinbaoxiang, DG = Daguang, CF = Chuangfang, PLJ = Panlongjiang, H = Haiheriver, GPG = Guangpugou, JJ = Jinjia, XBH = Xibahe, XYL = Xinyunling, XB = Xiaba, and YA = Yaoan.

levels were consistently low. In contrast, *nirK* genes of copper containing type have been found where diurnal DO swings are greater [24, 25]. This finding was of coincidence with that *E. crassipes* releases oxygen from roots, which facilitates the creation of aerobic microsites on the roots [26]. Even though the *nirK* and *nirS* are functionally equivalent, denitrifying bacteria harboring either nitrite reductase seems to be likely not under the same community assembly rules [27]. Philippot et al. [28] suggested that the existence of the two types of nitrite reductase (*nir*-gene) was due to differential niche preferences. This speculation was consistent with previously identified habitat preferences of *nirS*-gene and *nirK*-gene bearing organisms [29]. Moreover, *nirK* and *nirS* sequences may come from different sources. Jones and Hallin [27] found that most *nirK* sequences were derived from soil but that most *nirS* sequences were prominently derived from marine and estuarine environment. Bacteria suspended in water and attached to the root of *E. crassipes* may originate from many different sources. Autochthonous bacterioplankton populations that developed in the water column were likely to be mixed with allochthonous populations from forest soils, urbanized land, farm fields, and wetlands as well as hyporheic sediments in the rivers. This mixed origination, impacted by varied environmental parameters, seemed to be the main cause of the discrepancy of denitrifiers found in the eleven rivers. This, however, did not necessarily indicate that *nirK*-type denitrifiers contributed more or less in denitrification than *nirS*-type ones; rather it may only imply that the root of *E. crassipes* could provide a broad support for different kinds of microorganisms.

4.2. Relationship between Environmental Factors and Community Compositions of Denitrifying Genes on E. crassipes Root at Different Rivers. Dianchi Lake together with surrounding rivers comprised a plateau water catchment to provide ecological services and fresh water supply for more than seven million people in the area. Its geochemical characteristics have made the water pH relatively high (7.56–8.03) and its geophysical characteristics have made the water temperature moderate with winter months (December to March next year) around 12°C. Its heavy load of organic matters have made the DO level relatively low (0.20–3.80 mg L^{-1}) in the 11 rivers investigated. These environmental properties dominated the community assembly processes of the genetic makeup of the denitrifiers in the rivers. Nevertheless, specific environmental conditions in different rivers favored the variation in richness and diversity of different denitrifying genes.

The DGGE profiles for denitrification genes encoding nitrite and nitrous oxide reductase (*nirK*, *nirS*, and *nosZ*) on the root of *E. crassipes* growing in 11 rivers around Dianchi Lake supported our hypothesis of profound differences in community composition, although a complex picture of denitrifier community similarity emerged depending on which functional denitrification gene was evaluated. The correlations of denitrifying microbial community compositions with abiotic environmental factors, using redundancy analysis (RDA), confirmed that water temperature (Temp), dissolved oxygen (DO), and pH appeared to be the most important factors to alter the denitrifier community structures significantly by serving as essential conditions for the growth of microorganisms on the roots of *E. crassipes* (Table 5).

The results of this study indicated that the development of denitrifier communities on roots corresponded to different origins of rivers. The physiochemical characteristics of water from the river inlet varied with water origin and pollution

sources [22, 23, 30], resulting in the variation in DO, pH, pollutant species and concentrations, and organic carbons in rivers. These environmental factors, including DO, carbon content, water temperature, and pH, influenced denitrification rates in rivers [31] and as a consequence they might also affect the denitrifier community composition [32, 33]. Braker et al. [34] found that the change of temperature resulted in gradually changed denitrification activity but also in abundance mutative of nitrate reducers and in different denitrifier community compositions. There are some indications that temperature and pH may directly or indirectly influence the abundance and communities composition of denitrifiers [35, 36]. The excess O_2 resulted in reduced denitrifying bacterial growth and a smaller bacterial density versus nitrate reducing bacteria ration [37], which indicated that the development of the denitrifying bacteria was influenced by the DO concentration. Many investigators had found that the pH, temperature, and DO generally affect diversity and richness of denitrifier community [32, 38], and microbial community assembly was more dependent on local-scale environmental factors [39].

On the other hand, different microorganisms may have their physiological constraints for growth and reproduction within narrow pH ranges, specific DO, and nutrient availability, which affect the community structures directly [40, 41]. Activities of microorganisms could change the environmental properties that differed in the concentrations of enzymes and nutrients or DO, the form and amount of dissolved carbon present, and pH [42] hence to affect denitrifier community structure. Previous studies have found that growth of *E. crassipes* could regulate water at neutralize pH significantly [43], as a result of increase in the rate of denitrification in aquatic ecosystems [44].

5. Conclusions

The variation in abundance of denitrifier communities on *E. crassipes* roots, grown in rivers flowing into Dianchi Lake, corresponded to different water properties of rivers. The ratio of *nirK*/*nirS* gene copies abundance was always greater than 1, indicating that the surface of *E. crassipes* roots was more suitable for the growth of *nirK*-type denitrifying bacteria. The temperature of water, nitrate concentration, and pH greatly affected the *nirS*, *nirK*, and *nosZ* abundance than other factors. Meanwhile, the temperature of water, DO, and pH appeared to be the most important factors to alter the community structures of denitrifiers on the roots of *E. crassipes*. As process of denitrification is driven by denitrifies under the influence of environmental conditions, a variation of denitrification capability in different rivers would be expected.

Conflict of Interests

The authors declare that there is no conflict of interests regarding the publication of this paper.

Authors' Contribution

Neng Yi and Yan Gao contributed equally to this work.

Acknowledgments

The authors are grateful for the financial support from State Natural Science Foundation of China (no. 41401592), Natural Science Foundation of Jiangsu Province (no. BK20140737), and Independent Innovation of Agricultural Sciences in Jiangsu Province (no. CX(14)5047) and Jiangsu Province Science and Technology Support Plan Project (BE2013436).

References

[1] M. H. Hu, Y. S. Ao, X. E. Yang, and T. Q. Li, "Treating eutrophic water for nutrient reduction using an aquatic macrophyte (*Ipomoea aquatica* Forsskal) in a deep flow technique system," *Agricultural Water Management*, vol. 95, no. 5, pp. 607–615, 2008.

[2] Q. Yi, Y. Kim, and M. Tateda, "Evaluation of nitrogen reduction in water hyacinth ponds integrated with waste stabilization ponds," *Desalination*, vol. 249, no. 2, pp. 528–534, 2009.

[3] M. Rodríguez, J. Brisson, G. Rueda, and M. S. Rodríguez, "Water quality improvement of a reservoir invaded by an exotic macrophyte," *Invasive Plant Science and Management*, vol. 5, no. 2, pp. 290–299, 2012.

[4] Z. Wang, Z. Zhang, J. Zhang, Y. Zhang, H. Liu, and S. Yan, "Large-scale utilization of water hyacinth for nutrient removal in Lake Dianchi in China: the effects on the water quality, macrozoobenthos and zooplankton," *Chemosphere*, vol. 89, no. 10, pp. 1255–1261, 2012.

[5] N. Yi, Y. Gao, X.-H. Long et al., "Eichhornia crassipes cleans wetlands by enhancing the nitrogen removal and modulating denitrifying bacteria community," *CLEAN—Soil, Air, Water*, vol. 42, no. 5, pp. 664–673, 2014.

[6] Y. Gao, N. Yi, Y. Wang et al., "Effect of *Eichhornia crassipes* on production of N_2 by denitrification in eutrophic water," *Ecological Engineering*, vol. 68, pp. 14–24, 2014.

[7] V. Gagnon, F. Chazarenc, Y. Comeau, and J. Brisson, "Influence of macrophyte species on microbial density and activity in constructed wetlands," *Water Science and Technology*, vol. 56, no. 3, pp. 249–254, 2007.

[8] R. D. Sooknah and A. C. Wilkie, "Nutrient removal by floating aquatic macrophytes cultured in anaerobically digested flushed dairy manure wastewater," *Ecological Engineering*, vol. 22, no. 1, pp. 27–42, 2004.

[9] J. Green and B. J. M. Bohannan, "Spatial scaling of microbial biodiversity," *Trends in Ecology & Evolution*, vol. 21, no. 9, pp. 501–507, 2006.

[10] C. L. Lauber, M. Hamady, R. Knight, and N. Fierer, "Pyrosequencing-based assessment of soil pH as a predictor of soil bacterial community structure at the continental scale," *Applied and Environmental Microbiology*, vol. 75, no. 15, pp. 5111–5120, 2009.

[11] D. Radojkovic and J. Kušic, "Silver staining of denaturing gradient gel electrophoresis gels," *Clinical Chemistry*, vol. 46, no. 6, pp. 883–884, 2000.

[12] H. F. Luo, H. Y. Qi, and H. X. Zhang, "Assessment of the bacterial diversity in fenvalerate-treated soil," *World Journal*

of Microbiology and Biotechnology, vol. 20, no. 5, pp. 509–515, 2004.

[13] D. Roesti, R. Gaur, B. N. Johri et al., "Plant growth stage, fertiliser management and bio-inoculation of arbuscular mycorrhizal fungi and plant growth promoting rhizobacteria affect the rhizobacterial community structure in rain-fed wheat fields," *Soil Biology and Biochemistry*, vol. 38, no. 5, pp. 1111–1120, 2006.

[14] J. Lepš and P. Šmilauer, *Multivariate Analysis of Ecological Data using CANOCO*, Cambridge University Press, Cambridge, UK, 2003.

[15] A. J. Burgin and S. K. Hamilton, "Have we overemphasized the role of denitrification in aquatic ecosystems? A review of nitrate removal pathways," *Frontiers in Ecology and the Environment*, vol. 5, no. 2, pp. 89–96, 2007.

[16] A. C. Mosier and C. A. Francis, "Denitrier abundance and activity across the San Francisco Bay estuary," *Environmental Microbiology Reports*, vol. 2, no. 5, pp. 667–676, 2010.

[17] E. Lyautey, S. Hallin, S. Teissier et al., "Abundance, activity and structure of denitrifier communities in phototrophic river biofilms (River Garonne, France)," *Hydrobiologia*, vol. 716, no. 1, pp. 177–187, 2013.

[18] Y. Kim and W.-J. Kim, "Roles of water hyacinths and their roots for reducing algal concentration in the effluent from waste stabilization ponds," *Water Research*, vol. 34, no. 13, pp. 3285–3294, 2000.

[19] S. Kouki, N. Saidi, A. B. Rajeb et al., "Potential of a polyculture of *Arundo donax* and *Typha latifolia* for growth and phytotreatment of wastewater pollution," *African Journal of Biotechnology*, vol. 11, no. 87, pp. 15341–15352, 2012.

[20] C. C. Tanner, "Plants for constructed wetland treatment systems—a comparison of the growth and nutrient uptake of eight emergent species," *Ecological Engineering*, vol. 7, no. 1, pp. 59–83, 1996.

[21] A. M. Baxter, L. Johnson, T. Royer, and L. G. Leff, "Spatial differences in denitrification and bacterial community structure of streams: relationships with environmental conditions," *Aquatic Sciences*, vol. 75, no. 2, pp. 275–284, 2013.

[22] B. Wang, B. Huang, W. Jin et al., "Occurrence, distribution, and sources of six phenolic endocrine disrupting chemicals in the 22 river estuaries around Dianchi Lake in China," *Environmental Science and Pollution Research*, vol. 20, no. 5, pp. 3185–3194, 2013.

[23] Y. Huang, H. Wen, J. Cai et al., "Key aquatic environmental factors affecting ecosystem health of streams in the Dianchi Lake Watershed, China," *Procedia Environmental Sciences*, vol. 2, pp. 868–880, 2010.

[24] C. W. Knapp, W. K. Dodds, K. C. Wilson, J. M. O'Brien, and D. W. Graham, "Spatial heterogeneity of denitrification genes in a highly homogenous urban stream," *Environmental Science & Technology*, vol. 43, no. 12, pp. 4273–4279, 2009.

[25] A. García-Lledó, A. Vilar-Sanz, R. Trias, S. Hallin, and L. Bañeras, "Genetic potential for N_2O emissions from the sediment of a free water surface constructed wetland," *Water Research*, vol. 45, no. 17, pp. 5621–5632, 2011.

[26] K. K. Moorhead and K. R. Reddy, "Oxygen transport through selected aquatic macrophytes," *Journal of Environmental Quality*, vol. 17, no. 1, pp. 138–142, 1988.

[27] C. M. Jones and S. Hallin, "Ecological and evolutionary factors underlying global and local assembly of denitrifier communities," *The ISME Journal*, vol. 4, no. 5, pp. 633–641, 2010.

[28] L. Philippot, J. Čuhel, N. P. A. Saby et al., "Mapping field-scale spatial patterns of size and activity of the denitrifier community," *Environmental Microbiology*, vol. 11, no. 6, pp. 1518–1526, 2009.

[29] C. Desnues, V. D. Michotey, A. Wieland et al., "Seasonal and diel distributions of denitrifying and bacterial communities in a hypersaline microbial mat (Camargue, France)," *Water Research*, vol. 41, no. 15, pp. 3407–3419, 2007.

[30] Y. J. Yu, J. Guan, Y. W. Ma et al., "Aquatic environmental quality variation in Dianchi lake watershed," *Procedia Environmental Sciences*, vol. 2, pp. 76–81, 2010.

[31] J. L. Baeseman, R. L. Smith, and J. Silverstein, "Denitrification potential in stream sediments impacted by acid mine drainage: effects of pH, various electron donors, and iron," *Microbial Ecology*, vol. 51, no. 2, pp. 232–241, 2006.

[32] B. C. Crump and J. E. Hobbie, "Synchrony and seasonality in bacterioplankton communities of two temperate rivers," *Limnology and Oceanography*, vol. 50, no. 6, pp. 1718–1729, 2005.

[33] Z. H. Liu, S. B. Huang, G. P. Sun, Z. Xu, and M. Xu, "Phylogenetic diversity, composition and distribution of bacterioplankton community in the Dongjiang River, China," *FEMS Microbiology Ecology*, vol. 80, no. 1, pp. 30–44, 2012.

[34] G. Braker, J. Schwarz, and R. Conrad, "Influence of temperature on the composition and activity of denitrifying soil communities," *FEMS Microbiology Ecology*, vol. 73, no. 1, pp. 134–148, 2010.

[35] M. D. Wallenstein, D. D. Myrold, M. Firestone, and M. Voytek, "Environmental controls on denitrifying communities and denitrification rates: insights from molecular methods," *Ecological Applications*, vol. 16, no. 6, pp. 2143–2152, 2006.

[36] J. K. M. Walker, K. N. Egger, and G. H. R. Henry, "Long-term experimental warming alters nitrogen-cycling communities but site factors remain the primary drivers of community structure in high arctic tundra soils," *The ISME Journal*, vol. 2, no. 9, pp. 982–995, 2008.

[37] M. A. Gómez, E. Hontoria, and J. González-López, "Effect of dissolved oxygen concentration on nitrate removal from groundwater using a denitrifying submerged filter," *Journal of Hazardous Materials*, vol. 90, no. 3, pp. 267–278, 2002.

[38] S. Hallin, C. M. Jones, M. Schloter, and L. Philippot, "Relationship between n-cycling communities and ecosystem functioning in a 50-year-old fertilization experiment," *The ISME Journal*, vol. 3, no. 5, pp. 597–605, 2009.

[39] W. H. Hartman, C. J. Richardson, R. Vilgalys, and G. L. Bruland, "Environmental and anthropogenic controls over bacterial communities in wetland soils," *Proceedings of the National Academy of Sciences of the United States of America*, vol. 105, no. 46, pp. 17842–17847, 2008.

[40] I. R. Booth, "Regulation of cytoplasmic pH in bacteria," *Microbiological Reviews*, vol. 49, no. 4, pp. 359–378, 1985.

[41] W. Stumm and J. J. Morgan, *Aquatic Chemistry: Chemical Equilibria and Rates in Natural Waters*, John Wiley & Sons, New York, NY, USA, 2012.

[42] M. Kühl, L. F. Rickelt, and R. Thar, "Combined imaging of bacteria and oxygen in biofilms," *Applied and Environmental Microbiology*, vol. 73, no. 19, pp. 6289–6295, 2007.

[43] C. McVea and C. E. Boyd, "Effects of waterhyacinth cover on water chemistry, phytoplankton, and fish in ponds," *Journal of Environmental Quality*, vol. 4, no. 3, pp. 375–378, 1975.

[44] S. R. Carrino-Kyker, K. A. Smemo, and D. J. Burke, "The effects of pH change and NO_3^- pulse on microbial community

structure and function: a vernal pool microcosm study," *FEMS Microbiology Ecology*, vol. 81, no. 3, pp. 660–672, 2012.

[45] K. Kloos, A. Mergel, C. Rösch, and H. Bothe, "Denitrification within the genus *Azospirillum* and other associative bacteria," *Australian Journal of Plant Physiology*, vol. 28, no. 9, pp. 991–998, 2001.

[46] I. N. Throbäck, K. Enwall, Å. Jarvis, and S. Hallin, "Reassessing PCR primers targeting nirS, nirK and nosZ genes for community surveys of denitrifying bacteria with DGGE," *FEMS Microbiology Ecology*, vol. 49, no. 3, pp. 401–417, 2004.

[47] V. Michotey, V. Méjean, and P. Bonin, "Comparison of methods for quantification of cytochrome cd1-denitrifying bacteria in environmental marine samples," *Applied and Environmental Microbiology*, vol. 66, no. 4, pp. 1564–1571, 2000.

[48] G. Braker and J. M. Tiedje, "Nitric oxide reductase (norB) genes from pure cultures and environmental samples," *Applied and Environmental Microbiology*, vol. 69, no. 6, pp. 3476–3483, 2003.

[49] S. Hallin and P.-E. Lindgren, "PCR detection of genes encoding nitrite reductase in denitrifying bacteria," *Applied and Environmental Microbiology*, vol. 65, no. 4, pp. 1652–1657, 1999.